



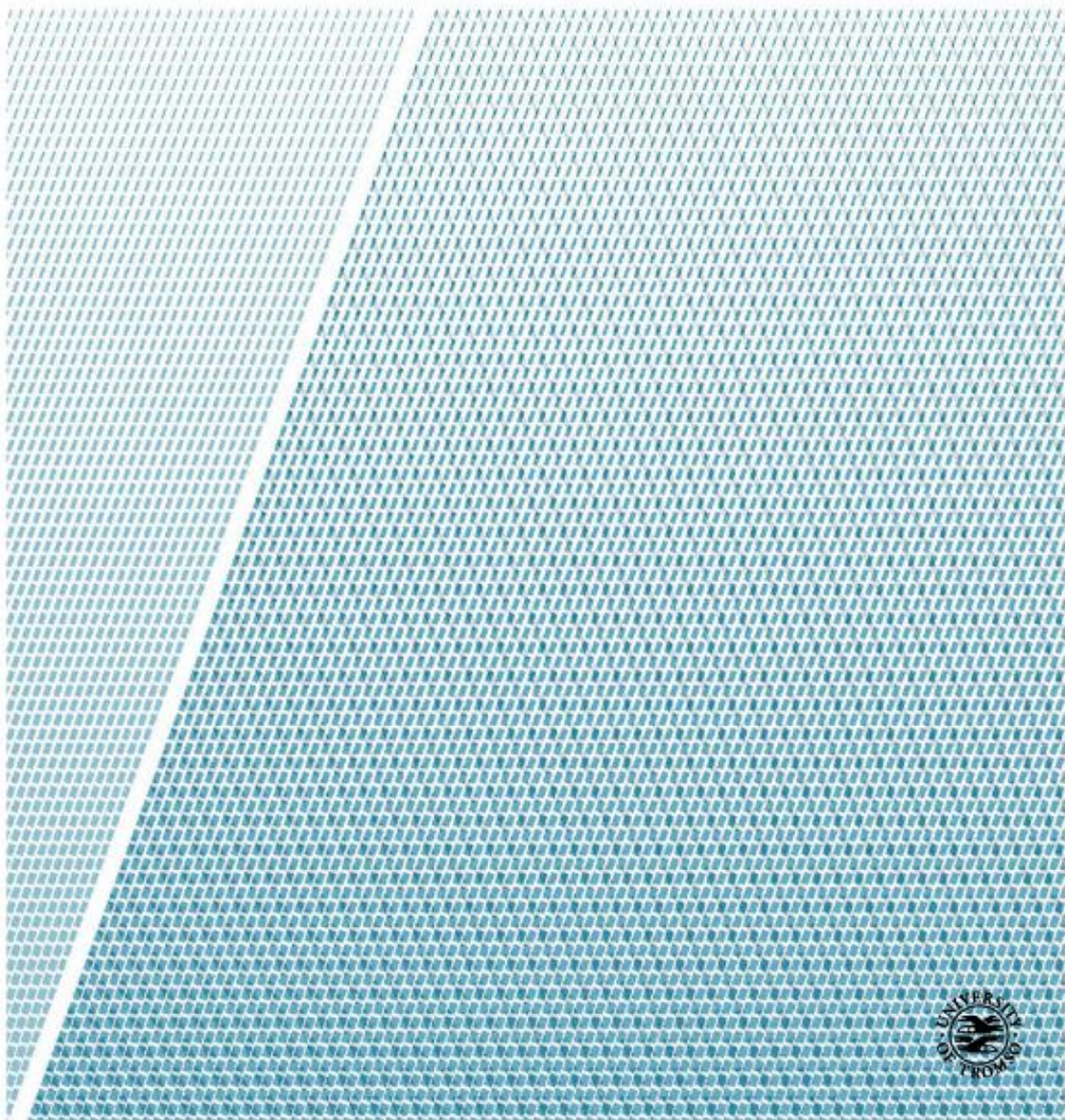
FACULTY OF ENGINEERING SCIENCE AND TECHNOLOGY

DUCT FANNED SHIELDING DESIGN FOR QUADROTORS

SETHURAM BALAKRISHNAN

Master Thesis in ENGINEERING DESIGN

JULY – 2016



Abstract

The master thesis work involved the design implementation of a duct fanned shielding for Quadrotors. This included the investigation of various settings for duct shielding and to identify the best possible option to safe guard propellers of the quadrotor. In addition, the work focused on improving the aerodynamic efficiency, reducing the mass of flight and the use of quadrotors in the arctic region.

The first goal was to understand and predict the necessary ways to improve the thrust with minimal increase in the mass of the quadrotor. The second goal was to check the durability of the duct.

In the elementary models, the duct was modelled as a rigid mass and preliminary tests were conducted using diverse software. Problems, were found in the core areas which had to be solved, independent of the size and shape of quadrotor. Initially before designing the shielding, preliminary research was incorporated for understanding different aspects of the quadrotor. This report is one such procedure, which focuses on different types of quadrotors, construction styles, market analysis, customer satisfaction, designing and simulation and manufacturing processes.

A study of the ducted principle culminates in the development of some simple structures and analysis which may prove useful in practice. Some comparisons between the conceptual models: rectangular concept of connection, aerodynamic concept with 45deg of connection, aerodynamic concept with 60deg of connection and cylindrical concept of connection have been made in order to access their strengths and highlight their various shortcomings.

The development of a final duct model for quadrotor shielding is discussed in detail with particular emphasis on thrust improvement (especially design features). A limited study on manufacturing approach has been conducted in order to gain some insight into the production equipment and to follow the evolution of the product. Future work in this area is indicated although the product is only for research purpose.

Preface

This report is the master thesis in Engineering Design study program at University in Tromsø (Narvik) and is the final work of the two-year master's degree study. The work is divided into two parts, one pre-thesis part of 5 weeks (25.01.2016 – 26.02.2016) and the main part of 18 weeks (01.03.2016 – 30.06.2016). The pre – project includes a presentation of the project, summary of the literature review, project planning with time schedule and important activities. The plan of manufacturing 3D printed model of all the concepts was changed in the end of the project owing to difficulties in executing the planned activities.

The programs which found its use in evolution of the product are,

- I. Solidworks 2015: This program was used to convert the hand sketches to 3D models, and to create mechanical drawings.
- II. Solidworks Flow simulation 2015: The tool was used to find the behaviour of the fluid using CFD (Computational fluid dynamics) and take decisions regarding the aerodynamics effect.
- III. Solidworks Simulations 2015: This tool was used to find the static and dynamic study regarding the structural stability of the material.
- IV. FLOW3D 10.1: This software was used to find the initial solution for our problem, which is also a powerful tool for complex fluid modelling problems.
- V. Granta CES 2015 selector: This tool was used to find the best material for our product and best suitable production process for the particular material.

Acknowledgement

The work described in this Thesis was carried out at the Faculty of Engineering Science and Technology at UiT – Norges Arktiske Universitet (Narvik campus) under the direction of Associate Professor Guy Beerli Mauseth. I am greatly indebted to him for his invaluable advice and encouragement throughout the work and for many suggestions for improvements to this thesis.

My thanks are due to Professor Meidell Annette, the Head of the Department, for allowing me to use the facilities of the Department. I also wish to thank Researchers Tor-Aleksander Johansen and Tom Stian Andersen for their interest in this research study.

I am deeply grateful to Professor Per-Arne Sundsbø, for his invaluable help in the enhancement of the simulation Flow-3D.

My thanks are also due to my Mom and Dad for their support and believing me that I will be successful.

I would also like to acknowledge the support of my fellow students, who were always willing to discuss aspects of my work with me.

I would like to express my gratitude to the readers for their patience and my apologies if there are any mistakes in the report.

Finally, many thanks to UiT – Norges Arktiske Universitet for its facilities and wonderful staffs, without which the work could not have been completed.

Sethuram Balakrishnan

Table of Contents

Abstract	
Preface	
Acknowledgement	
List of Figures	i
List of Tables	v
Notation.....	vi
List of Symbols	vi
Abbreviations	vii
Chapter 1. Introduction.....	1
1.1 General overview	1
1.2 Objective of the report.....	2
1.3 Customer-Focused Development	3
1.3.1 Voice of Customer	3
1.3.2 Phases of QFD Approach.....	3
Chapter 2. Background.....	5
2.1 Types of Quadrotors.....	5
2.1.1 Very Small Drones.....	5
2.1.2 Small Drones.....	5
2.1.3 Medium Drones	6
2.1.4 Large Drones.....	7
2.2 Standards for Unmanned Aircraft in Norway (11).....	7
2.3 Parts of a Quadrotor	8
2.3.1 Frame	8
2.3.2 Motors	9
2.3.3 Propellers	10
2.3.4 Flight Controllers	10
2.3.5 Electronic Speed Controllers (ESC)	11
2.3.6 Battery.....	11
2.3.7 Video system.....	11
2.3.8 Landing Gears.....	12

2.4	Mechanics of Flying.....	12
Chapter 3. Customer – Product planning.....		15
3.1	Problem Analysis	15
3.2	Problem description.....	15
3.3	Special attention on operation	15
3.3.1	Rotating blades.....	15
3.3.2	Batteries	15
3.3.3	Landing gears or rods.....	16
3.4	Possible predictable solutions	16
3.5	Customer Needs	16
Chapter 4. Market Research		17
4.1	Market Competitors.....	17
4.2	Market opportunity 1	18
4.3	Market opportunity 2.....	18
4.4	Market opportunity 3.....	19
4.5	Custom made ducts	19
4.6	Model Description.....	20
4.6.1	Frame (2.3.1).....	20
4.6.2	Motor (2.3.2).....	21
4.6.3	Propeller (2.3.3)	22
4.6.4	Frame plates (2.3.4)	23
4.6.5	Damping Legs (Landing gears)	24
Chapter 5. Research of basic Quadrotor structure.....		25
5.1	Speed and Power Calculation.....	25
5.2	Theoretical Thrust Calculation.....	26
5.3	Open rotor test results	28
5.4	Modelling of Existing Open Quadrotor	31
5.5	Flow simulation of Open Quadrotor for Thrust	32
5.6	Research results.....	33
Chapter 6. House of Quality		34
6.1	Introduction	34
6.2	Importance of this Design	34

Chapter 7. Ducted Principle.....	36
7.1 Construction of Ducted rotor.....	36
7.1.1 Diffuser Included Angle (Θ_d).....	37
7.1.2 Diffuser Length (L_d)	37
7.1.3 Blade Tip Clearance (δ_{tip})	38
7.2 Duct comparison	38
7.3 Simplifying Assumptions	41
7.4 Theoretical Derivations for Ducted rotor	41
Chapter 8. Developing Duct Concepts	47
8.1 Characteristics of Concepts	47
8.2 Rectangular concept of connection	49
8.2.1 Simulation of Concept I.....	50
8.3 Aerodynamic Concept with 45Deg of connection	52
8.3.1 Simulation of Concept II.....	53
8.4 Aerodynamic Concept with 60Deg of connection	55
8.4.1 Simulation of Concept III	55
8.5 Cylindrical concept of connection.....	57
8.5.1 Simulation of Concept IV	58
8.6 Selection of optimum Duct design	59
Chapter 9. Best concept Design.....	61
9.1 Concept design features	61
9.1.1 Beam	61
9.1.2 Duct wall.....	61
9.1.3 Structural connections.....	62
9.1.4 Top cover	63
9.2 Force on Impact Calculation	64
9.3 Material selection	66
9.3.1 Duct – Material selection	66
9.3.2 Top cover – material selection.....	75
9.4 Structural analysis on the Duct and top cover.....	78
9.4.1 Drop test on Duct	78
9.4.2 Impact test on Top cover.....	79

Chapter 10. Duct Performance.....	81
10.1 3-D Printing of duct.....	81
10.2 Duct thrust testing	82
10.3 Observation of Quad's	86
Chapter 11. Manufacturing Process	89
11.1 Duct and Top Cover Production.....	89
11.1.1 Raw material Description	89
11.1.2 Injection moulding	90
11.1.3 Injection molding requirements	90
11.2 Duct and Top cover manufacturing drawings	92
11.3 Assembly and Maintenance	93
Chapter 12. Conclusion.....	94
Chapter 13. Recommendations for Future studies	95
Appendix A.....	96
A.1 Thrust measuring test Procedure	96
Appendix B	97
B.1 Duct initial testing setup in Flow 3D.....	97
B.2 Flow simulation setup in Solidworks for open rotor	98
B.3 Flow simulation setup in Solidworks for ducted rotor	100
Appendix C.....	103
C.1 Procedure for drop test setup	103
C.2 Procedure for Impact test on Top cover	104
Appendix D.....	106
D.1 Bill of materials and Exploded view – Attachment 1 (Sheet: 1/3).....	106
D.2 Duct Mechanical drawing – Attachment 2 (Sheet: 2/3).....	106
D.3 Top cover Mechanical drawing – Attachment 3 (Sheet: 3/3)	106
Appendix E Task Description.....	107
References.....	110

List of Figures

Figure 1.1 Oehmichen No.2 Quadcopter (2)	1
Figure 1.2 De Bothezat Helicopter, 1923 (2).....	2
Figure 1.3 A photograph of the Convertawings quadrotor from May 1957 (3)	2
Figure 2.1 Prototypes of Nano-drones (7)	5
Figure 2.2 AAI RQ-7 Shadow UAV in Iraq (8)	5
Figure 2.3 Commercially used Quadrotors (9)	6
Figure 2.4 Flight trials at Parc Aberporth 2013 (10)	6
Figure 2.5 Large Drones (Google search on Large drones).....	7
Figure 2.6 Parts of a Quadrotor.....	8
Figure 2.7 Frame structure of a Quadrotor (13).....	9
Figure 2.8 MT-1306-10 3100 Kv brushless motor (16)	9
Figure 2.9 9x4.7 Carbon Fiber self-locking propellers (16)	10
Figure 2.10 TBS Bulletproof 30A ESC set (16)	11
Figure 2.11 Nano-tech LiPo (16).....	11
Figure 2.12 FPV Camera's (Google search on Sony FPV cams).....	12
Figure 2.13 Landing gears (Flame wheel F450 Landing gear search)	12
Figure 2.14 Flight dynamics (20).....	13
Figure 2.15 Quadrotor dynamics (21).....	14
Figure 4.1 Hubsan X4 H107C Protection covers (25).....	18
Figure 4.2 Lookatool® Upgrade JJRC H8D 4CH 5.8G FPV RC (26).....	18
Figure 4.3 UDI U830 RC Quadcopter Parts Protection Cover U830-04 (27).....	19
Figure 4.4 Custom made duct (Google image search on custom made ducts)	19
Figure 4.5 DJI Flame wheel F450 frame dimensions (13)	21
Figure 4.6 Frame arm Solidworks modelling	21
Figure 4.7 Dji Flame wheel F450 Motor (13).....	22
Figure 4.8 Motor model for quadrotor	22
Figure 4.9 Propeller modelling (13).....	23
Figure 4.10 DJI Flame wheel F450 Frame plates (13)	23
Figure 4.11 Power distributing board 1 solid modelling	23
Figure 4.12 Power distributing board 2 solid modelling	24

Figure 4.13 Damping leg modelling (13)	24
Figure 5.1 Propeller air flow	26
Figure 5.2 PWM example (PWM Wikipedia search)	28
Figure 5.3 PWM Vs thrust increase for open rotor	31
Figure 5.4 Open quadrotor modelling	31
Figure 5.5 Open rotor velocity flow section	32
Figure 5.6 Flow condition and thrust force data	32
Figure 5.7 Comparison of different results for an open quad	33
Figure 7.1 Cross section of ducted rotor	36
Figure 7.2 Ducted rotor parameters	37
Figure 7.3 Blade tip clearance	38
Figure 7.4 Negative draft angle modelling	39
Figure 7.5 Duct with Negative diffuser angle	39
Figure 7.6 Positive angle duct modelling	40
Figure 7.7 Duct with positive diffuser angle	40
Figure 7.8 Ducted rotor flow conditions (35)	41
Figure 7.9 Assumption value	42
Figure 8.1 Main characteristics of duct	48
Figure 8.2 Rectangular concept of connection	49
Figure 8.3 Velocity flow definition through Duct Inlet	49
Figure 8.4 Simplified model of duct and components for Flow simulation	50
Figure 8.5 Velocity flow section 1 in Concept I	51
Figure 8.6 Velocity of flow section 2 in Concept I	51
Figure 8.7 Velocity flow section 3 in Concept I	51
Figure 8.8 Flow trajectories in Concept Duct I	52
Figure 8.9 Thrust value Y-direction in Duct concept I	52
Figure 8.10 Aerodynamic concept II (45deg) modelling	53
Figure 8.11 Velocity flow section 2 in Duct concept II	53
Figure 8.12 Velocity flow section 3 in Duct concept II	54
Figure 8.13 Flow trajectories in Concept II	54
Figure 8.14 Thrust value Y direction in Concept II	54
Figure 8.15 Aerodynamic concept III (60deg) modelling	55

Figure 8.16 Velocity flow section in Duct concept III	55
Figure 8.17 Velocity flow section 2 in Duct concept III	56
Figure 8.18 Velocity flow section 3 in Duct concept III	56
Figure 8.19 Flow trajectories in Concept III.....	56
Figure 8.20 Thrust value Y direction in concept III	57
Figure 8.21 Cylindrical concept IV modelling	57
Figure 8.22 Velocity flow section 1 in Duct concept IV	58
Figure 8.23 Velocity flow section 2 in Duct concept IV	58
Figure 8.24 Velocity flow section 3 in Duct concept IV	58
Figure 8.25 Flow trajectories in Concept IV	59
Figure 8.26 Thrust value Y direction in Concept IV	59
Figure 9.1 Final concept modelling	61
Figure 9.2 Concept features	62
Figure 9.3 Top cover modelling.....	63
Figure 9.4 Sample Assembly process over duct	63
Figure 9.5 Impact Force on Quad	64
Figure 9.6 Actual Vs Simplified models.....	67
Figure 9.7 Young's Modulus Vs Density stage 1	72
Figure 9.8 Young's Modulus Vs Density stage 2.....	72
Figure 9.9 Young's Modulus Vs Density stage 3.....	73
Figure 9.10 Yield strength Vs Density final stage.....	73
Figure 9.11 Simplified model of top cover for Material selection	76
Figure 9.12 Yield strength Vs Density for top cover.....	77
Figure 9.13 Drop test analysis on duct.....	78
Figure 9.14 Max Von-Mises stress area on duct.....	79
Figure 9.15 Displacement result in the duct	79
Figure 9.16 Impact analysis on Top cover.....	80
Figure 10.1 MakerBot Replicator Z18 (43).....	81
Figure 10.2 Duct 3D printed for testing.....	81
Figure 10.3 3D Printed duct on Thrust testing machine	83
Figure 10.4 For simplified calculation of thrust	85
Figure 10.5 PWM vs thrust increase for Ducted quad.....	86

Figure 10.6 Thrust Vs speed curve	88
Figure 11.1 PA612 G30 raw material (Google image search on raw material PA612)	89
Figure 11.2 Parts made from PA612 (Google image search on PA612)	89
Figure 11.3 Injection molding machine and process (48).....	90
Figure 11.4 Mould forming process.....	91
Figure 11.5 Mold releasing principle (49)	92

List of Tables

Table 1.1 QFD Phases (5).....	4
Table 2.1 Dynamics of the quad-rotor (21)	14
Table 4.1 Manufacturers categorised Quadrotors (24)	17
Table 4.2 DJI Flame wheel F450 Quadrotor specification (13)	20
Table 5.1 Dimensions of motor and battery (13).....	25
Table 5.2 Manual test results for thrust	30
Table 5.3 Momentum theory parameters using flow simulation	33
Table 6.1 House of Quality.....	34
Table 8.1 Dimensions of Duct	48
Table 8.2 Thrust force generated from Duct Concept I.....	52
Table 8.3 Thrust force generated from Duct II.....	55
Table 8.4 Thrust force generated from Duct III.....	57
Table 8.5 Thrust force generated from Duct IV	59
Table 8.6 Brain storming for Duct principle.....	60
Table 9.1 Translation for duct material (41).....	68
Table 9.2 Ranking materials table	74
Table 9.3 Selected materials for Duct.....	75
Table 9.4 Translation for cover material (41).....	77
Table 10.1 3-D Printed model specification	82
Table 10.2 Ducted rotor test results	84
Table 10.3 % Increase in thrust.....	87

Notation

List of Symbols

ω	Angular velocity
A	Area of the propeller
D	Propeller diameter
γ	Velocity of air
ρ	Density
\dot{m}	Mass flow rate
T	Thrust
P	Power
g	Force of gravity
A_e	Diffuser exit plane area
σ_d	Expansion ratio
P	Pressure
Θ_d	Diffuser included angle
L	Length
δ_{tip}	Blade tip clearance
p	Pressure
t	Thickness
W	Workdone
S	Bending stiffness
E	Young's modulus
I	Second moment of Inertia
σ_y	Yield strength

Abbreviations

UAV	Unmanned Aerial Vehicle
QFD	Quality Function Deployment
CAA	Civil Aviation Authority
UAS	Unmanned Aircraft Systems
FPV	First Person View
EASA	European Aviation Safety Agency
GPS	Global Positioning Systems
ESC	Electronic Speed Controllers
RPM	Revolutions per minute
PWM	Pulse Width Modulation
PLA	Polylactic Acid
STL	Stereo Lithography

Chapter 1. Introduction

The use of Quadrotor's is expected to increase exponentially in the coming decades. Some of the proposed uses which are being implemented are fire rescue assistance, assistance bot for people working in dangerous heights like exterior workers, assistance during natural calamities like earthquake, tsunami etc. A quadrotor is a multi-rotor copter with four arms, each of which has a motor and a propeller at its end. The lift and thrust of a quadrotor is as similar to helicopters, rather than just one rotor, it has four rotors. The main difference between a quadrotor and helicopter is that a quadrotor does not have any tail to stabilize the craft as in case of a helicopter. To achieve stability, two of the propellers spin in one direction (clockwise) and the other two spin the opposite direction (counter clockwise). These rotors are directed upwards and are placed in a square formation with the centre of rotation of each of the rotor being equidistant from the centre of mass of quadrotor (1). Each arm of the quad produces its own thrust force and sum of all arm forces makes the quadrotor to lift. The lift/ thrust generated can be significantly improved using ducts around individual rotors, which also plays a role in improving safety by eliminating the chance of rotor hitting an obstacle or personnel on the ground.

In recent years the quadrotors have received considerable attention from researchers as the complex phenomena of quadrotors has generated several areas of interest. A quadrotor is a simple structure for typical design of small unmanned aerial vehicles (UAV)

1.1 General overview

The very first experimental attempts of taking off with a rotorcraft were mostly done with multirotor. It was around 1907, Jacques and Louis Breguet, French brothers built and tested Gyroplane No.1, a quadrotor. Perhaps it managed to take-off, but the system considered as a failure attempt, because unstable and impractical (2). In 1922 a French engineer, Etienne Oehmichen built the first quadrotor Oehmichen No. 2 (Figure 1.1), which was a six full – scale rotary winged vehicle and further development featuring the “X” design, which found its usage in current quadrotor styles (3).

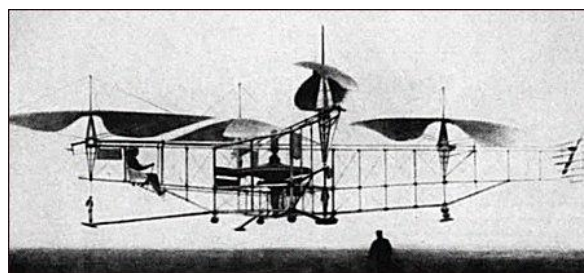


Figure 1.1 Oehmichen No.2 Quadcopter (2)

This equipment had a single 120HP engine, powering all four rotors and it was found difficult to control the altitudes and speed, so to overcome this trouble four small propellers were added to control the movement, further it can fly at an altitude of 360m. Throughout 1900's there was numerous design phases to achieve a perfect physical platform for quadrotors. Along in 1923 Dr. George de Bothezat and Ivan Jerome developed a six bladed rotors at the end of an X-

shaped design (Figure 1.2), they were powered by two small propellers with varying pitch to control thrust and yaw (2).



Figure 1.2 De Bothezat Helicopter, 1923 (2)

By the end of 1956 attachments of rotors were replaced by wings as an improvement in design. This newly developed model came to be known as Convertawing's Model 'A' (Figure 1.3) in which the craft was controlled by two engines of varied power. Since then quadrotors had undergone several design changes and several researches have focused on improving the technology in rotor design.

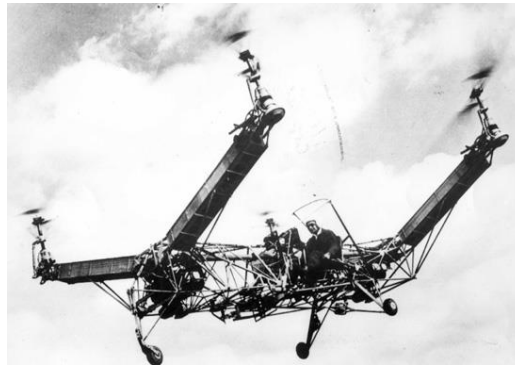


Figure 1.3 A photograph of the Convertawings quadrotor from May 1957 (3)

1.2 Objective of the report

The objective of this report is to gain an understanding of the performance improvements and basics thrust changes of a quadrotor through the application of momentum theory, testing and simulation predictions. This will be done in multiple steps.

The existing quadrotor was studied applying Quality Function Deployment (QFD) and an understanding of the open quadrotor and its structure. This provided an overview of the problem and aerodynamics of a quadrotor. The problem description pointed to market research of existing products and their short comings. Further research was conducted on the open rotor in terms of momentum theory to gain an understanding of the open rotor. Tests for thrust development have been done manually and in software and design changes were made on open quadrotor for improving the thrust.

These simulations and tests were expanded to ducted concepts for a full calculation of ducted rotor flow fields and three-dimensional calculations include ducted and un-ducted cases for the sake of comparison. The goal of the 3D cases and testing is to explore, in detail, the implications of a duct and cover. Thrust distribution and critical conditions were analysed. The design of

the duct was evaluated for withstanding impacts and material analysis was carried out to explore suitable materials for the safety of the duct.

The final objective is to model accurately the dimensions and develop the complex features, such as struts and connections inside the duct. Additionally, production methods were evaluated to customer satisfaction.

1.3 Customer-Focused Development

Quality Function Deployment (QFD) is a systematic process of defining customer's needs or requirements and translating them into specific implementation on the product. The "Voice of Customer" is stated in variety of ways: direct discussion, surveys, customer specification, observation etc., This observation of customer needs is then summarised in a product planning matrix or "House of Quality". These details are transferred to the table to distinguish the lower and higher level of differences and meet the customer needs.

Using QFD in this report will tie all the process of marketing, needs, design, quality, manufacturing etc.... together to establish a best product. This methodology helps in understanding the essential requirements, internal capabilities, and constraints and design the product, so that all the processes are in place to achieve the desired outcome – a satisfied customer (4).

1.3.1 Voice of Customer

Quality function deployment requires that the basic customer needs are identified. Frequently, customers will try to express their needs in terms of "how" the need can be satisfied and not in terms of "what" the need is. The limits consideration of development alternatives. Development and marketing objective should ask "why" until they are properly formulated what the need is.

After the needs are gathered together, they need to be organised. The needs, required documents, market research and product details need to be distilled into a handful of statements that express key customer needs. Problems statements are formulated in tables and diagram to avoid any misinterpretation. In addition to stated and spoken customer needs, "unstated" or "unspoken" needs or opportunities should be identified. Also marketing team advice is identified and documented (5).

1.3.2 Phases of QFD Approach

To develop a product successfully there are following four phases in QFD and each phase describes certain activities of the product development process

- I. Product planning,
- II. Assembly/ Part Deployment,
- III. Process planning,
- IV. Process/ Quality control.

These phases are described in the flow chart Table 1.1.

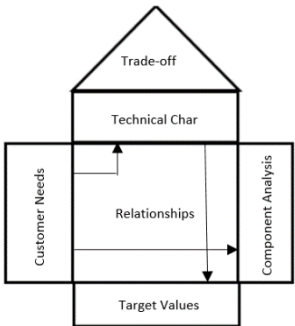
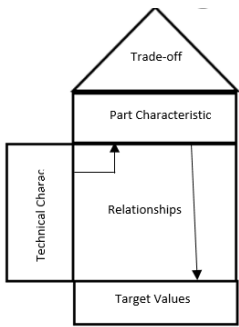
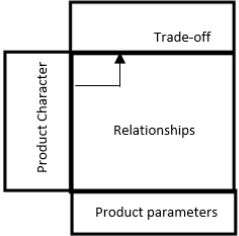
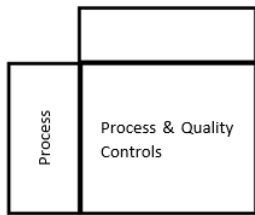
S. No	Phases	Description
1	<p style="text-align: center;">Product Planning</p> 	<p>I. Define and prioritize customer needs, II. Analyse competitive opportunities, III. Plan a product to respond to needs & opportunities, IV. Establish critical characteristics target values.</p>
2	<p style="text-align: center;">Assembly/ Part Deployment</p> 	<p>I. Identify critical parts & assemblies, II. Flow down critical products characteristics, III. Translate into critical part/assembly characteristics & target values.</p>
3	<p style="text-align: center;">Process Planning</p> 	<p>I. Determine critical processes and process flow, II. Develop production equipment requirements, III. Establish critical process parameters.</p>
4	<p style="text-align: center;">Process/Quality Control</p> 	<p>I. Determine critical process and characteristics, II. Establish process control methods and parameters, III. Establish inspection & test methods and parameters.</p>

Table 1.1 QFD Phases (5)

Chapter 2. Background

2.1 Types of Quadrotors

Quadrotors fly without human pilots inside the vehicle and are controlled by remote controls or computers. Quadrotors are classified according to their shape and size, but there is no perfect standard to differentiate each of them (6). Based on its size and use, for example in military, research, adventure etc., a quadrotor can be classified as very small to large drones.

2.1.1 Very Small Drones

These are usually called as Nano or micro quadrotors and these are in the range of 50mm long. Having the size of insects, they are used for biological welfare and spying and its rotors are in the shape of small rotary or flapping wings as shown in Figure 2.1.



Figure 2.1 Prototypes of Nano-drones (7)

2.1.2 Small Drones

Small drones have dimensions varying from 50mm to 2m. These kinds of drones have fixed rotors and the design construction is based on purpose, in some cases. Due to small size and low power consumption, they find their applications in commercial areas and defence. An example of small drones which is used in US army is RQ7 shadow (8) is shown in Figure 2.2 and Figure 2.3 shows the commercially used quadrotor.



Figure 2.2 AAI RQ-7 Shadow UAV in Iraq (8)



Figure 2.3 Commercially used Quadrotors (9)

2.1.3 Medium Drones

These kind of drones are bigger than the ‘Small drones’, but smaller than the light aircrafts. They have a wing span of 5-10m and can carry up to 200kgs. The shape of the craft is based on the wing model as shown in Figure 2.4, which is used in United Kingdom military (10). The ‘Watchkeeper’ gathers information about pinpoint targets, it senses all kind of movements in ground and accurately fixes the target for ground forces.



Figure 2.4 Flight trials at Parc Aberporth 2013 (10)

2.1.4 Large Drones

These kind of drones are in the shape of small aircrafts and are used in the places where human cannot enter due to security risks and are mainly used for military purpose (Figure 2.5). and can be further classified based on their performance. They have varying ranges and flying abilities depending on air conditions. Normally, the maximum flight time for large drones is 36 hours and they have the capability to fly at a height of 30000ft above sea level. They are used in high end surveillance.



Figure 2.5 Large Drones (Google search on Large drones)

2.2 Standards for Unmanned Aircraft in Norway (11)

There are currently no regulations governing the use of systems of unmanned aircraft for neither commercial/utility operation nor areal sports/ recreation. Civil Aviation Authority (CAA) has initiated efforts to develop regulations for this sector, and has strengthened staffing to work on this. More and more players want to develop and test fly systems of unmanned aircrafts, also known as Unmanned Aircraft Systems (UAS). A UAS comprises one or more unmanned aircraft, along with ground stations and data links for transmission of control signals and sensor information between the ground and aircraft. As of now, regulation for the so called First Person View (FPV) flight by model exists, this is also included in the term UAS.

Use of UAS involve number of issues that have not previously existed, and much pioneering work is still being carried out. This relatively new field is characterised by a very rapid technological development, where it is important to ensure that the regulations implemented are sufficiently dynamic to follow this trend. Rules for UAS with aircrafts having a mass of 150kg will be prepared by European Aviation Safety Agency (EASA) in accordance with European Union (EU) directive 1592/2002.

(EASA) directive Annex 2 National regulation will therefore be established for unmanned aircraft with maximum take-off mass up to 150 kg. Overall objective in this context is to ensure the safety of other users of the airspace and, not the least safety of people and property on ground. The requirements of UAS equipment, operations and personnel qualifications must be set so that the overall risk level for another air traffic and people and property on the ground being acceptable, and not inferior to similar operations manned aircraft.

CAA will set requirements for a reporting system for incidents and accidents involving UAS, as for manned aviation. Ref BSL A 1-3 (Regulation 2006-12-08 No. 1393 on the notification and reporting requirements related to aviation accidents and incidents etc., CAA approach will be a regulatory framework based on general practice and development with elements from similar systems in our neighbouring countries and Europe. Furthermore, the structure of the regulations being developed by EASA will be applied, despite the fact that the target audience for this legislation is manned aviation systems with greater honesty aircraft.

It is important that a future national legislation largely aligned with the cast of European and global standards to enable operations across borders smoothly. If there are specific plans to operate UAS, notification to CAA on awareness of this at an early stage, so that plans are adapted to the existing requirement. Until specific regulations are in place for such operation will CAA be constructive with a view to finding solutions that enable UAS operations in Norwegian airspace (12) and the full description on the present standards on Regulations concerning aircraft without a pilot on-board etc., is given in Civil Aviation Authority department and for reference see (11).

2.3 Parts of a Quadrotor

Commercial and research based quadrotors consists, some of the commonly used components, where the electronics section of a quadrotor is mainly characterised by the motor capacity and the kind of research the structure is used. An overview of all the components of a quadrotor is shown in Figure 2.6.

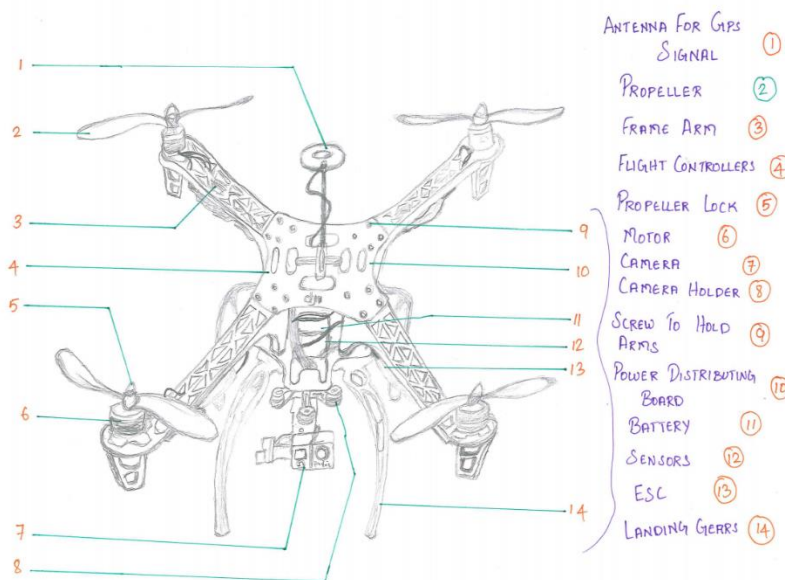


Figure 2.6 Parts of a Quadrotor

2.3.1 Frame

As for all mechanical structures, the actual work of frame is same as for a quadrotor. It is the structure that joins the motors to the rest of the aircraft and strength to lift the quad. The frame consists of four different arms connecting to the main power distributing circuits. In some cases, it can be a single unit such that the rotors do not collide with each other while in

operation. Depending on the use, the size and the material of the frame is decided which in turn also affects the weight of the quadrotor. A shape of a typical frame is shown in Figure 2.7.



Figure 2.7 Frame structure of a Quadrotor (13)

The construction of the frame should carry the built in wires towards the rotor from the circuit batteries (14) & (15). The frame is also connected to the landing gear, so that craft can be grounded safely without damaging the electronics boards. The structure must also absorb instant load in case of crash and thus, it should be tested thoroughly before use.

2.3.2 Motors

The motors spin the propellers to provide lifting thrust, and choosing a right motor is the first step to build a good electronics for a quadrotor. Since motors are expensive, research should be carried out before selecting the right configuration of motor for a specific function. Mostly for the function of quadrotors “brushless” motors are used owing to minimal friction (as shown in Figure 2.8). Propeller is mounted on top of the motor with proper safety arrangements, so that the propeller will not be flawed from the motor (16).



Figure 2.8 MT-1306-10 3100 Kv brushless motor (16)

As shown in Figure 2.8, a brushless motor has a cylindrical shell of magnet rotating on precision bearings around a core of tightly coiled wire. The working of the motor is common as other motors, and reasonable care should be taken to avoid from dirt since coils are very important in providing thrust. These motors are specified with Kv ratings, (not to be confused with kilovolts kV) which denotes the motor velocity in terms of revolution per minute (RPM) that a motor will achieve when a potential difference of 1V is applied with zero load.

2.3.3 Propellers

Propellers are also one of the important components, as they control the size and price of a quadrotor. Materials, dimensions and shape play a critical role in propeller design, and based on this, calculations for vibrations are carried out. In a quadrotor, small vibrations are allowed. Cheaper propellers generally are not precisely manufactured and more prone to create vibration. Quadrotor propeller should be properly designed and manufactured like an airplane propeller optimised for multirotor system (16). Usually quadrotors use two clockwise (CW) and two counter-clockwise (CCW) propellers and they are classified by pitch and length, for example 9x4.7 propellers means 9inch long and pitch of 4.7 as shown in Figure 2.9



Figure 2.9 9x4.7 Carbon Fiber self-locking propellers (16)

In a quadrotor, depending upon the length of propellers, the frame arm is mounted which also gives a good balance with increased propeller efficiency even when a small increase in propeller is done. A Propeller with low pitch can generate more torque while higher pitched propeller shifts greater amount of air, which could create turbulence and cause the craft to wobble during hovering (17). In selection of propellers, the motor Kv ratings plays an important role; while a higher Kv rating results in smaller propeller sizes which allow greater speeds with reduced efficiency. Larger propeller with corresponding low Kv motors is easy to fly steadily, use less current and lift more weight.

2.3.4 Flight Controllers

A Flight controller is a circuit board that reads sensing data and user commands, and makes adjustments to the motor speed in order to keep the quadrotor balanced and in control. Most of the quadrotors presently used now have Gyro (Gyroscopes) and an Acc (accelerometer). In addition to these, some application based crafts have Barometer (Barometric pressure sensors), compass and GPS. Thus, there is no perfect hardware or sensors for a quadrotor, it depends on the purpose and characteristics of craft.

There are several flight controllers in the market. Researchers generally build their own controllers based on their uses and research purpose, some of the commonly used FC are CC3D, APM2.6, BrainFPV, Naza M lite, Naza M V2 etc., “Autonomous flying” (18) i.e., a flight without any touch controls, involves in important features like auto take-off and landing for which waypoint flying and data telemetry should be included.

2.3.5 Electronic Speed Controllers (ESC)

Each motor in a quadrotor has its own ESC units which connects flight controllers. Speed adjustments and balancing of multiple motors are done by ESC, which is critical in case of multi-rotors (16). A type of ESC is shown in Figure 2.10

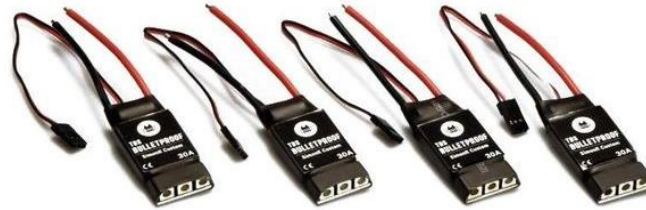


Figure 2.10 TBS Bulletproof 30A ESC set (16)

2.3.6 Battery

Lithium-ion polymer (LiPo) batteries (Figure 2.11) are used to fly quadrotors, these batteries are light weighted, compact, and offering high discharge rates. In LiPo, single cell supplies a nominal voltage of 3.7 V and when additional batteries are added these ratings are increased. LiPo packs also have C ratings that indicates, the maximum rate at which a battery can be discharged, with C standing for capacity. Capacity is one of an important factor which determines the maximum discharge up to 80,000mA, or 80A.



Figure 2.11 Nano-tech LiPo (16)

Life of a LiPo battery is less for low cost batteries and vice-versa. Excessive heat production in batteries is a bad sign for battery life and to reduce the heat, normally it should not be drained below 80% because the voltage drops rapidly when charge is depleted. Due to this some controllers have protection mechanisms to help or prevent over-discharge.

2.3.7 Video system

Camera or video setup is an optional part of a quadrotor. Today's development in video technology has brought camera, as an important part of a quadrotor. The quality of the systems is based on the quality of the video transmitter and the image quality of the goggles or monitor display. Quad's used commercially have FPV (First Person View) camera as shown in Figure 2.12, which uses its own quad power. But military or heavy clearance area quadrotors uses intelligent cameras which uses separate power box for operating systems.



Figure 2.12 FPV Camera's (Google search on Sony FPV cams)

2.3.8 Landing Gears

Landing gear is one of an important component that plays in quadrotor safety, this absorbs the maximum force applied on the quad while in destruction, accordingly the landing gears are designed and manufactured (Figure 2.13). Basically landing gears depends on the size of quad and different models has different landing gears. To avoid crash and heavy impact on quads system these gears should be higher and wider. Gears are wider because the footage of gears in video recording will promptly a problem. It should be light as much possible to avoid an extra weight on the quad.



Figure 2.13 Landing gears (Flame wheel F450 Landing gear search)

2.4 Mechanics of Flying

An advantage of quadrotor over a traditional helicopter is fixed rotor propulsion mode, which uses rapidly spinning rotors to push air downwards thus creating a thrust force keeping the helicopter aloft. Helicopter configurations require complicated machinery to control the direction of the motion for which a swashplate is used to change the angle of attack on the main rotor. The complicated design of the rotor and swashplate mechanism presents some problems, increasing construction costs and design complexity.

In case of quadrotors the controlling is quite different and also difficult as in helicopter, but interesting problem which has six degrees of freedom (three translational and three rotational) shown in Figure 2.14. It has four independent inputs (rotor speeds), and in order to achieve the six degrees of freedom, rotational and translational motions are coupled (19). To remain stable in its position while flying it should have its own damping because it has very little friction. Each rotor is aligned such that, to have opposite two rotors in one direction and other two in

opposite direction. This movement cause the torque from each rotor to cancel by the corresponding motor rotating in opposite direction (Figure 2.14).

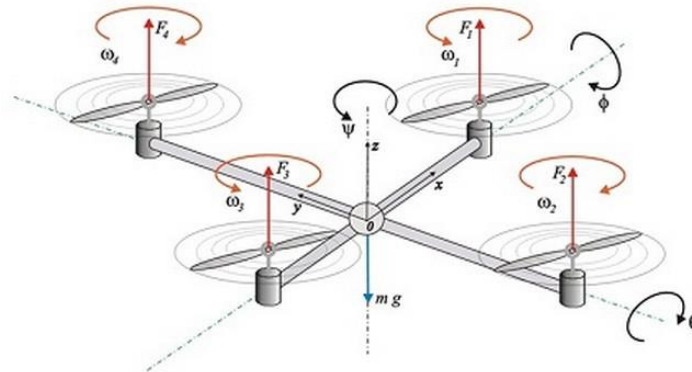


Figure 2.14 Flight dynamics (20)

Let us consider the quadrotor moving in counter clockwise from the front propeller and F_i be the force of each rotor's, where $i= 1,2,3$ and 4 respectively as shown in Figure 2.14, such that the rotors F_1 and F_3 rotate in counter-clockwise and F_2 and F_4 rotate in clockwise. As mentioned earlier to perform the stationary hover, all the four rotors rotate at the same rate and the total thrust of the craft is equal to its mass, m (21). The total thrust can be represented by $u= F_1+F_2+F_3+F_4$ and F_i is the force of rotor i . Yawing, moving left and right, pitching and rolling is shown in Table 2.1,

S. No	Movement	Description	Result
1.	Yaw movement – Counter-clockwise	F_1 and F_3 are sped up inversely proportional to F_2 and F_4 .	Net torque on the craft is negative and it will yaw while remaining in same altitude.
2.	Upwards and downwards	F_1 and F_3 do not increase proportionally to F_2 and F_4 decreasing.	Craft will move in z-direction, because the net thrust will be no longer equal to zero.
3.	Yaw movement - Clockwise	F_2 and F_4 must increase proportionally to F_1 and F_3 decrease.	Net torque on the craft is positive and it will yaw while remaining in same altitude.
4.	Roll to left	Decreasing the speed of F_2 and increasing the speed of F_4	Roll towards left is achieved, Note: Both the decreasing and increasing should be done at the same rate, to maintain the zero net torque.
5.	Roll to right	Increasing the speed of F_2 and decreasing the speed of F_4	Roll towards right is achieved.
6.	Pitching forward	Decreasing the speed of F_1 and increasing the speed of F_3	Pitch towards left is achieved.
7.	Pitching to right	Increasing the speed of F_1 and decreasing the speed of F_3	Pitch towards right is achieved.

Table 2.1 Dynamics of the quad-rotor (21)

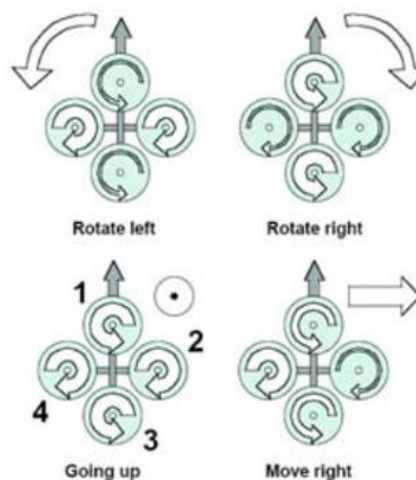


Figure 2.15 Quadrotor dynamics (21)

Chapter 3. Customer – Product planning

3.1 Problem Analysis

Quadrotors with autonomous operating system will be a part of the future. Several researches confirm that quadrotors are even capable of doing some aggressive maneuvers (22). Also some of the quadrotors is able to lift some couple of kilograms. As quadrotors has many degrees of freedom, it is considered as a challenge or problem and in addition to this is dynamics of quadrotor, which includes stable arrangement and risk of damaging flight controllers, sensors, propellers, motors etc.,

In this thesis Duct fanned shielding design for quadrotors, we can concentrate on how to protect the rotor blades of quadrotors and what factors influence the aerodynamic design. Prior to the solution, various problems are analysed on protection covers and thrust improvement.

3.2 Problem description

When the parts are assembled in the main system, the rotor arrangement has no protection towards any damage in hazardous condition this open arrangements will make difficult for flying as the control has many degree of freedom. Usually the craft propellers are made of plastics and light weighted to give quadrotor lift, which is prone to damage quickly. Aerodynamics of the craft has a problem in increasing the thrust.

In the process of research, the type of quadrotor used will be normally small drones in which all the four rotors will be in open arrangement. When there is loss in battery charge or even sudden obstacle obviously cause the quad to fall towards the ground, damaging the propeller totally. Damage to the propeller will also effect the motors which is connected in series to the propeller. So, when we design a protection cover, it should be more effective in controlling the damage. Protection covers cannot be added blindly, because it will also cost extra weight. This extra weight will reduce the thrust produced from rotor, so protection cover design should also improve the thrust.

3.3 Special attention on operation

During operation of quadrotor's major safety rules should be followed and these problems should be controlled under supervision. Also even humidity may affect quadrotor's electronics and result in unpredictable behaviour or a crash (23).

3.3.1 Rotating blades

A quadrotor must be operated only by a trained professional and it should be kept away from other people because touching of flying quadrotor can cause deep cuts and serious wounds. Also safety goggles should be used to prevent damage to eyes.

3.3.2 Batteries

As discussed in 2.3.6 the type of battery used is LiPo batteries, if wrongly used they can even explode. It is not allowed to use them outside the range of -20C to 60C, the voltage should never go below 3V per battery cell neither should it go above 4.2V per cell during charging.

Also the batteries should be avoided with serious impact and usage of sharp objects is prohibited on batteries (23).

3.3.3 Landing gears or rods

In case of serious impacts on quadrotors, the landing gears may break or come off. Again, it is important to keep the quadrotor away from non-user. Using proper protection is very important, since small splinters may remove from sides.

3.4 Possible predictable solutions

- I. Protection cover can be added in the shape of a wind tunnel.
- II. Each rotor can be designed with separate duct and structurally attached together.
- III. Top of the propeller can be protected by a top cover (Either can be integrated or made as separate component).

These predictions are prepared by design department and when it is combined with customer needs, it becomes a successful product.

3.5 Customer Needs

The result of these problems discussed above can be solved using some design change with the aerodynamics of the quadrotor. Also the shape of the quadrotor can be changed in this situation and based on the constraints described, the materials and the dimensions of the parts can be fixed. According to QFD approach customer satisfaction is the main aim and as our customer is internal research unit, we formulate the needs which are mentioned prior to design,

- I. Minimal mass,
- II. Improved thrust,
- III. Physical protection for the rotors,
- IV. Added strength/ integrity for the rest of the design,
- V. Minimal vibrations,
- VI. Usage in cold climate/ arctic regions,
- VII. Aesthetics,
- VIII. Easy,
- IX. Easy service and maintenance.

Chapter 4. Market Research

4.1 Market Competitors

In this market study, manufacturers of quadrotors are collected and the quadrotor product which is required for the thesis is selected. As mentioned in Types of Quadrotors 2.1, categorized quadrotors along with some manufacturers are shown in below Table 4.1

S. No	Application Categories	Manufacturers
1	Radio-Controlled UAV, Lightweight, Electric motorized	R & Drone Mechatronics
2	Quadrotor UAV, Rotary Air foil, Civilian, Inspection	Xamen Technologies
3	Helicopter UAV, Civilian	DJI Innovation company limited
4	Multicopter UAV, Rotary air foil	Birdpilot GMPH
5	Mini UAV, Rotary air foil, Civilian	Carbon-Based technology Inc
6	Mini UAV, Rotary air foil, Civilian	Uconsystem Co.Ltd
7	Quadrotor UAV, Rotary air foil, Civilian	Cyberflight Ltd
8	Mini UAV, Rotary air foil, Civilian	Aeryon Labs Inc
9	Quadrotor UAV, Rotary Air foil, Civilian	Fly-n-Sense UAV systems

Table 4.1 Manufacturers categorised Quadrotors (24)

As mentioned in 3.2 small drones are perfectly suited for our operation and research purpose. This market research is carried out to minimize the risk of accepting a wrong quadrotor, by this way the thrust will be improved along with other factors. Accepting small drones has an advantage of reduction of material price and weight of rotors in a broad way. Basically to achieve the thrust along with weight reduction, the manufactures follow some of the solutions such as,

4.2 Market opportunity 1

The first model in Figure 4.1 shows the protection cover for Hubsan X4 model where the protection is created for the rotors of the quadrotor and this covers only the bottom portion of the rotor. In this case all the parts are made of plastics, so in case when the weight is increased due to camera or other parts it can manage to fly. The difference between the materials to space ratio is high so that the thrust will not be affected in either way. The main dis-advantage of this model is the protection is not sufficient in all directions and a crash will damage the quadrotor in the front or in top.

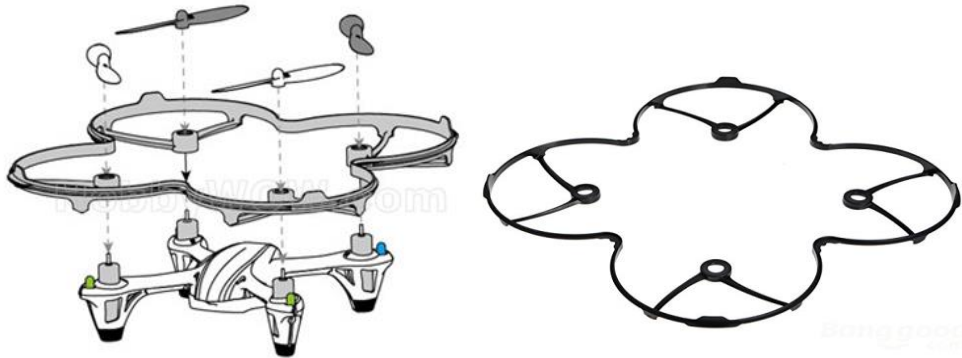


Figure 4.1 Hubsan X4 H107C Protection covers (25)

4.3 Market opportunity 2

As shown in Figure 4.2 this is one of type of protection cover for quadrotor's which is in same condition as mentioned above. In our protection covers this dis-advantages should be covered to create a possible protection in all directions. Also the protection covers are removable as shown in Figure 4.1 & Figure 4.2 which can be attached integral with the quadrotor if possible.



Figure 4.2 Lookatool® Upgrade JJRC H8D 4CH 5.8G FPV RC (26)

4.4 Market opportunity 3

The protection cover in Figure 4.3 gives the maximum protection in all directions in single wired way but the safety is still a constraint in this case. In this cover the thrust will be the same as open quadrotors. The propellers are likely to damage due to large opening in side.



Figure 4.3 UDI U830 RC Quadcopter Parts Protection Cover U830-04 (27)

4.5 Custom made ducts

Due to increasing culture of quadrotors in the market, interest on developing ducts also concerned researchers. A model of this kind of custom made duct is shown in Figure 4.4



Figure 4.4 Custom made duct (Google image search on custom made ducts)

The custom made covers are one of the similar solutions to the product that we are dealing with and usually these custom made ducts are used only to improve safety and reduce the power usage. The figure shows the construction type of the duct and the structural connection to ducts. But as per market search there was no product in the market with duct and top cover combined together to increase the thrust.

Apart from the above market opportunities there are multiple number of manufacturers who are leaders in production of quadrotors and protection covers. But our basic need is research, hence we go for small drone type, make from DJI Innovation Company limited with particular model of DJI Flame wheel F450. All the construction styles and dimensions are noted from this quadrotor.

To develop this research and customer's requirement the quadrotor product that we select from the market has no duct previously. The configuration of the quadrotor that we selected is discussed in the next section

4.6 Model Description

The DJI Flame wheel F450 quadrotor comes with the following model specifications (Table 4.2) (13),

S. No	Part list	Capacity/ Dimensions	Quantity	Weight
1	ESC (2.3.5)	30 Amps OPTO	4	-
2	Motors (2.3.2)	2212/920 KV (22 x 15mm/ 22 x 12mm)	4	212g
3	Propellers 9443(2.3.3)	10 x 4.5in; 8 x 4.5in	4	-
4	Frame (2.3.1), Material: PA66-GF30-02 (30% long glass fiber reinforced, heat stabilized, Nylon 6/6)	8.5" each arm Total length through centre = 19.5"	4 arms	282g (whole frame)
5	Battery (2.3.6)	3S ~ 4S LiPo	-	-
6	Frame Plates (2.3.1), PCB material	-	-	-
Total Quadrotor specification: Diagonal wheel base = 450mm Take-off weight = 800g ~ 1600g				

Table 4.2 DJI Flame wheel F450 Quadrotor specification (13)

As mentioned above, DJI flame wheel F450 model has its own specification and based on the manual measurements, the dimensions of quad are sketched.

4.6.1 Frame (2.3.1)

The frames which are used in the quadrotor is of PA66-GF30-02 material, basically this material is 30% long glass fiber reinforced plastic and also heat stabilised. This material has density of 1.36 g/cm^3 and about 30% of the weight is filler material so the weight to strength ratio is good when compared to PVC or ABS. Dimensions of the existing frame is shown in Figure 4.5. The frame is strengthened with ribs in the middle as shown.

All the four frame legs are made of same material and have the same dimensions to reside the stiffness. Dimensions are then transferred to Solidworks Figure 4.6 to model the frame leg, the model is also mentioned with screw holes to hold the power distributing plates and motor. The

weight of a single frame leg is 54 grams which will be approximately equal to 216grams for all the four legs.

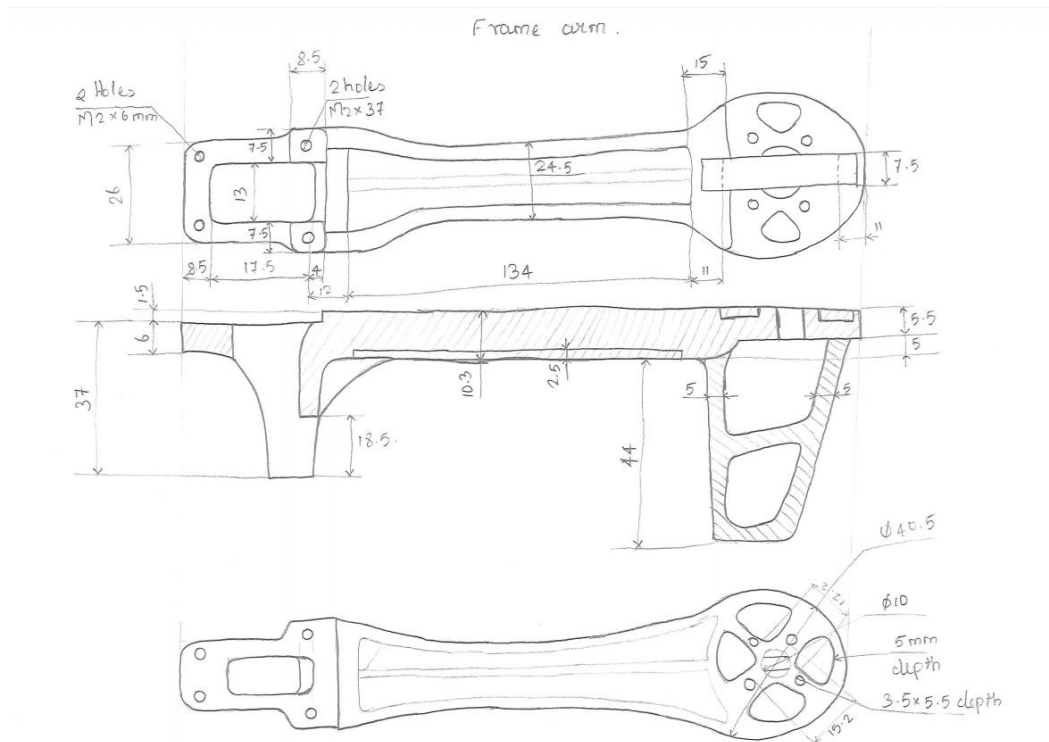


Figure 4.5 DJI Flame wheel F450 frame dimensions (13)

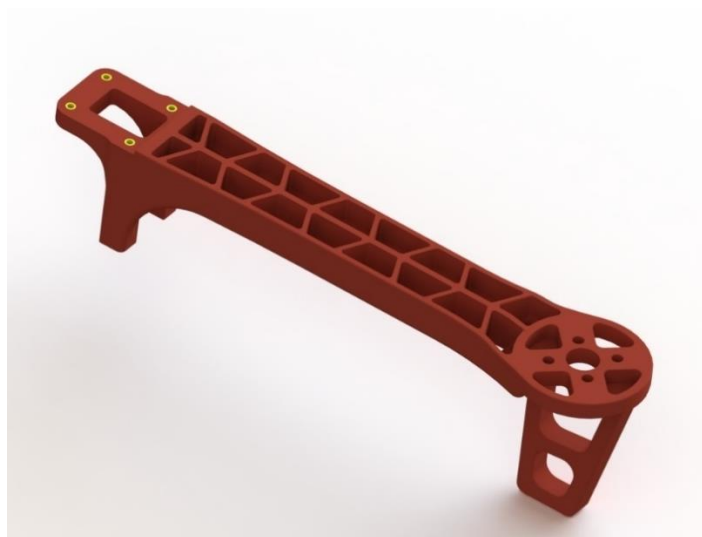


Figure 4.6 Frame arm Solidworks modelling

4.6.2 Motor (2.3.2)

The motor shell is made of aluminium alloy material to reduce the weight and inside the shell placed the windings and bearings to hold the rotation. Sealed bearings are clamped using a C clamp outside the shell. As it is a brushless motor, maintenance is less included with weight of 53grams and the total weight of all four motors will be 212grams. The overall dimensions of motor are shown in Figure 4.7. Two motors rotate in clockwise motion and the other two motors

rotate in anti-clockwise motion, this difference in motion create thrust which is required to lift the quadrotor and to move in its required path.

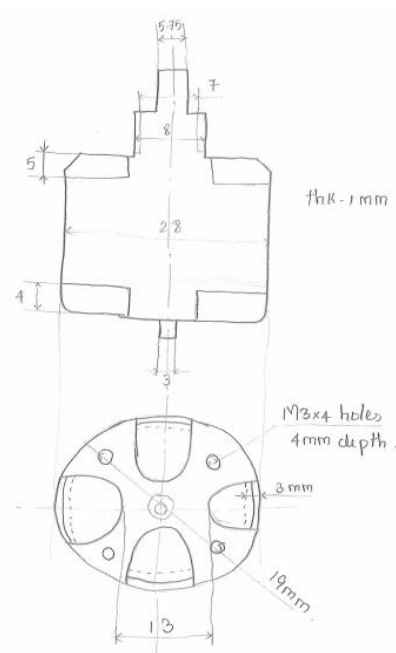


Figure 4.7 Dji Flame wheel F450 Motor (13)



Figure 4.8 Motor model for quadrotor

4.6.3 Propeller (2.3.3)

The type of propeller used for our model is self-locking propeller 9443 made of plastic. The weight of propeller is 9gms approximately, and the overall diameter of the propeller is 242mm (0.242m). The dimensions of the propeller are difficult to measure using normal hands, hence the propeller is scanned completely in all the directions. Also the angles in the propeller vary with the model of the propeller as shown in Figure 4.9. The scanned files are transferred to scan converter software and they are combined to a single part using Solidworks. Normally in quadrotors as mentioned earlier two wings rotate in one direction and other two in opposite direction, so the propellers also manufactured accordingly. Scanning process is done for both

clockwise and anti-clockwise prop in co-ordination with their respective motors. A view of DJI Flame wheel 450 anti-clockwise propeller is shown in Figure 4.9.



Figure 4.9 Propeller modelling (13)

4.6.4 Frame plates (2.3.4)

The thickness of the frame plates is around 1.5mm and the weight is approximately 40gms. The Power distributing board is PCB (Printed circuit board) which is useful in flow of current and soldering. Overall dimensions of the plates are measured for reference as shown in Figure 4.10.

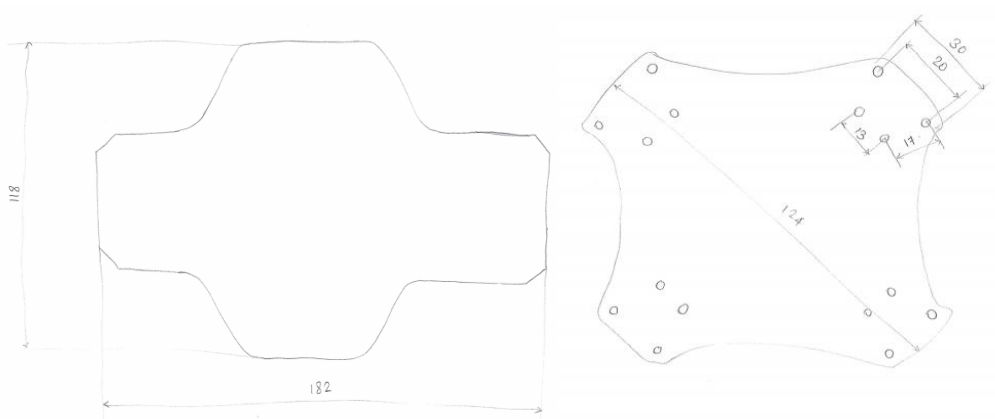


Figure 4.10 DJI Flame wheel F450 Frame plates (13)

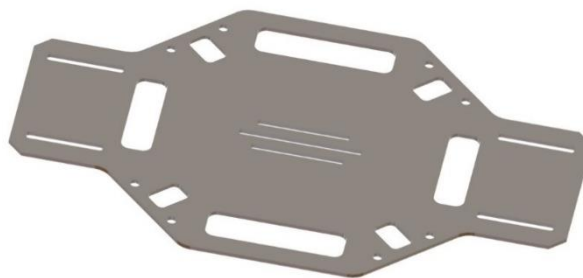


Figure 4.11 Power distributing board 1 solid modelling



Figure 4.12 Power distributing board 2 solid modelling

4.6.5 Damping Legs (Landing gears)

Damping legs are separately mountable parts of a quadrotor, this part allows the quad for smooth landing, accordingly the legs are designed to absorb the shock of 4 kgs or even when the quad dropped from a height of 15m. Material used for these legs is plastic reinforced with fiber glass G10/G11, with less weight and great damping property. The product is perfectly designed to maintain a smooth landing, with some openings in the middle of the legs to increase the flexi property as shown in Figure 4.13.



Figure 4.13 Damping leg modelling (13)

Chapter 5. Research of basic Quadrotor structure

In this chapter reference geometry and basic thrust calculation is defined. This chapter also defines motor position and its direction of rotation with some simulation results of open rotor system at different speed levels. The last part of this chapter is modelling assembly of open quad with final thrust developed by the model.

5.1 Speed and Power Calculation

Speed calculation is the first step to find out the thrust which can be developed from the motor. Power transmitted by the motors to the propellers are calculated in terms of RPM (Revolutions per minute) and this power is based on the propeller constants and power factor for the propellers that are used to create thrust (28).

$$\text{Power} = \text{Propeller constant} * \text{rpm}^{\text{power factor}} \quad (5.1)$$

For the purpose of calculation, we approximate from the datasheet of aircraft technology based on our propeller size 10x3.8 inch and choose APC Slow fly series propellers (28).

$$\text{Propeller Constant} - 0.136$$

$$\text{Power factor} - 3.40$$

Dimensions of the DJI 2212/920 Kv motor 2.3.2 and battery discharge is also used for calculating power and some of its specifications (Table 5.1).

Rating	920 Kv
Battery	3s, 4s
Voltage per cell	3.7 v
Standard current	15 – 25 A
Max current	30 A
RPM motor can run in no-load condition	Kv (RPM per volt) = 920

Table 5.1 Dimensions of motor and battery (13)

In our testing we use 3s battery with 3.7v and under no-load condition the rpm is measured as

$$\begin{aligned} 3s &= 3.7 * 3 = 11.1 v \\ &= 920 * 11.1 = 10212 rpm \end{aligned}$$

As we know that under continuous rating the motor will be running 75% approximately of it's no load rpm

$$3s = 10212 * 0.75 = 7659 rpm$$

This loaded speed is inserted in equation (5.1) (29).

$$\text{Power} = 0.136 * 7.659^{3.4} = 137.950W \quad (5.2)$$

5.2 Theoretical Thrust Calculation

Thrust calculation is determined using Momentum theory, which is also known as disk actuator theory is a theory describing a mathematical model of an ideal actuator disk such as propeller or helicopter rotor, by W.J.M Rankine (1865), Alfred George Greenhill (1888) and R.E. Froude (1889) (30).

In the theory the propeller is considered as a thin disc rotating at some constant velocity in its axis of rotation. In this condition the propeller creates a flow around, which is given in mathematical terms between power, radius of rotor, torque and induced velocity. This hovering condition does not experience energy losses due to frictional drag (31).

Basic thrust equation

$$T = A * \rho * \omega * \gamma \quad (5.3)$$

T – Thrust (N),

A – Area of propeller rotor,

D – Propeller diameter (m),

ω – Velocity of air at the propeller (m/s),

γ – Velocity of air accelerated by propeller (m/s),

ρ – Density of air (1.225 Kg/m³).

From the above equation we can calculate the thrust approximately, and we can consider the full power of the motor without losses as shown in Figure 5.1.

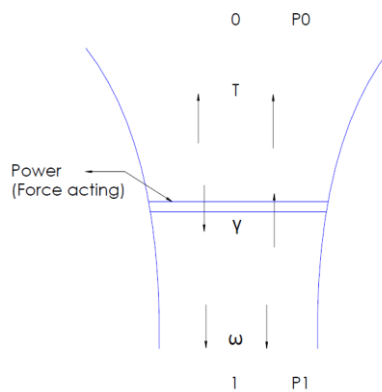


Figure 5.1 Propeller air flow

In the flow diagram shown P0 and P1 are the pressure difference of air flow before and after propeller. We can derive the mass flow and rate of change of flow as shown below,

$$\text{Mass flow rate } \dot{m} = \rho * A * \gamma \quad (5.4)$$

$$\text{Momentum conservation } T = \dot{m} * \omega \quad (5.5)$$

(Rate of change of momentum)

The change in kinetic energy is given by,

$$\text{Change in Kinetic energy / sec} = \frac{1}{2} * \dot{m} * \omega^2 \quad (5.6)$$

Substituting equation (5.4) in terms of mass flow in equation (5.6) to calculate energy conservation,

$$\text{Energy conservation } T * \gamma = \frac{1}{2} * \rho * A * \gamma * \omega^2 \quad (5.7)$$

The energy conservation is considered when there is no loss. In the equation (5.7) power is considered as a product of force and velocity which is a common derivation.

Substituting equation (5.4) and (5.5) in equation (5.7)

$$\begin{aligned} \rho * A * \gamma * \omega * \gamma &= \frac{1}{2} * \rho * A * \gamma * \omega^2 \\ \omega &= 2 * \gamma \end{aligned} \quad (5.8)$$

Substitute equation (5.8) in equation (5.5) to equate thrust in terms of velocity,

Therefore *Thrust* $T = \rho * A * \gamma * 2 * \gamma$

$$\text{Thrust } T = 2 * \rho * A * \gamma^2 \quad (5.9)$$

From the Figure 5.1 we know that area is the function of rotor diameter, so we substitute for area which is $A = \frac{\pi}{4} D^2$ (31).

$$\begin{aligned} T &= 2 * \rho * \frac{\pi}{4} * D^2 * \gamma^2 \\ T &= \rho * \frac{\pi}{2} * D^2 * \gamma^2 \end{aligned} \quad (5.10)$$

From the equation (5.7) we know that power is the product of force and velocity (in our case thrust is given in force exerted) which can be also derived in terms of velocity $\gamma = \frac{P}{T}$ to use in equation (5.10).

$$\begin{aligned} T &= \rho * \frac{\pi}{2} * D^2 * \frac{P^2}{T^2} \\ T^3 &= \rho * \frac{\pi}{2} * D^2 * P^2 \\ T &= \left(\rho * \frac{\pi}{2} * D^2 * P^2 \right)^{\frac{1}{3}} \end{aligned} \quad (5.11)$$

For our designed quad the thrust force approximately can be calculated from the above equation and the result from this momentum theory will be the maximum thrust without frictional losses,

Diameter of the propeller $D = 242\text{mm}$ (0.242m),

Density of air $\rho = 1.225 \text{ Kg/m}^3$,

Power of the motor transmitted to propeller P (equation(5.2)) = 137.950 W,

$$T = \left(\frac{\pi}{2} * 0.242^2 * 1.225 * 137.950^2 \right)^{\frac{1}{3}}$$

Thrust $T \approx 12.895 \text{ N}$

Therefore, the thrust calculated is for one rotor, and as we know four rotor thrust will be approximately equal to **51 N**.

5.3 Open rotor test results

In this phase we can read about some manual tests on the open quadrotor and actual thrust difference between theoretical calculation and actual manual tests. This can be also tested using software and the results can also be predicted which will be shown in this report later,

For testing we use Pulse Width Modulation (PWM) to calculate the transmission partly, instead of rpm tachometer. PWM or PDM (Pulse-duration modulation) is a modulation technique used to encode a message into a pulsing signal. Although this modulation technique can be used to encode information for transmission, its main use is to allow the control of the power supplied to electrical devices. The average value of voltage and current fed to the load is controlled by turning the switch between supply and load on and off at a fast rate (32).

As mentioned above PWM senses the voltage with very low power loss in the switching devices. There is practically no current when the switch is turned OFF and when the switch is turned ON, the current is directly transmitted to the load without power-loss or voltage drop. An example of how PWM work is shown in Figure 5.2, in which the blue indicator shows the voltage source as a series of pulses, which results in sine-like current in the red indicator.

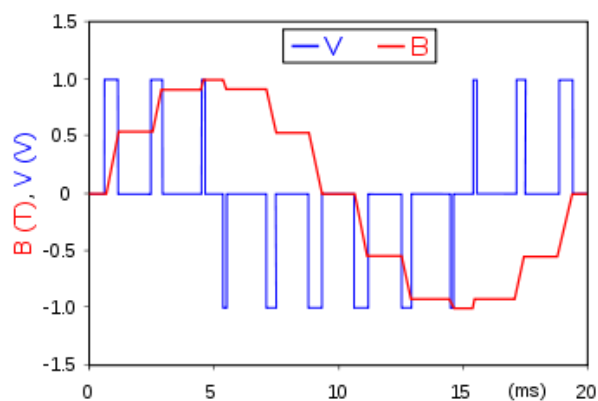


Figure 5.2 PWM example (PWM Wikipedia search)

The PWM is controlled using specially designed software by my co-ordinator and the motor speed is controlled. The experimental equipment for open quadrotor consisted of some primary components:

- I. Quadrotor motion parts (Propeller & motor),
- II. Battery and ESC controller,
- III. PWM setup software and converter equipment,
- IV. Thrust stand,

Procedures to conduct the test and the details regarding the test equipment is explained in Appendix A. Initially the speed control is started from 1100 PWM as per the setup, and the speed is gradually increased until the motor reaches its maximum speed limit and at this point the maximum PWM is 2000. The thrust values are noted down in kilograms and converted to Newton's after approximating through gravity. The thrust values are then calculated to make the setup symmetric, because we have difference in length of thrust stand (Explained properly in the Appendix A). The final thrust value received at highest power and speed is the maximum achieved thrust, which in our case is displayed in the Table 5.2.

The achieved thrust for a single rotor is then added with all other rotors, which is our net thrust for this kind of quadrotor.

S. No	PWM	Thrust		
		Mass (Kg)	Force (N)	Thrust (N) After model symmetricity (Appendix A.1)
1	1100	0	0	0
2	1200	0.0347	0.340407	0.26849
3	1250	0.0616	0.604296	0.476628
4	1300	0.092	0.90252	0.711847
5	1350	0.1215	1.191915	0.940102
6	1400	0.1554	1.524474	1.202402
7	1450	0.1955	1.917855	1.512674
8	1500	0.25	2.4525	1.934366
9	1550	0.3109	3.049929	2.405578
10	1600	0.3627	3.558087	2.806378
11	1650	0.4328	4.245768	3.348775
12	1700	0.5032	4.936392	3.893492
13	1750	0.581	5.69961	4.495467
14	1800	0.6523	6.399063	5.047148
15	1850	0.7462	7.320222	5.773696
16	1900	0.836	8.20116	6.468521
17	1950	0.842	8.26002	6.514945
18	2000	0.845	8.28945	6.538158

Table 5.2 Manual test results for thrust

These test results are plotted in graph (Figure 5.3) to show the increase in thrust in accordance to the PWM rating, which shows that the maximum thrust which can be achieved by a single rotor is **T = 6.538158N**,

For the four rotor the net thrust which can be achieved is approximately

$$T = 4 * 6.538158 = \mathbf{26.1526 N}$$

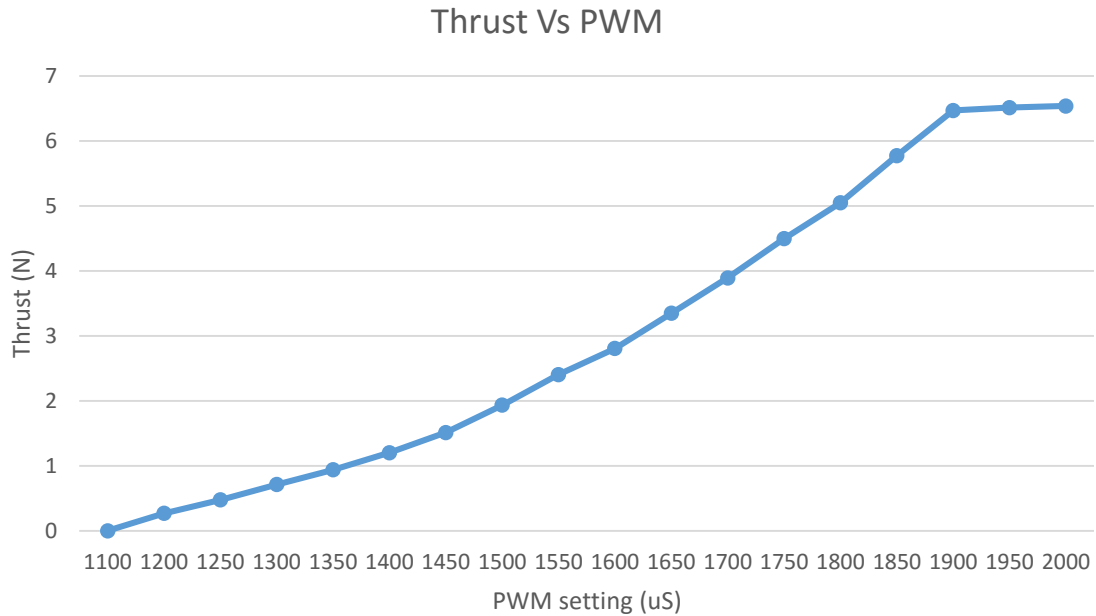


Figure 5.3 PWM Vs thrust increase for open rotor

5.4 Modelling of Existing Open Quadrotor

Designing of open quadrotor is modelled in Solidworks, using assembly view, where all the separate components (motor, frame, etc.) are combined together to form a full model as shown in (Figure 5.4). Special screws are used as fasteners to mate the parts in modelling. All the parts are mated exactly as in actual quad, to structure the critical portions.



Figure 5.4 Open quadrotor modelling

5.5 Flow simulation of Open Quadrotor for Thrust

The model developed is checked for its thrust values to compare the manual tests Vs software results. To continue with the simulation, the following are the important data's,

- I. Direction of rotation: Clockwise,
- II. Force applied towards gravity,
- III. Rotational speed of Propeller ω : 7659 RPM,
- IV. Air density ρ : 1.225 Kg/m³,
- V. Diameter of propeller D: 0.242m.

These data are plugged in the flow simulation software using Solidworks, for our simulation we consider one rotor propeller as in test results 5.3 to compare the results. From the Figure 5.5, we can see the velocity profile over the propeller, the low pressure area is shown in the blue colour above the propellers allows to lift the system. As discussed the loss of thrust in the form of vortex and noise is created in the sides of the propeller, shown in red colour in the sides.

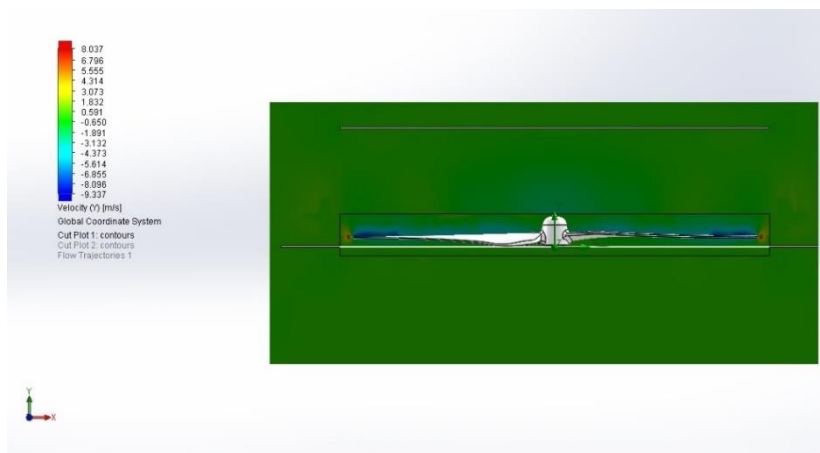


Figure 5.5 Open rotor velocity flow section

The flow of air due to propeller in actual quadrotors and the thrust achieved due to it is shown in the below Figure 5.6. The force in the Y direction is considered as the thrust force.

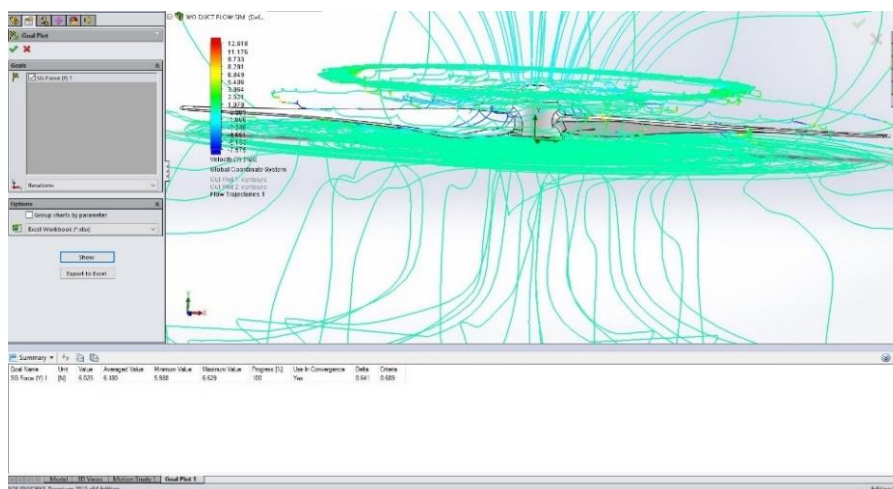


Figure 5.6 Flow condition and thrust force data

Table 5.3 is a summary of the recorded data used to access the performance of the open rotor,

Name	Unit	Value	Progress	Use in convergence
SG Force (Y) or Thrust	N	6.025	100%	Yes

Table 5.3 Momentum theory parameters using flow simulation

5.6 Research results

By comparing the manual, test and simulation calculations, a quadrotor thrust is fixed, from which our next design process will be carried out. In order to improve the values, these results are compared using a chart as shown in Figure 5.7.

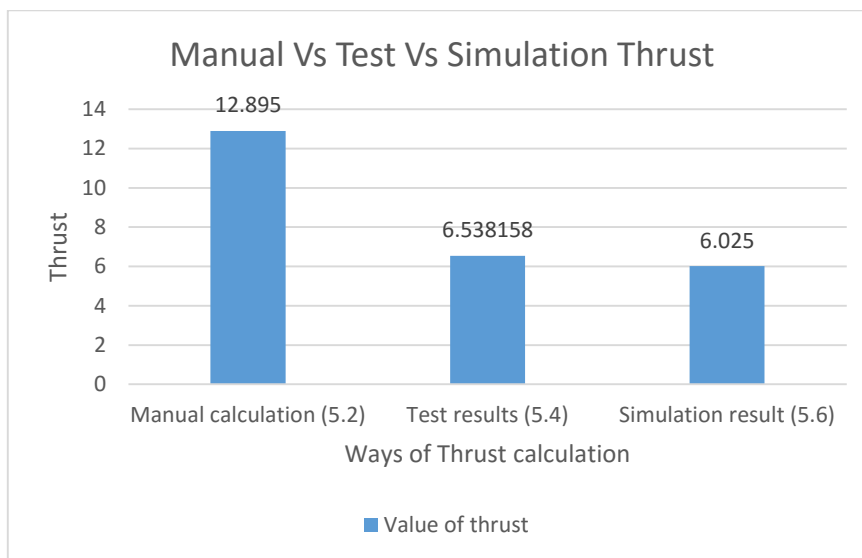


Figure 5.7 Comparison of different results for an open quad

Thrust from the manual calculation shows approximately the maximum thrust that the motor can develop at its maximum power, which shows that the test and simulation results are similar to the exact result while the quadrotor in action. To improve the thrust value even when load is included and to improve the aerodynamics design of quadrotor, duct is additionally added to the open propeller. These research results are formulated in QFD approach and House of Quality is created to correlate the customer needs and available resources.

Chapter 6. House of Quality

6.1 Introduction

A house of quality matrix is a diagram, which is a part of QFD and utilizes a planning matrix to relate what the customer wants and how our product is meeting the requirements. According to the Table 6.1 shown below, it looks like a house with a “correlation matrix” as its roof, “technical requirements” below the roof, “customer requirements” in the left side, “customer wants vs technical requirements vs product features” in the middle, “competitor’s evaluation” in the right side” and “target values” at the bottom.

Correlation		Relationships		Direction of Improvement									Customer Competitive Assessment						
+	Important Correlation	●	Strong (9)										Direction of Improvement ▼ Minimize ▲ Maximize						
-	Less correlation	○	Moderate (3)																
	No Correlation	△	Weak (1)																
Row S.No	Importance out of 5 in %	Cust. requirement importance	Maximum relationship	Customer Requirements	Weight	Shape of the duct	Assembly feasibility	Temperature	Overall dimensions	Durability	Life	Cost of production	Power usage	Our Product	Competitor 1: Hubsan X4 cover	Competitor 2: Lookatel JJRC cover	Competitor 3: UDI/U830 RC cover	Competitor 4: Custom made cover	Comparison with competitors
1	16	4	5	Minimal mass	●	○	△		●	○		○	●	2	3	4	3	2	
2	20	5	5	Improved thrust	●	●		●	●				●	5	2	2	2	4	
3	16	4	5	Physical protection for rotors	△	●	○		○	●	○			5	1	1	2	4	
4	8	2	5	Added strength	●	○	○		○	●	○	○		3	1	1	2	3	
5	4	1	5	Minimal vibrations	△	○	●	△	△	△	○		△	3	3	4	3	2	
6	8	2	5	Usage in cold climate		○		○					○	3	1	1	2	2	
7	4	1	5	Aesthetics		●							○	2	3	4	3	1	
8	12	3	5	Easy service and maintenance	△	●	●		○		○			3	3	4	2	2	
9	12	3	5	Safety	○	●	○	○		○				5	1	2	3	4	
				Target Functions	Requirement 1	Requirement 2	Requirement 3	Requirement 4	Requirement 5	Requirement 6	Requirement 7	Requirement 8	Requirement 9						
				Maximum relationship	9	9	9	9	9	9	9	9	9	9					
				Technical importance rating	464	684	268	244	436	304	120	84	376						
				Relative weight in %	16	23	9	8	15	10	4	2	13						
				Our Product	3	5	3	3	4	5	5	2	3						
				Competitor 1: Hubsan X4 cover	4	0	0	4	0	3	2	4	3						
				Competitor 2: Lookatel JJRC cover	4	0	0	3	0	3	3	4	3						
				Competitor 3: UDI/U830 RC cover	3	0	0	3	0	2	3	4	3						
				Competitor 4: Custom made cover	3	4	3	4	4	4	3	2	3						
				Technical Comparison with competitors															
				Column S.No	1	2	3	4	5	6	7	8	9						

Table 6.1 House of Quality

6.2 Importance of this Design

From the result of open rotor and house of quality it can be proved that the design of ducted system should be calculated as a better output when compared to open rotor. As discussed in the marketing section the different products available in the market is compared to our products

importance and evaluated to its best. The table also shows the different technical characteristics that our product should contain, also showing more importance on the duct shape which affects the air flow.

Shape of the duct has strong correlation with the weight of the duct, i.e., when the thickness is increased to improve the strength it will affect the performance of the duct. The current strengths and weakness of the duct is compared with the competitors and as per the table there is no competitors who are manufacturing ducts for a specific purpose. But some researchers as mentioned are manufacturing ducts for their specific purpose to enhance the design of quad.

In our product quality function deployment is an extremely useful methodology to facilitate the communication, planning and decision-making of quadrotor. This will give next milestone in our product closer to the intended target, and importance of duct in our quad. In the next section we can have a brief description of the product features and duct concepts.

Chapter 7. Ducted Principle

The ducted rotor configuration has emerged as the most popular choice for quadrotors, because of inherently safety of the design and the potential for significant performance improvements. In this configuration, the rotor is surrounded by basic form of a cylindrical duct or shroud, which resembles an annular airfoil or ‘ring-wing’, with camber (angle) and finite thickness that vary along its length, and with a rounded ‘leading edge’ and smoothly ‘trailing’ edge which form, respectively, the inlet and exit or diffuser sections of the duct Figure 7.1. This investigation on ducted rotor configuration is carried out over half a century and found to result in significant gains in aerodynamic performance compared to open rotor.

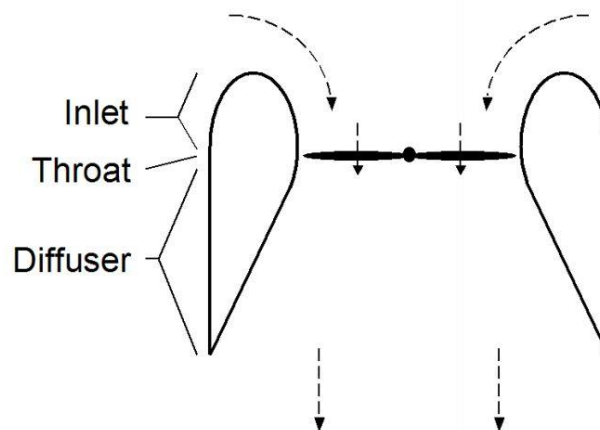


Figure 7.1 Cross section of ducted rotor

For a duct with a profile that is angled inwards, like that shown in Figure 7.1 and which accelerates the flow towards the rotor, the performance gain is principally in static and near static conditions. Also there is some benefits when the quad is moving forward or backward in high speed as well. Other than performance increase ducted rotor encounter also advantages like

- I. The duct can potentially reduce the noise signature of rotor, which is an advantage for military purpose,
- II. The duct serves as safety feature.

The performance benefit of ducting the rotor derives principally from the ability of the diffuser section of the duct to restrain the natural contraction of the flow after it passes through the rotor. For any fluid dynamics propulsive device, the increase in velocity of the exit over the free stream velocity of air is great in the generation of thrust. Also this include in the additional losses of the fluid due to turbulence.

7.1 Construction of Ducted rotor

In this case of ducted rotor, the change in area of the air or the slipstream outside the duct is determined by the shape of the diffuser. The slipstream can be forced to either maintain a constant cross-sectional area or to actually increase in area by using a cylindrical diffuser. So by doing in this way the air which moves out the diffuser increases in pressure and reducing

the power requirements for operations. Just as open rotor, momentum theory can be used for the first-order prediction of the performance but the only difference is the slip stream has expanded back to normal atmospheric pressure at exit plane.

As shown in Figure 7.2 the very important parameter in determining the performance of a shrouded rotor is diffuser expansion ratio (σ_d), which is equal to the ratio of the diffuser exit plane area (A_e) to the area of the rotor disk (A), In the Figure 7.2 D_t is the Diameter of the duct.

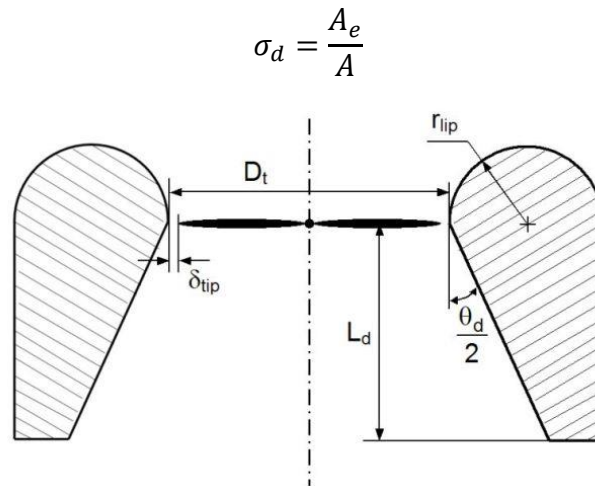


Figure 7.2 Ducted rotor parameters

In case of an open rotor, $T_{rotor} = T_{total}$, which exactly predicts the value of the ‘expansion’ that momentum theory predicts for an open rotor. But in case of ducted rotor the total thrust is $T_{total} = T_{rotor} + T_{duct}$, so from this to predict the exact condition where the thrust increases depends on the duct. These thrust fractions are functions of the expansion ratio only, and are independent of the precise shape of the duct, and that as σ_d is increased, the rotor’s contribution to the total thrust decreases, while the duct contribution increases. The duct contribution will be $T_{duct} = T_{inlet} + T_{diffuser}$.

In a duct the parameters which affect the rotor performance are,

7.1.1 Diffuser Included Angle (Θ_d)

Although more calculations are made on diffuser angles, still flow characteristics are not fully understood. The uniformity of flow in a wind tunnel can be greatly improved if an expansion section is maintained perfectly as shown in Figure 7.2. Efficient designing of the diffuser angle will greatly affect the flow separation or reverse flow, and it is defined as the natural movement of the air in a diffusion process is to break away from the walls of the diverging passage, reverse its direction and flow back in the direction of the pressure gradient (33). The angle of the diffuser greatly depends on different test results and based on the height, and in our case there are assumptions made on the diffuser angles which is shown below in 7.3.

7.1.2 Diffuser Length (L_d)

Diffuser length shows greatly the effect of the air flow without any pressure loss and the length will be at least equal to 30% of the diameter of the duct. Improvements in thrust or decrease in power consumption is determined by this length. Studies on length shows that when the length

increases the power consumption increases in reasonable way. As mentioned earlier this value also depends on test results. The additional thrust developed from the rotor is injected around the sides of the duct along its length.

This flow around an airfoil experiences a pressure recovery in the tail of diffuser and the air pressure expands again to its ambient atmospheric pressure. In some cases, the inner surface of the diffuser experiences suction pressure and generates a negative thrust. However, the positive thrust from the inlet is always large enough that the net duct thrust remains positive (34).

7.1.3 Blade Tip Clearance (δ_{tip})

Tip clearance depends on the expansion ratio of the duct, which effects greatly the performance of the duct. As shown in Figure 7.3 when the quad in motion low pressure area is created on the top of rotor and the high pressure is flowing under the surface of rotor tries to move upwards along the sides of the propeller which creates vortex in sides. So due to this vortex loss in energy occurs in term of noise and heat, hence the efficiency of duct depends dramatically on this distance.

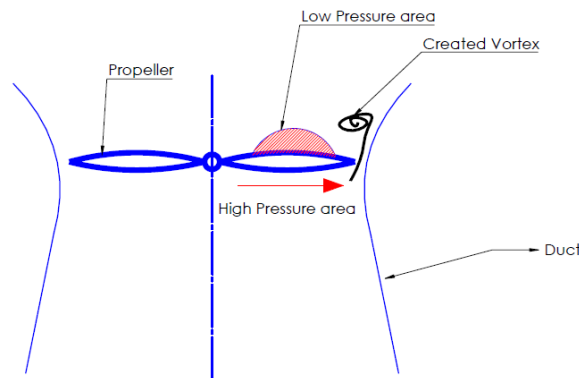


Figure 7.3 Blade tip clearance

Lower the distance, lesser the creation of vortex and the energy wasted is utilised to transform as lift and thrust development.

7.2 Duct comparison

Initially to test these parameters, comparisons is done between two kinds of ducts, i.e., duct with positive diffuser angle and duct with negative diffuser angle. The benefits of this comparison will provide the flow of this report to proceed further. In this comparison we use flow 3D simulation to check the pressure force and amount of shear force which increases or decreases the pressure lift.

The models are created considering the diameter of the propeller and is modelled in simple sketch, without forming the thickness. The geometry and the meshing details are explained in Appendix B.1. As we can see from the Figure 7.4 the angle of the duct convergence is negative and if the propeller is rotating at high speed, it will not achieve its optimum expansion ratio to increase the thrust.

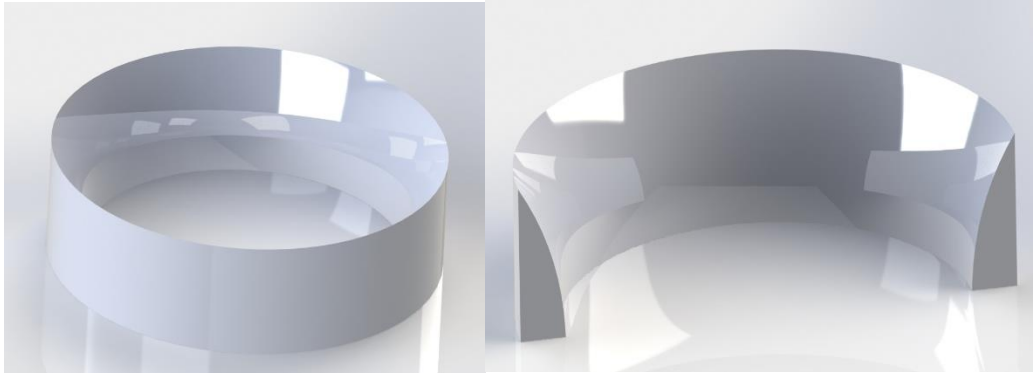


Figure 7.4 Negative draft angle modelling

The preliminary model is loaded in Flow-3D software with the help of one of my supervisor, then the final results of the negative angled duct is achieved which shows that the velocity magnitude after the propeller area is high and hence rather than reducing the velocity after the flow it increases in that converging area, which has no use with the thrust improvement. The maximum values are shown in red coloured area in Figure 7.5.

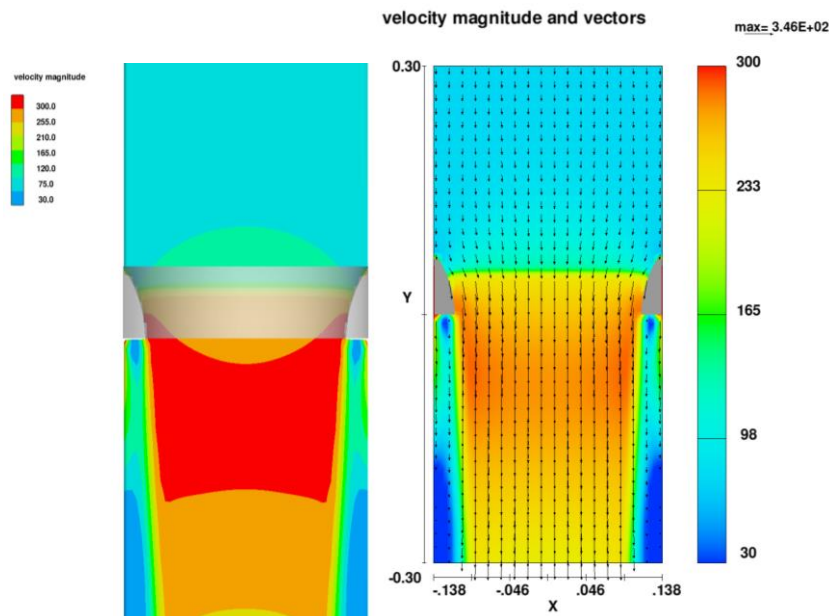


Figure 7.5 Duct with Negative diffuser angle

The next examination is on the positive angled duct (Figure 7.6). The angle used after the converging section of the duct is approximated from the market research, and we believed that it will make a significant difference in the performance of duct. The resistant force developed is the thrust force to lift the quad. The modelled positive angled duct is then loaded to the software.

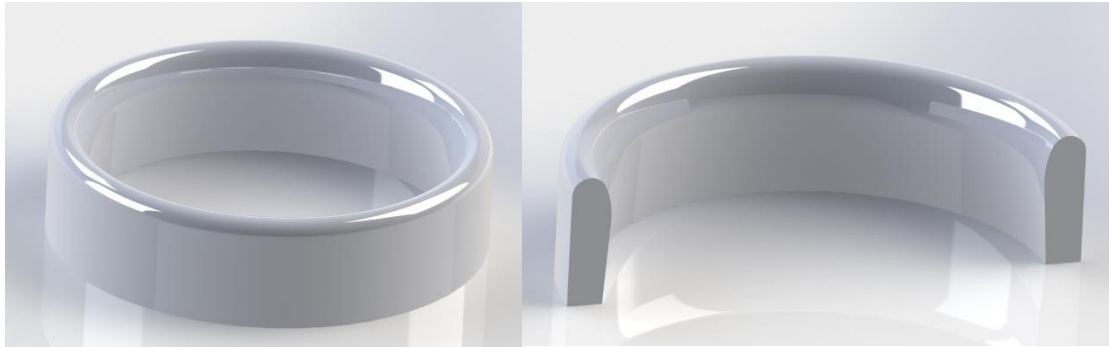


Figure 7.6 Positive angle duct modelling

The velocity magnitude is less as expected, although the tip clearance of the rotor is more, there is still expected to be a strong influence from the angle of the duct wall, which is what is seen when the velocity field on the duct examined in Figure 7.7.

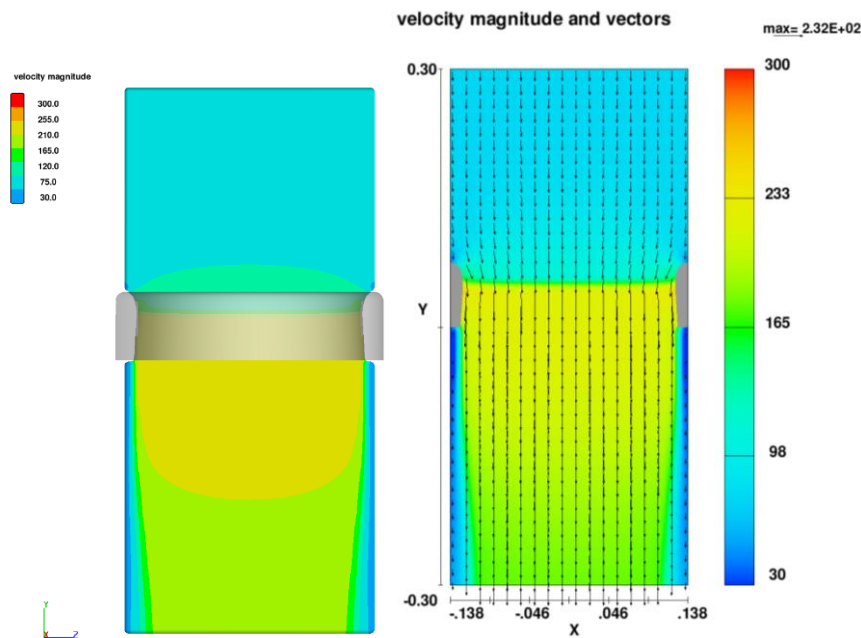


Figure 7.7 Duct with positive diffuser angle

The effects of the different diffuser angles indicating the increase in velocity profiles in the contracted area is 232 m/s and 346 m/s respectively for positive and negative angles. Also the pressure and shear force in Y direction is,

- I. Duct with positive diffuser angle
Y Pressure force = 617.9N
Y shear force = 6.0N
- II. Duct with negative diffuser angle
Y Pressure force = 820.5N
Y shear force = 29.8N

The pressure and shear forces acts on the contraction surface of the ducts to achieve maximum thrust, but in case of negative angle the shear forces act to reduce the pressure and increase the velocity. This cause the improvement of turbulence and vortex creation at the sides which is

clearly shown in figures, this is the reason the jet engines are always designed with positive angles.

Also reducing the diffuser angle to 0° causes a deterioration in performance, while increasing it to more positive causes an even greater deterioration. The same conclusions can be drawn from the variations seen along the length of the diffuser. Prior to design the duct proper assumptions should be made to reduce this pressure deviations and velocity vortex.

7.3 Simplifying Assumptions

Two simplifying assumptions were made prior to performing the analysis are presented in this chapter.

- I. The first was that the values of the various quantities did not vary significantly between the tested rotational speeds of 0 – 8220 rpm, and that the values used in the analysis comparing the various duct-rotor models could therefore be those obtained by averaging all the measurements made at all rotational speeds within this range.
- II. The second assumption was the measurements on the blade tip distance, diffuser duct length and angle to make the simulation more realistic and to compare the results with the actual test results.

$$\delta_{tip} = 0.1\% D_t$$

$$\gamma_{lip} = 13\% D_t$$

$$\theta_d = 7^\circ/2$$

$$L_d = 30\% \text{ to } 50\% D_t \text{ (Depending on the results)}$$

These assumptions are made to reduce the simulation work and reduction of cost in terms of 3D printing.

7.4 Theoretical Derivations for Ducted rotor

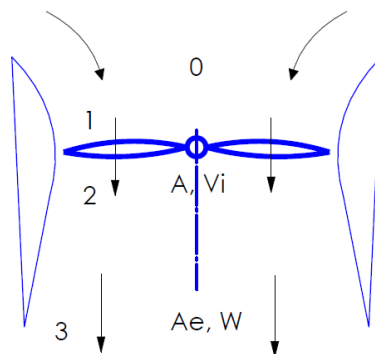


Figure 7.8 Ducted rotor flow conditions (35)

In this section, the general performance characteristics of the ducted rotor are discussed, followed by the thrust improvements in tested conditions are presented. The calculations of the thrust are based on the momentum theory for ducted rotor and logical assumption of $T_{total} = T_{rotor} + T_{duct}$ (35).

$$\text{Diffuser expansion ratio } \sigma_d = \frac{A_e}{A} \quad (7.1)$$

A_e = Diffuser exit area

A = Area of the rotor disc.

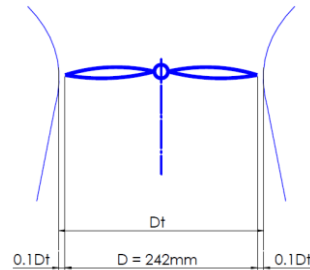


Figure 7.9 Assumption value

Assumptions I (7.3),

$$\delta_{tip} = 0.1\% D_t$$

$$D_t = 0.1\% D_t + D + 0.1\% D_t$$

From equation we know that Diameter of the rotor is 242mm (0.242m),

$$D_t = 0.2\% D_t + D$$

$$D = D_t - 0.2\% D_t$$

$$0.242 = 0.998 D_t$$

$$D_t = \frac{0.242}{0.998} = \mathbf{0.2424849m}$$

$$\delta_{tip} = 0.1\% * 0.24248$$

$$\delta_{tip} = \mathbf{0.000242m}$$

$$\text{Area of the rotor disc } A = \frac{\pi}{4} D^2 \quad (7.2)$$

$$A = \frac{\pi}{4} * 0.242^2 = 0.045996m$$

$$\text{Diffuser exit area } A_e = \frac{\pi}{4} D_t^2 \quad (7.3)$$

$$A_e = \frac{\pi}{4} * 0.2424849^2 = 0.0461805m$$

Substitute equation (7.2) and (7.3) in equation (7.1),

$$\sigma_d = \frac{0.0461805}{0.045996}$$

Diffuser expansion ratio $\sigma_d = \mathbf{1.004011}$

Assumptions II 7.3,

Lip radius $\gamma_{lip} = 13\%D_t$

$$\gamma_{lip} = \frac{13}{100} * 0.2424849$$

$$\gamma_{lip} = \mathbf{0.031523\ m}$$

Assumptions III 7.3,

$$\theta_d = 7^\circ/2$$

$$\theta_d = \mathbf{3.5^\circ}$$

Assumptions IV 7.3,

$$L_d = 40\% D_t$$

$$L_d = \frac{40}{100} * 0.2424849$$

$$L_d = \mathbf{0.096993\ m}$$

From Figure 7.8 the flow field of ducted rotor in the hovering – flight condition we can identify that the air is flowing in Y direction which is point 0 representing the free-stream. Point 1 and 2, respectively lie just above and below the plane of the rotor disc. Point 3 is at the exit plane of the ducted diffuser or far wake, infinitely downstream of rotor. The following identities and definitions therefore arise (35) & (36):

I. Velocities

$$v_0 = 0$$

$$v_1 = v_2 = v_i$$

$$v_3 = w$$

II. Areas:

$$A_1 = A_2 = A$$

$$A_3 = A_e = \sigma_d A$$

III. Pressures:

$$p_0 = p_3 = p_{atm}$$

$$\Delta p = p_2 - p_1$$

The development of ducted principle is as follows,

Conservation of Mass:

$$\dot{m} = \rho * A * v_i = \rho * A_e * w \quad (7.4)$$

$$w = \frac{v_i}{\sigma_d} \quad (7.5)$$

Conservation of Momentum:

$$T_{total} = \dot{m} * w = \rho * A * \frac{v_i^2}{\sigma_d} \quad (7.6)$$

$$v_i = \sqrt{\frac{\sigma_d * T_{total}}{\rho * A}} \quad (7.7)$$

Conservation of Energy:

$$P_i = \frac{1}{2} * \dot{m} * w^2 = \frac{1}{2} * \rho * A * \frac{v_i^3}{\sigma_d^2} \quad (7.8)$$

$$P_i = \frac{T_{total}^{3/2}}{\sqrt{4 * \sigma_d * \rho * A}} \quad (7.9)$$

The actuator – disc model of the rotor itself will be equal to the pressure difference to the area of the rotor,

$$T_{OR} = \Delta p * A \quad (7.10)$$

This is used to derive our thrust provided by the rotor alone:

$$T_{rotor} = \Delta p * A \text{ or } \frac{1}{2} * \rho * A * w^2 \quad (7.11)$$

$$\frac{T_{rotor}}{T_{total}} = \frac{\frac{1}{2} * \rho * A * w^2}{(\rho * A * v_i) * w} = \frac{1}{2 * \sigma_d} \quad (7.12)$$

The contribution of the total-ducted rotor thrust provided by the diffuser alone can be found by applying the conservation laws to a controlled volume consisting of the fluid within the diffuser only. The control volume is therefore bounded by diffuser walls, the rotor disc plane and the diffuser exit plane. Applying the momentum equation and summing the forces in the z-direction, where +z is an axial co-ordinate in the direction of the flow (opposite to the direction of the rotor)

$$\Sigma F_z = \Sigma v_z(\rho * \vec{A} * \vec{v}) \quad (7.13)$$

$$\begin{aligned} F_{diff} + (p_2 * A_2) - (p_3 * A_3) \\ = -(v_2 * \rho * A_2 * v_2) + (v_3 * \rho * A_3 * v_3) \end{aligned}$$

Where F_{diff} is the force exerted by the diffuser on the control volume,

$$F_{diff} + (p_2 * A) - (p_{atm} * \sigma_d * A) = -(\rho * A * v_i^2) + (\rho * \sigma_d * A * \frac{v_i^2}{\sigma_d^2})$$

$$F_{diff} = \rho * A * v_i^2 * \left(\frac{1}{\sigma_d} - 1\right) + A * (\sigma_d * p_{atm} - p_2) \quad (7.14)$$

Applying the Bernoulli equation (conservation of energy):

$$p_2 + \frac{1}{2} * \rho * v_2^2 = p_3 + \frac{1}{2} * \rho * v_3^2$$

$$= p_{atm} + \frac{1}{2} * \rho * \frac{v_i^2}{\sigma_d^2}$$

$$p_2 = p_{atm} + \frac{1}{2} * \rho * v_i^2 * \left(\frac{1}{\sigma_d^2} - 1\right) \quad (7.15)$$

Substituting equation (7.15) into equation (7.14) and simplifying, we obtain:

Note that $-F_{diff}$ is the force exerted by the control volume on the diffuser, in the +z direction. Therefore, the thrust (which is in the -z direction) on the diffuser due to control volume is equal to $-(-F_{diff})$. The net thrust on the diffuser is equal to the sum of the forces (in the -z direction) due to both the control volume and the external atmosphere. This latter quantity is equal to $-p_{atm} (A_3 - A_2) = -p_{atm} A (\sigma_d - 1)$. Adding this to F_{diff} from equation (7.15)

$$Net\ thrust\ on\ diffuser = T_{diff} = -\frac{\rho * A * v_i^2 (\sigma_d - 1)^2}{2\sigma_d^2} \quad (7.16)$$

Making use of equation (7.6), we obtain the final result:

$$\frac{T_{diffuser}}{T_{total}} = -\frac{(\sigma_d - 1)^2}{2 * \sigma_d} \quad (7.17)$$

Given expressions for the thrust fractions from the rotor (equation (7.12) and the diffuser (equation (7.17)), the thrust fraction from the inlet is directly obtained:

$$\frac{T_{inlet}}{T_{inlet}} = 1 - \frac{T_{rotor}}{T_{total}} - \frac{T_{diffuser}}{T_{total}}$$

$$= \frac{\sigma_d}{2} \quad (7.18)$$

From equation (7.12), the thrust sharing between the duct and the rotor is:

$$\frac{T_{duct}}{T_{rotor}} = \frac{1 - \frac{1}{2\sigma_d}}{\frac{1}{2\sigma_d}} = (2\sigma_d - 1) \quad (7.19)$$

Which shows that as the expansion ratio is increased, the duct increasingly offloads the rotor.

Chapter 8. Developing Duct Concepts

The efficiency of a ducted rotor is determined straight forward by the application of the momentum theory, discussed in section 7.4.

However, the thrust may also be nonstationary depending on the design. This section investigates the different concepts of a duct development and various different factors which influences the design activities. The assumptions used in the section 7.3 will be taken for the development phases and also the structural stiffness based on drop test and impact tests carried out in Solidworks will be considered. Therefore, the generality of the discussion is not restricted by the consideration of thrust and air flow ratio.

In practice, the integrated duct for a quadrotor can be not successful due to:

- I. The purpose of the design improvement on quadrotor depends on our customer; basic purpose of our design is research based on thrust improvement. So, only models are developed for testing and not as mass production.
- II. Changes in the existing quadrotor Flame wheel F450 is not incorporated over long-term.

To address the design, all the assumptions should be used and if there is a difference in dimensions the thrust and lift of quad will be significantly changed. If there is no difference the practical tests will achieve the exact results according to the hand theory excluding the losses due to weight and air resistance.

By means of manual testing it has been investigated if there is a difference between the thrust production with the tests and software results. The results are given in this section and the best product is chosen using quality function deployment method. Overview of the best concept is described in the next section.

8.1 Characteristics of Concepts

In this characteristics of concepts, we will discuss about the main features in duct which are made constant without changing in dimensions as discussed in 7.1. The basic structure of the duct is in the form of a nozzle, which contracts and expands to atmospheric pressure. As calculated earlier the common dimensions of the developed concepts are given in Table 8.1 Dimensions of Duct and also shown in Figure 8.1.

S. No	Details	Dimensions
1	Diameter of the Propeller D	0.242m
2	Distance between propeller and duct $\delta_{tip} = 0.1\% D_t$	0.000242m
3	Inner Diameter of the duct D_t	0.242484m
4	Length of the Diffuser $L_d = 40\% D_t$	0.096993m
5	Angle of the Diffuser $\theta_d = 7^\circ/2$	3.5°
6	Lip radius $\gamma_{lip} = 13\% D_t$	0.031523m
7	Thickness of the duct T	0.0012m

Table 8.1 Dimensions of Duct

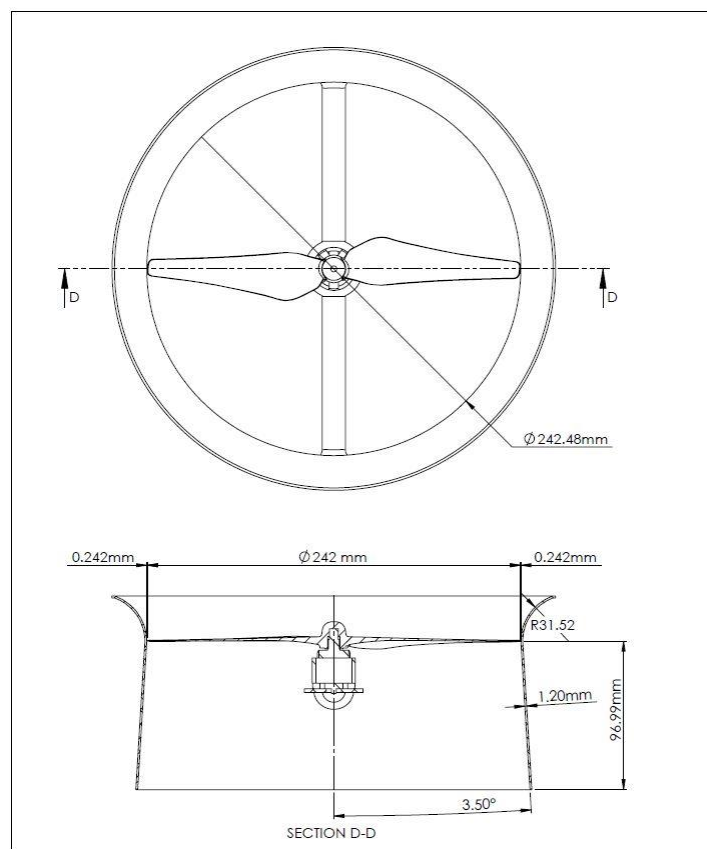


Figure 8.1 Main characteristics of duct

As shown in Figure 8.1 the distance between the propeller and duct is maintained, so that the vortex created is reduced. In the figure the basic dimensions are maintained same for all concepts and so that the design is only created on the connection areas to the frame. This is because the flow area is the important part of the thrust development. Various models and different cross sections are developed for connection areas where the air flow passes to make the air flow as smooth to avoid turbulent and maintain the pressure.

8.2 Rectangular concept of connection

In this connection the cross-section of the duct to motor cross is rectangular, as shown in Figure 8.2 all the mating parts with the duct and to the motor is rounded. This concept is basically developed to increase the strength of the duct; in this kind of duct no extra brackets are needed to improve strength. The cross section of the system is 10*40*1.5mm, so the weight of the system increases to 50gms extra, and about 5% of the thrust loss occurs. As the flow area is obstructed by the flat region, turbulence occurs and the pressure decreases and velocity increases, which is also important factor to be considered.

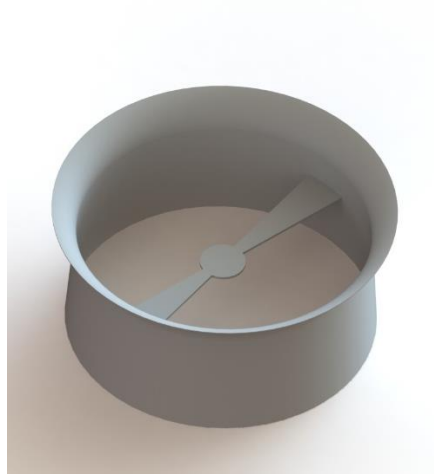


Figure 8.2 Rectangular concept of connection

From the Figure 8.3 we can see that the flow is towards the ground which is in $-Y$ direction, the air flow through the duct inlet and crosses the contraction in σ_d region with increase in pressure and expands in the diffuser area to normal atmospheric pressure. The flow is being pressurised by the propeller when rotating at high speed. The flow is distributed in the analysis flow simulation and the results are extracted to improve the duct for further process.

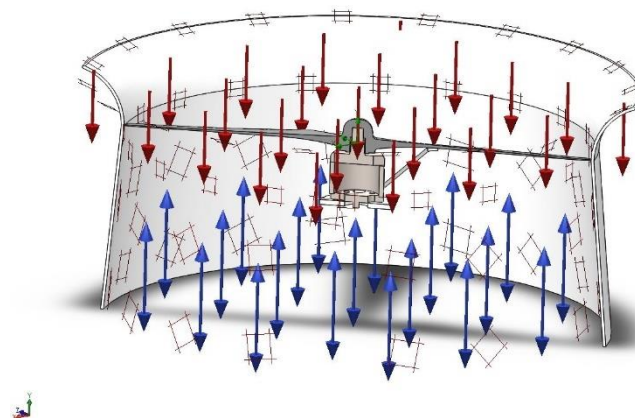


Figure 8.3 Velocity flow definition through Duct Inlet

8.2.1 Simulation of Concept I

Three dimensional, viscous, compressible flow simulation were conducted on the rotor/duct configuration, provided by the Table 8.1, so this case could be compared to the other concepts. For the initial simulations, only one duct is used to check the thrust confirmation and the hub is also simplified as shown in Figure 8.4. The goal of the simulations is to gain an understanding of the overall flow and disturbances before exploring how additional features, such as above openings and frame, will impact the flow. It is also important to note that the rotor used for the experimental purpose was not originally designed to be used in a ducted rotor.

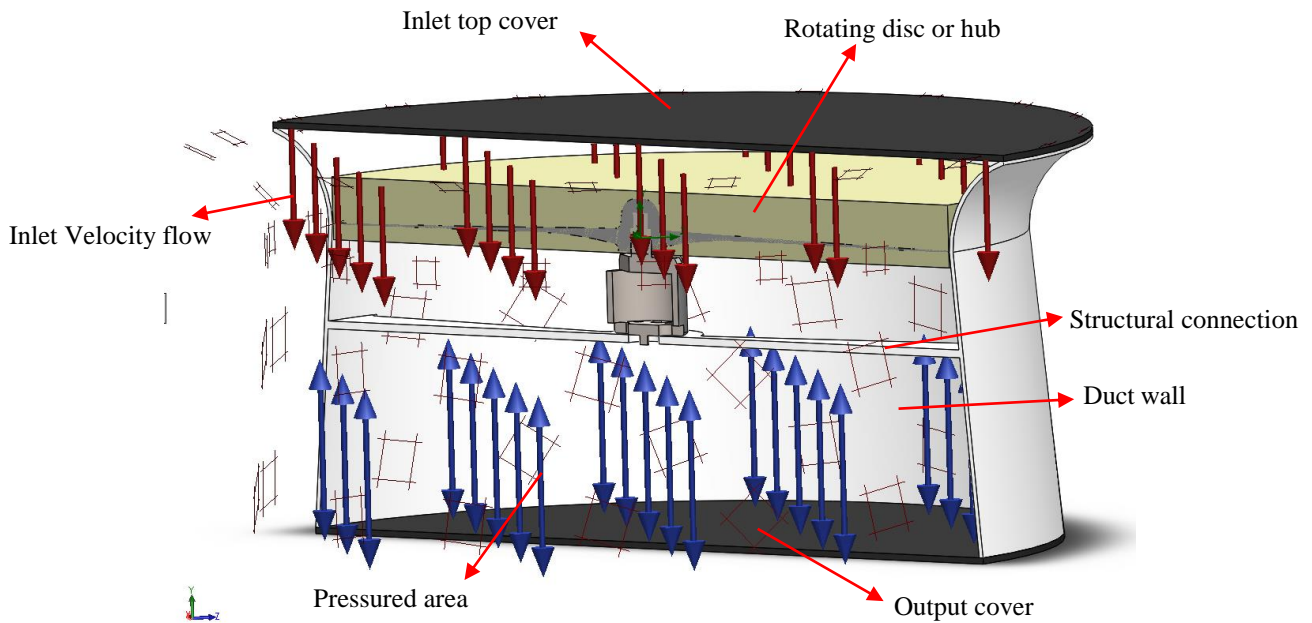


Figure 8.4 Simplified model of duct and components for Flow simulation

This part of the design process is to treat the tip to prevent leakage which is a large amount of flow passing between the duct wall and the rotor blade tip. By using this simulation flow around the tip can be predicted.

The setup of the model and mesh distribution on the ducts are kept the same, and all the procedure's regarding this is shown in Appendix B.3. The simulation is continued until the pressure contours developed from start-up flow to end of the diffuser as mentioned earlier and the thrust of both rotor and the duct no longer varied with time. The pressure contours along the rotor blades and duct were also checked to ensure that the distribution was consistent and normal as expected.

Low pressure areas were detected where each of the blades of the rotor were passing the duct wall which is shown in blue colour in Figure 8.5. High velocity area shown in thick red colour in the figure proves that, this type of section would increase the thrust, but still if the structure of the connection in duct is changed, we will be able to see better results.

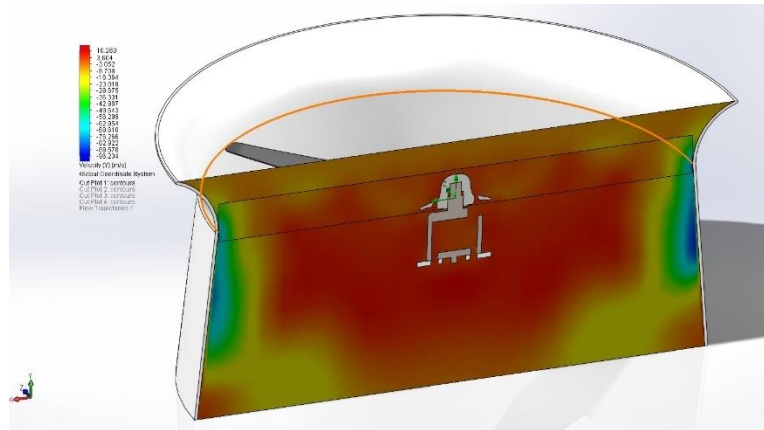


Figure 8.5 Velocity flow section 1 in Concept 1

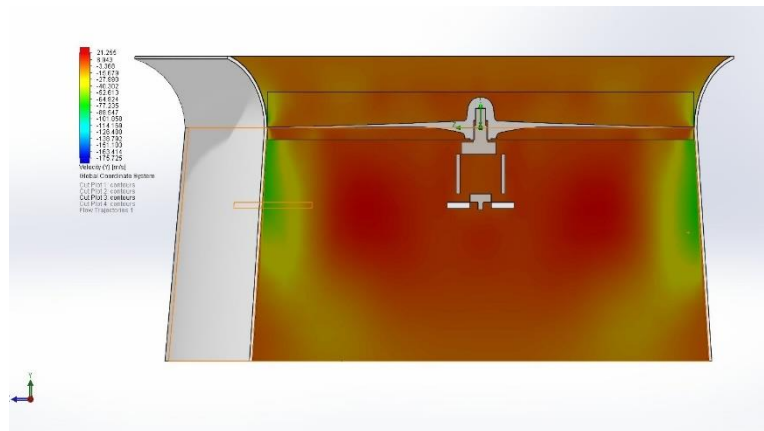


Figure 8.6 Velocity of flow section 2 in Concept 1

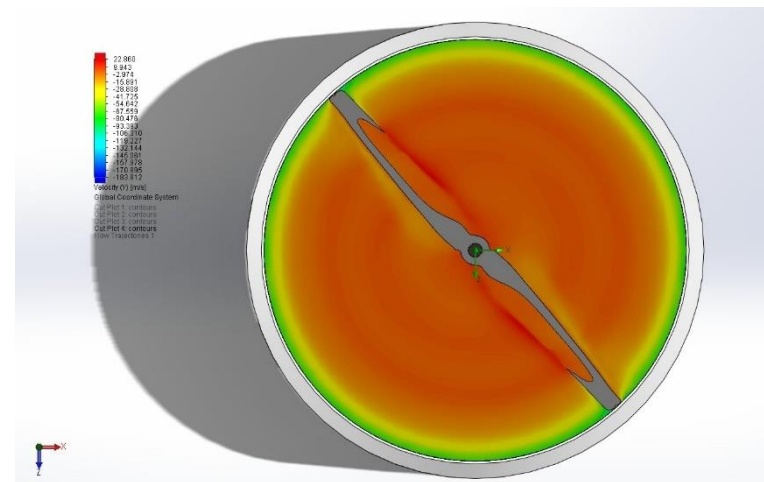


Figure 8.7 Velocity flow section 3 in Concept 1

Figure 8.8 shows the air flow condition inside the duct, at the rotor blade, the velocity is high, but the pressure is low in that area and this impact extends towards the structural barrier in the duct. Also it can be seen that rectangular type of section causes the pressure break in the area and which also reduces the thrust.

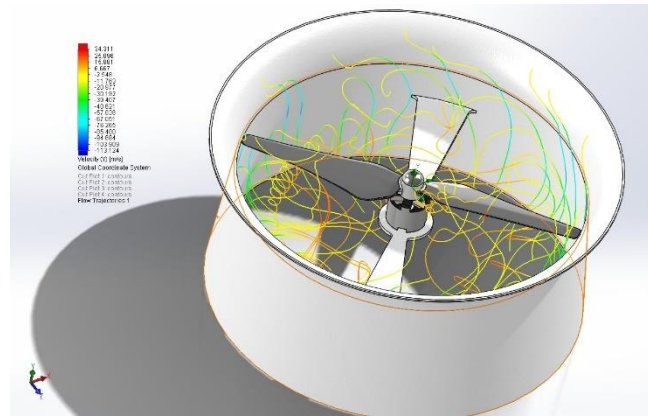


Figure 8.8 Flow trajectories in Concept Duct I

As discussed in open rotor, force in Y direction is considered as the thrust force and this allows the quadrotor to take off from the ground against the gravity.

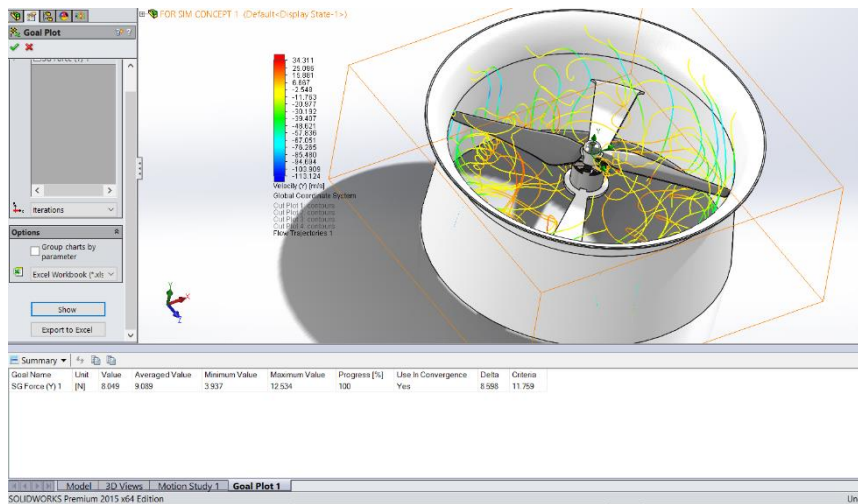


Figure 8.9 Thrust value Y-direction in Duct concept I

Name	Unit	Value	Progress	Use in convergence
SG Force (Y) or Thrust	N	8.049	100%	11.7592411

Table 8.2 Thrust force generated from Duct Concept I

8.3 Aerodynamic Concept with 45Deg of connection

This concept is mainly developed to eliminate the disadvantages of the previous concept. In this concept the air flow is not disturbed by a flat structure instead an aerodynamic flow piece is designed with 45° angle. So the high pressure air is not disturbed in a way that it will get escaped using the angular foil as shown in Figure 8.3. The cross-section is shown in the below figure. The weight of the system is increased by 3% and approximately 4% of thrust is

improved but due to the weight there is a minimum loss in the thrust. The procedure of airflow is same as mentioned in 8.2.1.

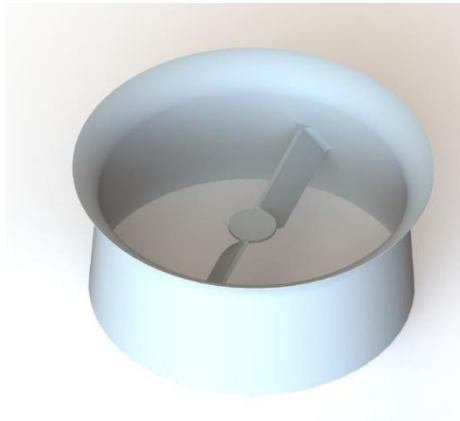


Figure 8.10 Aerodynamic concept II (45deg) modelling

8.3.1 Simulation of Concept II

As mentioned above the setting of the part and meshing is done and the results are displayed below.

The low pressure area is improved when compared to the first concept and the value of the velocity is also reduced (Figure 8.11) below the propeller which indicates a positive sign to use the duct, but to have a better look, in our next step we can design a duct with 60° aerodynamic cross section.

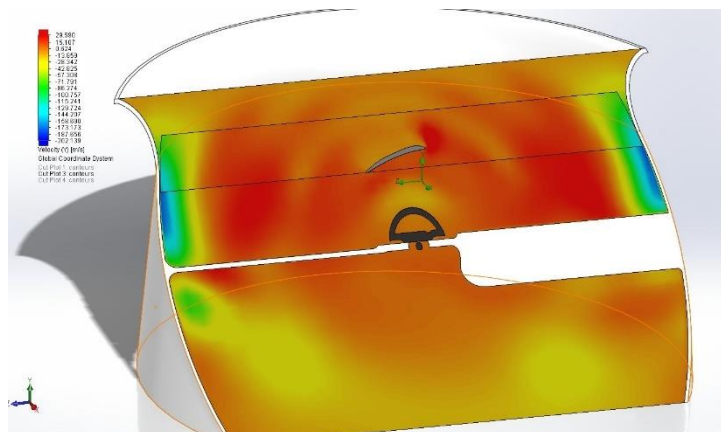


Figure 8.11 Velocity flow section 2 in Duct concept II

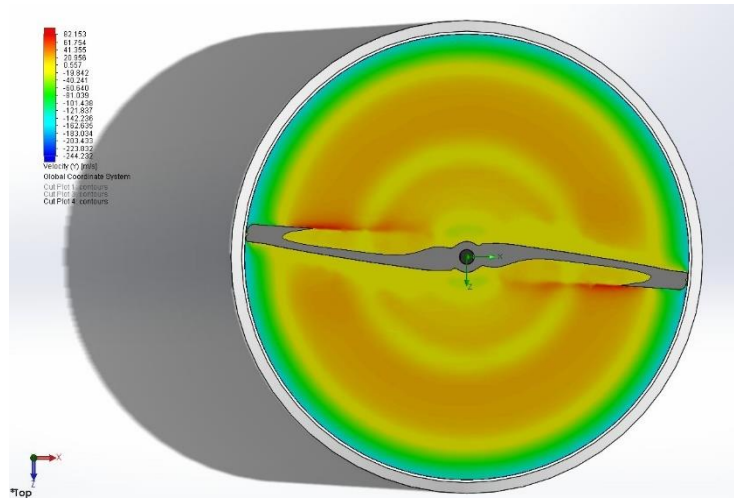


Figure 8.12 Velocity flow section 3 in Duct concept II

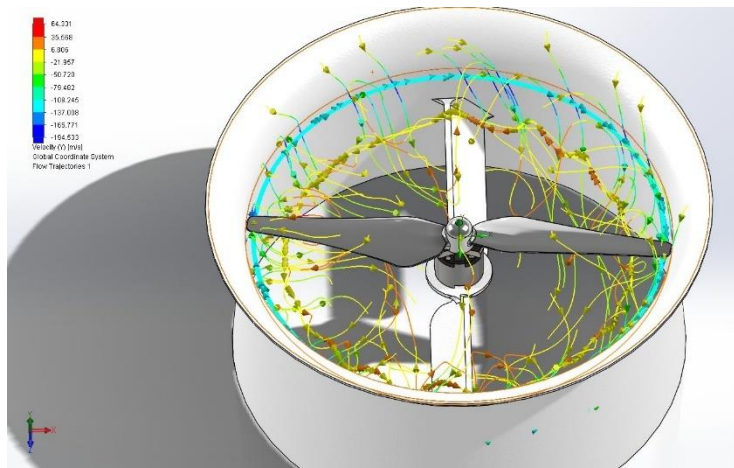


Figure 8.13 Flow trajectories in Concept II

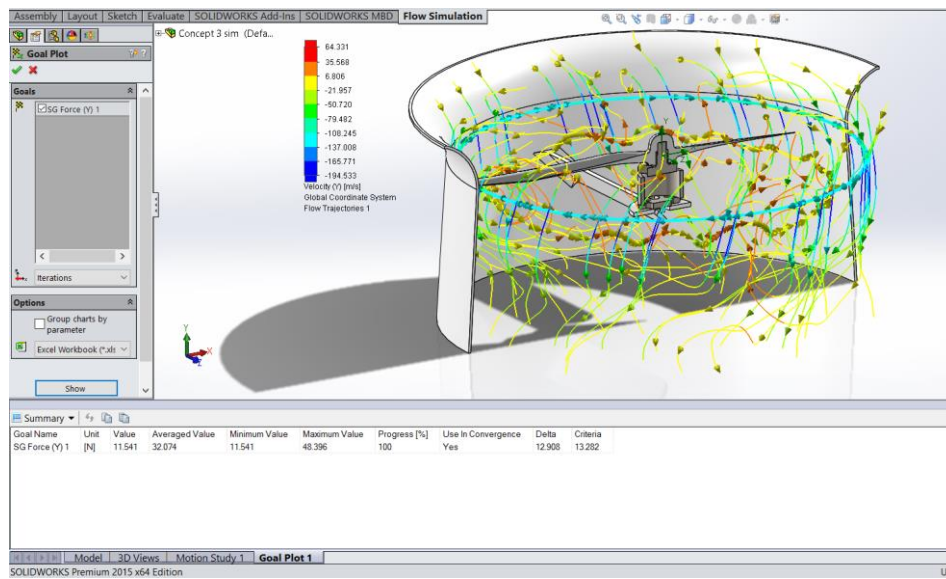


Figure 8.14 Thrust value Y direction in Concept II

Table 8.3 is a summary of the recorded data used to access the performance of the 45° aerodynamic concept ducted rotor,

Name	Unit	Value	Progress
SG Force or Thrust force (Y)	N	11.541	100

Table 8.3 Thrust force generated from Duct II

8.4 Aerodynamic Concept with 60Deg of connection

Mainly this concept is developed to check the difference in the flow between the 45° and 60° connection concept. The air flow will be same as in concept II, but the flow distribution simulation will be explained in detail. The angular foil of 60° concepts cross section is shown in Figure 8.16. The weight of the system is same as in previous concept, but when compared to results the thrust loss is approximately 2% as shown in Figure 8.15.

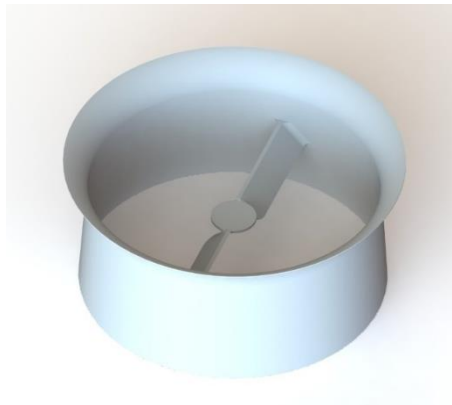


Figure 8.15 Aerodynamic concept III (60deg) modelling

8.4.1 Simulation of Concept III

As mentioned above the setting of the part and meshing is done and the results are displayed below.

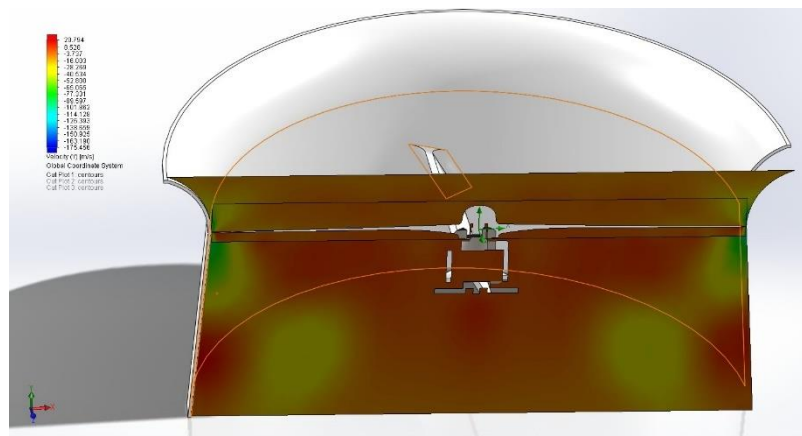


Figure 8.16 Velocity flow section in Duct concept III

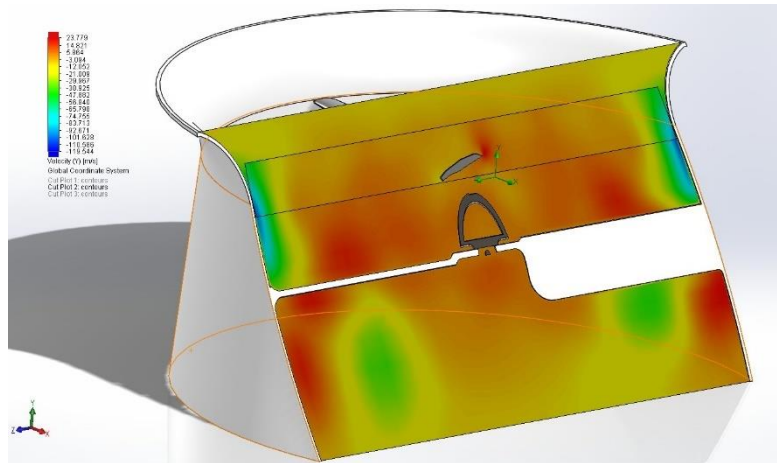


Figure 8.17 Velocity flow section 2 in Duct concept III

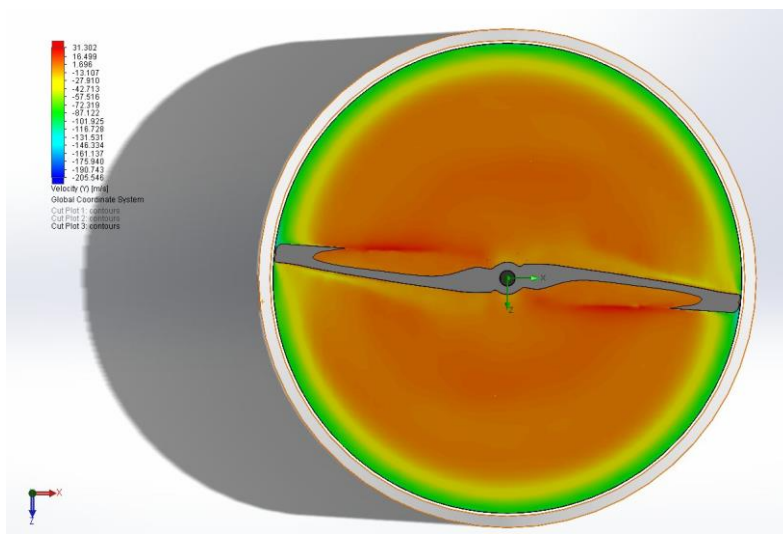


Figure 8.18 Velocity flow section 3 in Duct concept III

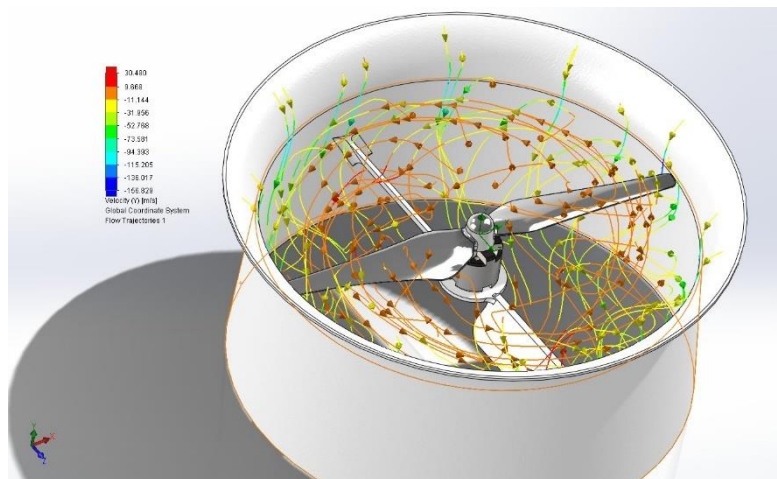


Figure 8.19 Flow trajectories in Concept III

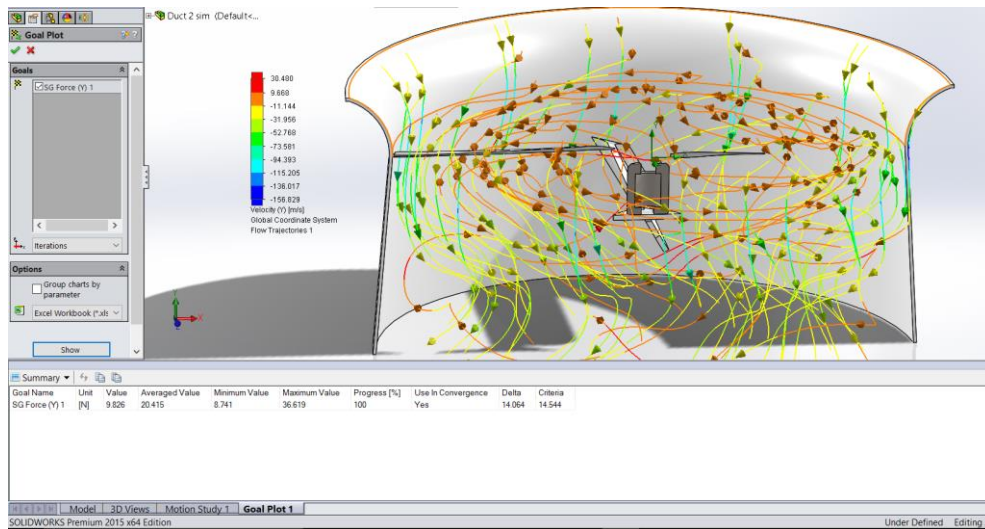


Figure 8.20 Thrust value Y direction in concept III

Table 8.4 is a summary of the recorded data used to access the performance of the 45° aerodynamic concept ducted rotor,

Name	Unit	Value	Progress
SG Force or Thrust force (Y)	N	9.826	100

Table 8.4 Thrust force generated from Duct III

8.5 Cylindrical concept of connection

In this concept the connection of the hub to duct is using cylindrical tube with a diameter of 15mm, and is developed mainly to reduce the weight and increase the stiffness. Also in addition, flow is not being affected by any uneven shape of the outlet. In this condition the air flow is like on a cylindrical rod or on a ball. The cross section of the duct concept is shown in Figure 8.21.

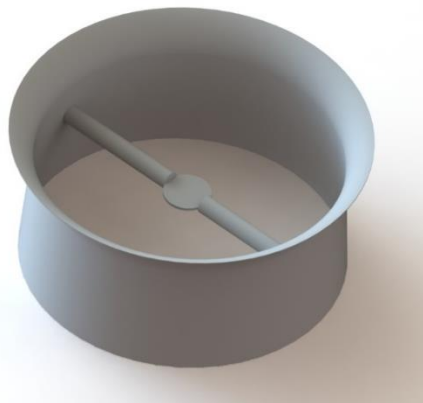


Figure 8.21 Cylindrical concept IV modelling

8.5.1 Simulation of Concept IV

As mentioned above the setting of the part and meshing is done and the results are displayed below. As expected the Figure 8.22 shows clearly the difference in the velocity region below the propeller and after passing through the cylindrical connection.

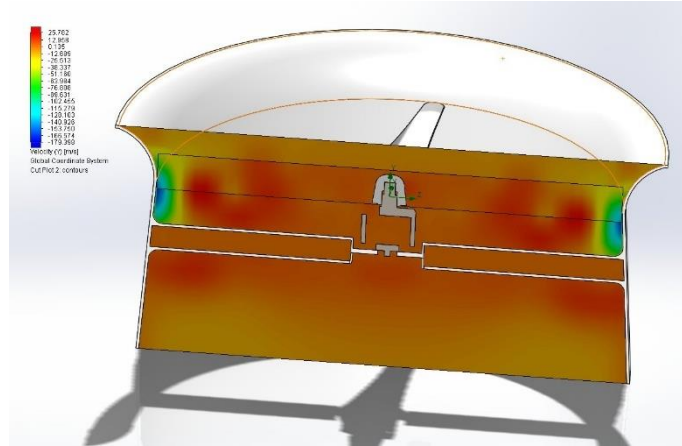


Figure 8.22 Velocity flow section 1 in Duct concept IV

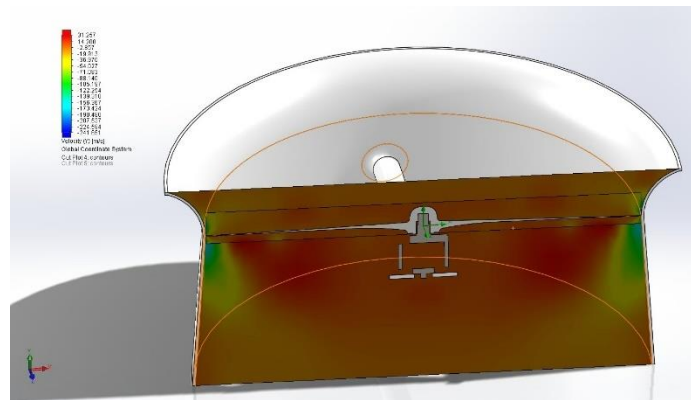


Figure 8.23 Velocity flow section 2 in Duct concept IV

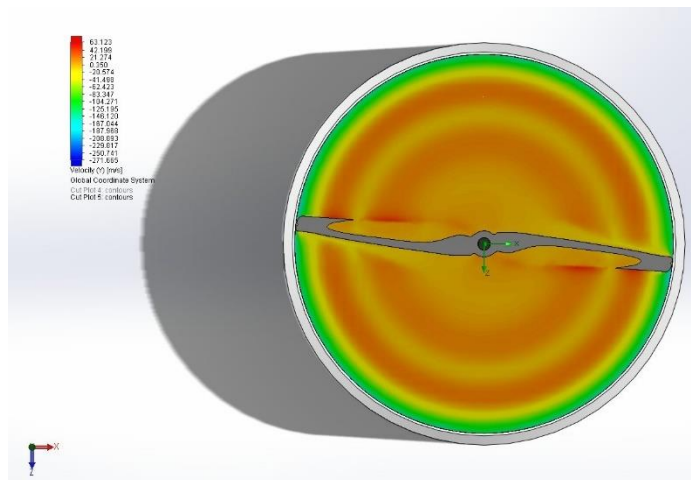


Figure 8.24 Velocity flow section 3 in Duct concept IV

The flow trajectory shown in Figure 8.25 has a high velocity over the propeller area and towards the end of the duct the velocity decreases (brown at the end of duct). So, this also confirms that the positive improvement on the duct.

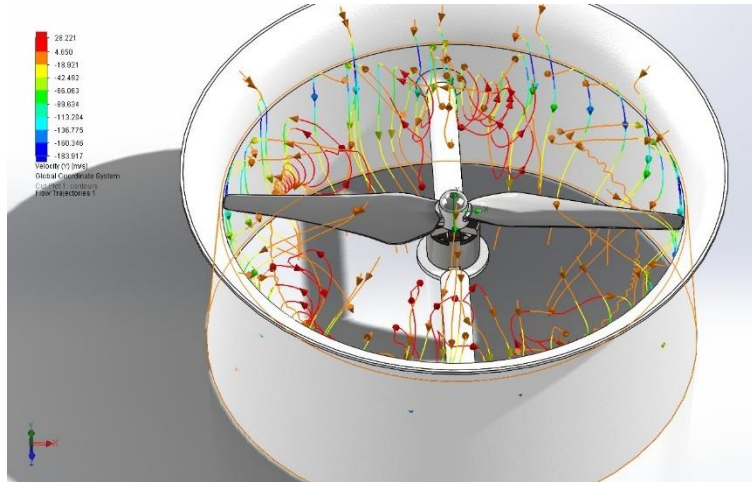


Figure 8.25 Flow trajectories in Concept IV

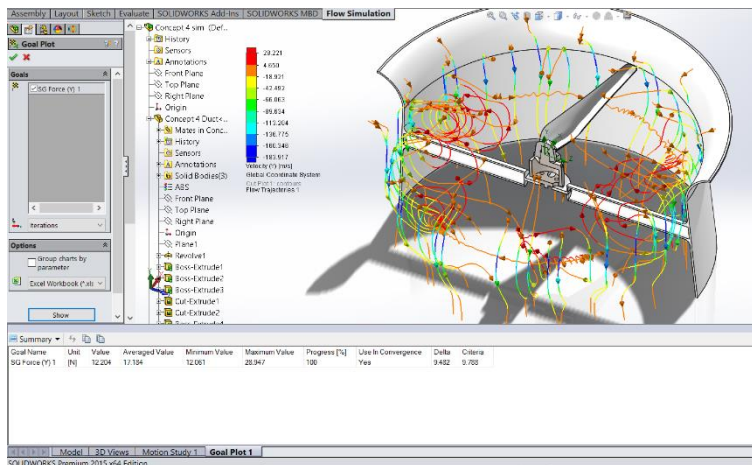


Figure 8.26 Thrust value Y direction in Concept IV

When compared to the above concept's thrust results, the developed thrust by concept four is 50% to open rotor thrust. Table 8.5 is a summary of the recorded data used to access the performance of the cylindrical concept ducted rotor,

Name	Unit	Value	Progress
SG Force or Thrust force (Y)	N	12.204	100

Table 8.5 Thrust force generated from Duct IV

8.6 Selection of optimum Duct design

At this stage, we want to estimate the optimum duct concepts for our purpose in payload condition. i.e., the difference between the ducted and non-ducted rotor should be greater than

the weight of the duct for a given power input. From the simulation results and concepts of different quadrotor ducts this selection process can be selected and final explanation of the product will be discussed in the next chapters. To make the selection process specific again QFD is used, but in this stage we can use some brainstorming principles.

Features	Concept Design			
S.No	I	II	III	IV
Duct diffuser shape	Diffuser Positive angle 	Diffuser Negative angle 	-	-
Connecting beam cross section	Rectangular Cross section 	Aerodynamics concept of 60deg 	Aerodynamics concept of 45deg 	Cylindrical cross section
Duct air flow diffuser angle	$\Theta = 7/2 = 3.5^\circ$	$\Theta = 10/2 = 5^\circ$	$\Theta = 15/2 = 7.5^\circ$	$\Theta = 20/2 = 10^\circ$
Duct structural design aesthetics				-
Duct cover closing				-
Duct thickness	1.2 mm	1.5 mm	2 mm	2.5mm
Duct structural stiffness				-

Table 8.6 Brain storming for Duct principle

The brain storming Table 8.6 points out the best alternatives that fits our design and which suits our thrust improving principle also. At this end of QFD, customer needs and the technical characteristics are meeting in line to form a good product. It is interesting to note that the simulation results and the technical details are significantly correlated to increase the thrust. It is also important to note that the ducted rotor with top cover for propeller will reduce the thrust at least by 3%. In the next chapter we can have a brief description about the selected concept.

Chapter 9. Best concept Design

Based on the previous discussion, the final design choice for the duct construction incorporated cylindrical beam cross-section and custom made top cover. These were mounted on frame structure with structural extensions for four rotor connections. The overall design features and material selections of duct fanned quadrotor is explained below.

9.1 Concept design features

The duct component of the quad follows a conventional design. A cylindrical rod made of same material as duct is used to connect all the ducts for rotor, this will reduce the manufacturing cost. Inside the duct two connecting beams are used to hold the duct in position and to improve structural stiffness Figure 9.1.

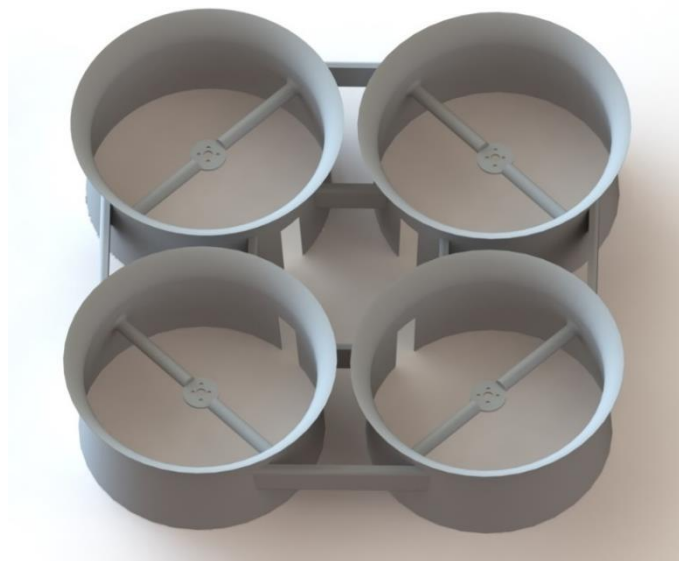


Figure 9.1 Final concept modelling

9.1.1 Beam

The cross-section of the beam is cylindrical tubular with 15mm diameter and 1.2mm thickness, it connects with motor fitting part of duct. Despite flow separation and recirculation, the thrust level of the rotor did converge, however, the thrust level of the duct continued to show a few fluctuations over time in the flow region because of the cylindrical structure in the middle. Also surface finish of the beam is an important factor to be considered, because air flow causes some friction losses.

9.1.2 Duct wall

Thickness of 1.2mm is maintained all the areas of duct. Top side of the duct is made more aerodynamic as shown in Figure 9.2 to improve the inlet flow. Our case is partly turbulent flow, so the frictional co-efficient depends on the Reynolds number and roughness of the duct or pipe wall (37). Absolute roughness co-efficient k for plastic (PVC) kind of material is 0.0012-0.007 (m) 10^{-3} , and to find the relative roughness we use Colebrook equation (38).

$$\text{Relative roughness } r = k/d_h \quad (9.1)$$

Where,

r = Relative roughness,

k = Roughness of duct, pipe or tube surface (m),

d_h = Hydraulic diameter (m)

$$r = \frac{0.007}{0.2427} = 0.02884$$

The roughness which is approximately calculated should be maintained to avoid the frictional losses of 145pas (from internet data for the duct length). Also the difference between duct and propeller is 0.000242m, and the surface finish has to be in microns.

In the duct a small opening is carved in the bottom to make the assembly easy and feasible to fit in the top of the frame leg, as shown in Figure 9.2.

9.1.3 Structural connections

All the four ducts are connected using rectangular beam section of 10x35mm (Figure 9.2 in Section C-C). Since these structural connections are the one which breaks in critical times, it should stiff enough to handle the impact loads, so impact tests are performed

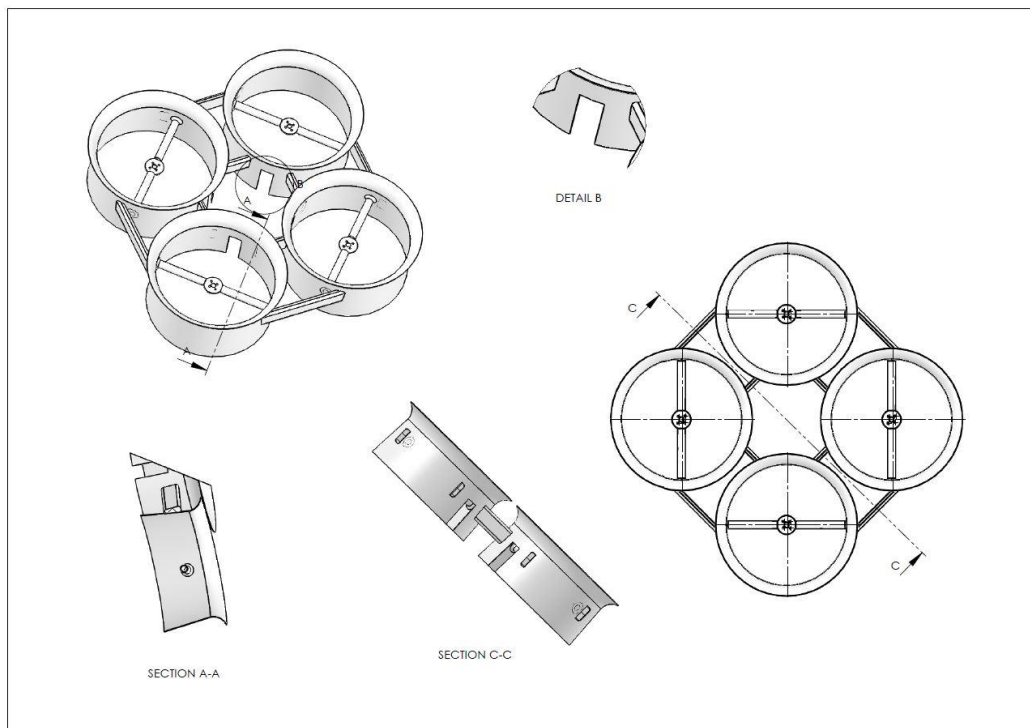


Figure 9.2 Concept features

9.1.4 Top cover

Studies shows that ducts fitted with top covers experience reductions in thrust even 10% of its overall thrust. To control this, our duct is designed specifically to reduce this loss and to improve the air flow. The problem of impact to propeller is also reduced in spite of air flow and structural stiffness. Special locking arrangements Figure 9.3 is used to fit cover to duct, this will improve the maintenance work.



Figure 9.3 Top cover modelling

No special arrangements are designed in the duct except a small rib at the end of the duct as shown in Figure 9.3, the cover has a closing rib in the opposite direction and this is to fit the top part to the bottom part. Basically the design is formulated to reduce the cost and weight of the material on the duct. The cover is 5mm in thickness and is stiff enough to withstand the load when falling from a height of 10m. As shown in Figure 9.4 the construction of the cover is designed with ribs around the top surface of the duct unlike of other cover designs provided with closed meshes.

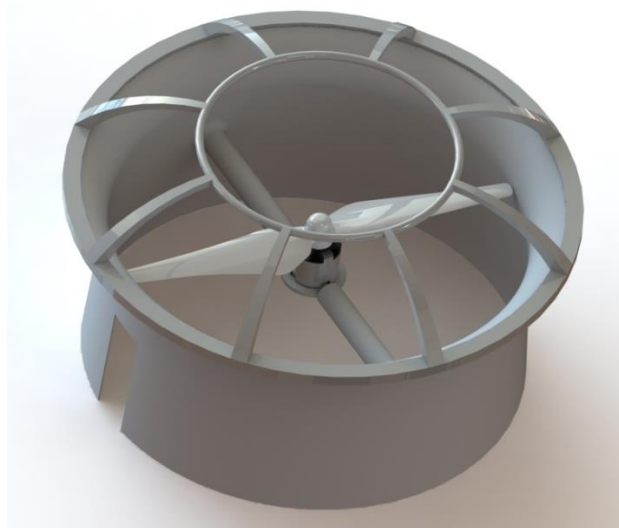


Figure 9.4 Sample Assembly process over duct

9.2 Force on Impact Calculation

The impact force or work force on the quadrotor due to force of gravity on a falling object from some distance from ground is calculated. This force calculated is applied on the quadrotor and its ducts to confirm that it holds the impact load. For this calculation relation between workdone by gravity and force acting on quad over a distance at which the force acts are taken into consideration (39) & (40). Also this calculation can be confirmed using relation of work that the force of gravity does on the quad to negative change in objects potential energy.

As shown in Figure 9.5 quadrotor falls from a distance of 10m approximately to ground,

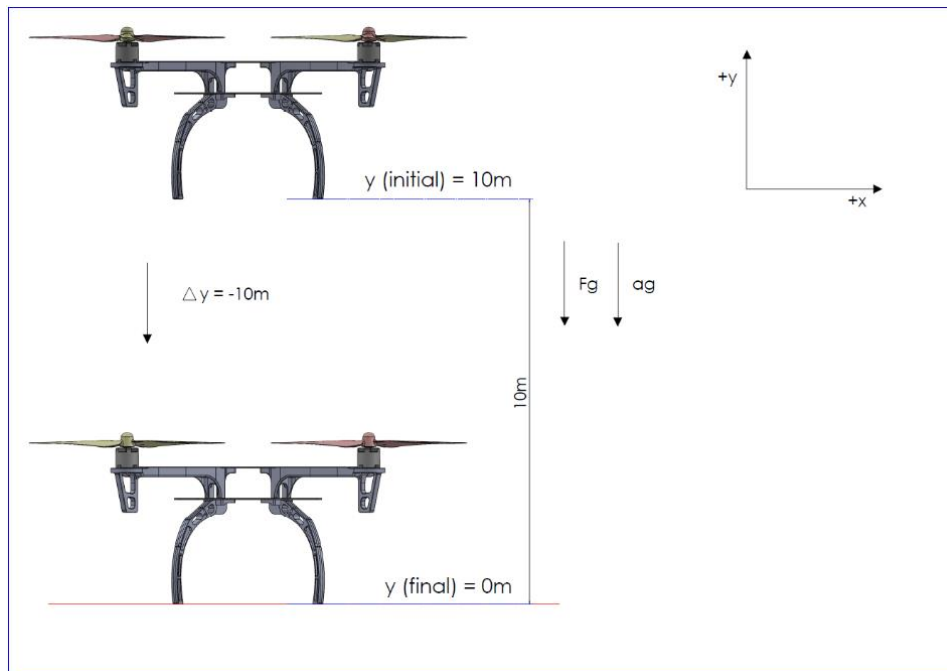


Figure 9.5 Impact Force on Quad

The impact defining the points at ground as $y=0\text{m}$ and the quad fall distance as $y=10\text{m}$, so our initial height will be $y=10\text{m}$ with final as $y=0$. As our quad is falling in downward direction and our $\Delta y = -10\text{m}$, which concludes that force of gravity is the only force acting on the quad causing to accelerate in the downward direction and we ignore all the forces such as air resistance. As shown in figure force of gravity is the only force acting on the quad causing it to do positive work on the quad as it accelerates in downward direction, means that the force will increase the velocity of quad as it falls which we know from the study of dynamics (40).

$$W = F \cdot d \quad (9.2)$$

W = Workdone by gravity on quadrotor,

F = Force due to gravity,

D = Distance the quad falls down,

In this case force is mass to acceleration with final and initial distances and which will be,

$$W = -m \cdot g \cdot \Delta y \quad (9.3)$$

$m = 1.24\text{kgs}$ Mass of quadrotor,

$g = 9.81\text{m/s}^2$ Acceleration due to gravity,

$\Delta y =$ Distance from which the quadrotor falls to the distance of which the quadrotor ends, in this case this distance is negative, because $y_f - y_i = 0 - (10) = -10\text{m}$

$$W = -1.24 * 9.81 * (-10)$$

$$W = 121.644 \text{ J or N-m}$$

Therefore, the force of gravity transfers about 121.644 J of energy as it falls from a distance from a distance of 10m. To confirm this workdone we calculate the negative change in potential energy (40),

$$\text{Workdone } W = -(m * g * \text{final ht}) - (m * g * \text{initial ht}) \quad (9.4)$$

$$W = -(0 - m * g * Y_i)$$

$$W = 1.24 * 9.81 * 10 = 121.644 \text{ J or Nm.}$$

Velocity at which the impact is created can be calculated using the gravity and height which will be further used to calculate the impact force on the duct,

$$\text{Velocity } v = \sqrt{2 * g * h} \quad (9.5)$$

$$v = \sqrt{2 * 9.81 * 10} = 14.007 \text{ m/s}$$

When the duct is dropped from the height of 10m at a velocity of 14m/s and approximately if the duct reaches the impact distance of 0.1mm (0.0001m), then the impact force will be

$$F = \frac{121.644}{0.0001} = 1216440 \text{ N}$$

Now, we apply this force to find the maximum designed stress at which the duct fracture or fail.

$$\text{Designed stress } D_s = \frac{\text{Force}}{\text{Area (From modelling)}} \quad (9.6)$$

Surface area for duct is calculated from the modelling and inserted in the above equation (9.6), (Solidworks surface area of Duct = 235917.82 mm²),

$$D_s = \frac{1216440}{235917.82} = 5.15 \text{ N/mm}^2 \text{ (MPas)}$$

From our standard study (2.2), we know that the equipment that we are using is in connection with human inter-relations, hence we can assume a Factor of Safety to our product and which can be 2 times the Designed stress calculated.

$$\text{Factor of safety (FOS)} = \frac{\text{Yield stress } (Y_s)}{\text{Designed stress } (D_s)} \quad (9.7)$$

$$Y_s = FOS * D_s$$

$$Y_s = 2 * 5.15 \approx \mathbf{10 MPas}$$

The force applied is in the form of downward force, this gravitational force can cause damage to the quadrotor in some unfortunate situations, so the duct that we design should withstand this force to save the propellers from damage. To achieve this our second step is to find the best material for the parts and the properties of the materials selected should be more than the impact properties of the force.

9.3 Material selection

This section will highlight the approaches taken to understand the materials of ducts and cover. First, the data's that required for the basic selection process will be explored. These data's use the broad knowledge which we discussed from the report. Our material selection process starts with selecting an optimum material of low cost and ends with selecting a manufacturing technique for our products.

9.3.1 Duct – Material selection

Important in a variety of applications, the property of duct particularly impact resistance will help to select the proper material, impact strength in our case is the ability of the duct to absorb the shock load and dissipating the energy without varying in shape. Shape variation will cause the duct to hit the propeller which will be a major problem. The impact property of the material is tested to its ability in the analysis which also depends on the geometry, temperature, stress and speed (41). Considering this impact property, the functions, constraints and objectives of the material is formulated,

9.3.1.1 *Material requirements for the Duct*

Our selected material should meet all the design requirements for duct having,

- I. High material strength,
- II. Low density,
- III. High stiffness.
- IV. Required that the material can be moulded.

9.3.1.2 *Assumptions on design and structure*

Some assumptions are made according to the size and loading characteristics on duct, and this also make the part simplified to perform the action.

- I. Our model is cylindrical in shape of equal thickness all over the area, applied force is travelled equally. Simplifying the model and we consider a rectangular plate or panel on which force is applied, this will make the calculation more precise.
- II. Considering rectangular section having second moment of inertia I and section modulus Z (Appendix B.1, B.2, B.3, B.4 in (41)),

$$I = \frac{b * t^3}{12} \quad (9.8)$$

$$Z = \frac{b * t^2}{6} \quad (9.9)$$

Where,

b = width (m),

t = height or thickness (m),

III. The plate is loaded and the deflection will be as in Figure 9.6.

9.3.1.3 Loads acting on the Duct

The loads which are acting on the duct are shown in Figure 9.6, as discussed earlier gravity is also one of the force which is acting on the duct due to its self-weight, combined with the wind force from sides.

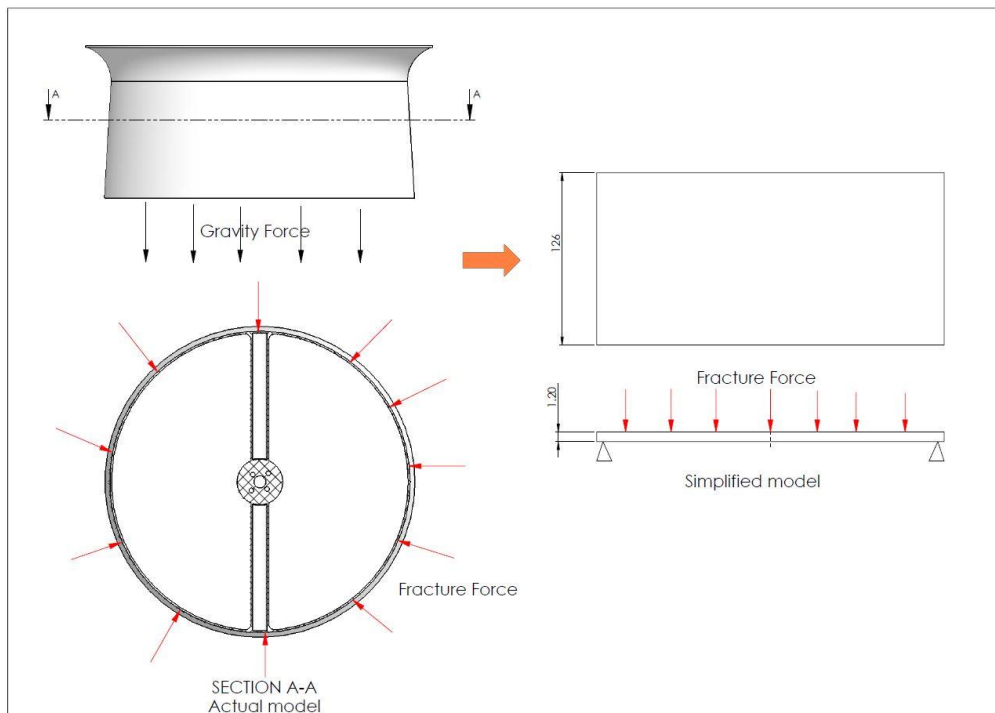


Figure 9.6 Actual Vs Simplified models

9.3.1.4 Design requirements for the Duct

A duct should provide safety protection for propellers and motors operating inside, also it should absorb the load as impact applied.

- I. The duct should be strong enough to resist the stress applied when forcing it.
- II. It must be stiff enough to prevent collision with the propeller under impact loads and elastic enough to repel force.
- III. Duct construction needs to be as light as possible to minimize the power usage to lift the weight, as we decided in our Ducted design section 9.1.

Function	Plate or panel
Constraints	Plate must support bending load F without deflecting too much meaning that Bending Stiffness S (Functional constraint) Length l and width b (Geometric constraints)
Objective	Minimizing mass (m)
Free variables	Plate thickness t Material of choice

Table 9.1 Translation for duct material (41)

9.3.1.5 Derivation for material indices

The objective function for the mass of the plate is,

$$\text{Mass } m = A * \rho * l \quad (9.10)$$

Where,

A = Area of the plate (m),

ρ = Density of the material (kg/m³),

l = Length of the plate (m).

$$\text{Area of the plate } A = b * t \quad (9.11)$$

$$\text{Bending stiffness } S = F/\delta \quad (9.12)$$

F = Force applied on the plate (N),

δ = Deflection of the plate due to the force (m),

From (Appendix B.1, B.2, B.3, B.4 in (41)),

The deflection of plate is given by,

$$\delta = \frac{F * l^3}{C_1 * E * I} \quad (9.13)$$

Substitute equation (9.13) in stiffness equation

$$S = \frac{F}{\frac{F * l^3}{C_1 * E * I}}$$

$$S = \frac{C_1 * E * I}{l^3} \quad (9.14)$$

As given in (Appendix B.1, B.2, B.3, B.4 in (41)), C_1 is a constant that depends on the distribution of the loads. Second moment of inertia I is from assumptions section above and E is young's modulus of material we insert the equation (9.8) in above equation (9.14),

$$S = \frac{C_1 * E * \left(\frac{b * t^3}{12}\right)}{l^3}$$

$$S = \frac{C_1 * E * b * t^3}{12 * l^3}$$

$$S = \frac{C_1 * E * b}{12} \left(\frac{t}{l}\right)^3$$

$$\frac{t}{l} = \left(\frac{12 * S}{C_1 * E * b}\right)^{1/3}$$

$$t = \left(\frac{12 * S}{C_1 * E * b}\right)^{1/3} * l \quad (9.15)$$

To eliminate t from the above equation equating it with mass in equation (9.10),

$$m = b * t * l * \rho$$

$$m = b * \left(\frac{12 * S}{C_1 * E * b}\right)^{1/3} * l^2 * \rho$$

$$m = \left(\frac{12 * S}{C_1 * b}\right)^{1/3} * (bl^2) * \left(\frac{\rho}{E^{1/3}}\right) \quad (9.16)$$

In the above equation,

$\left(\frac{12 * S}{C_1 * b}\right)^{1/3}$ is the Functional constraint,

(bl^2) is the Geometric constraints,

$\left(\frac{\rho}{E^{1/3}}\right)$ is the material properties,

Where S , l , b and C_1 are specified; the only freedom of choice left is the property of material. The index is the group of material properties, which we invert such that a maximum is sought: The best materials for a weightless, stiff plate are those with greater values of M_1 (material index) (41),

$$M_1 = \frac{E^{1/3}}{\rho} \quad (9.17)$$

$$\frac{E^{\frac{1}{3}}}{\rho} = C$$

$$\frac{1}{3} \log E - \log \rho = \log C$$

$$\log E = 3 \log \rho + 3 \log C$$

$$y = 3x + \text{constant}$$

The slope for selecting material using CES software should be 3 with E (Young's modulus) in the Y-axis and ρ (density) in the X-axis.

To make the calculation more precise another material index to reduce the weight to the given design loads is found (strength). In this our design goal is simple, which consider the strength at low weight. The design requirements are nearly same as above.

From (Appendix B.1, B.2, B.3, B.4 in (41)),

$$F_f = C * Z * \frac{\sigma_y}{l} \quad (9.18)$$

As given in (Appendix B.1, B.2, B.3, B.4 in (41)), C is a constant that depends on the distribution of the loads. Section modulus Z (m^3) is from assumptions section above and σ_y is Yield strength (N/m^2) of the material of material we insert the equation (9.10) in above equation (9.18),

$$F_f = C * \frac{b * t^2}{6} * \frac{\sigma_y}{l}$$

$$t^2 = \frac{6 * l * F_f}{C * b * \sigma_y}$$

$$t = \left(\frac{6 * l * F_f}{C * b * \sigma_y} \right)^{1/2}$$

To eliminate t from the above equation equating it with mass in equation (9.10),

$$m = b * t * l * \rho$$

$$m = b * \left(\frac{6 * l * F_f}{C * b * \sigma_y} \right)^{1/2} * l * \rho$$

$$m = \left(\frac{b}{b^{1/2}} * l * l^{1/2} \right) * \left(\frac{6 * F_f}{C} \right)^{1/2} * \left(\frac{\rho}{\sigma_y^{1/2}} \right)$$

$$m = (b^{1/2} * l^{3/2}) * \left(\frac{6 * F_f}{C} \right)^{1/2} * \left(\frac{\rho}{\sigma_y^{1/2}} \right) \quad (9.19)$$

In the above equation,

$\left(\frac{6*F_f}{c}\right)^{1/2}$ is the Functional constraint,

$(b^{1/2} * l^{3/2})$ is the Geometric constraints,

$\left(\frac{\rho}{\sigma_y^{1/2}}\right)$ is the material properties,

Where σ_y , l, b and C are specified; the only freedom of choice left is the property of material. The index is the group of material properties, which we invert such that a maximum is sought: The best materials for a weightless plate which can withstand impact loads are those with greater values of M_2 (material index) (41),

$$M_2 = \frac{\sigma_y^{1/2}}{\rho} \quad (9.20)$$

$$\frac{\sigma_y^{1/2}}{\rho} = C$$

$$\frac{1}{2} \log \sigma_y - \log \rho = \log C$$

$$\log \sigma_y = 2 \log \rho + 2 \log C$$

$$y = 2x + \text{constant}$$

The slope for selecting material using CES software should be 2 with σ_y (Yield strength) in the Y-axis and ρ (density) in the X-axis.

9.3.1.6 Material selection and Screening using CES Edu pack 2015

Finally, we are at the stage where we will list appropriate material candidate and select the one with highest material index. From the software we can generate graphs for different material indices, and limiting many types of material parameters which would ease material selection process. Initially young's modulus vs density graph is plugged in and slope value of 3 is entered as shown in Figure 9.7. In the first stage of limiting the materials yield strength value less than 8MPas materials are eliminated.

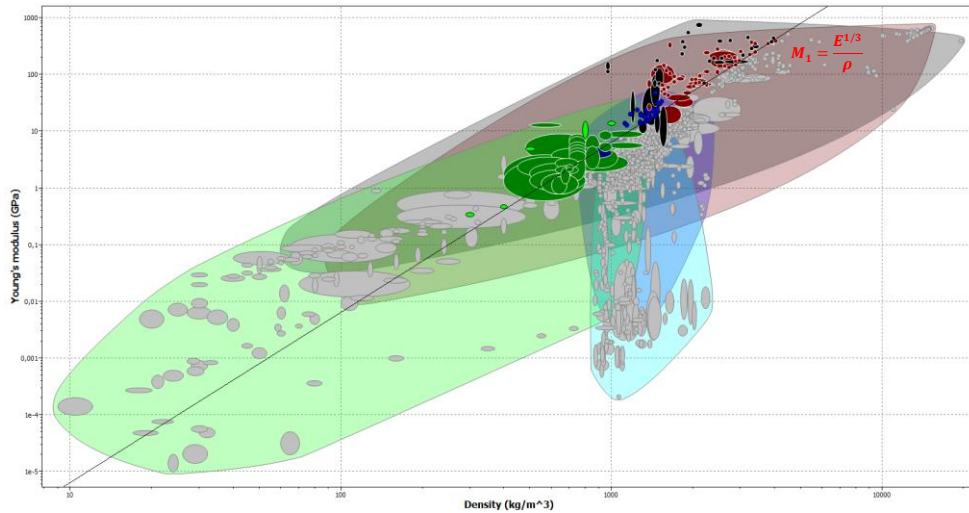


Figure 9.7 Young's Modulus Vs Density stage 1

In the next stage as we need better elastic property also we eliminate the materials which has less than 10GPa of young's modulus.

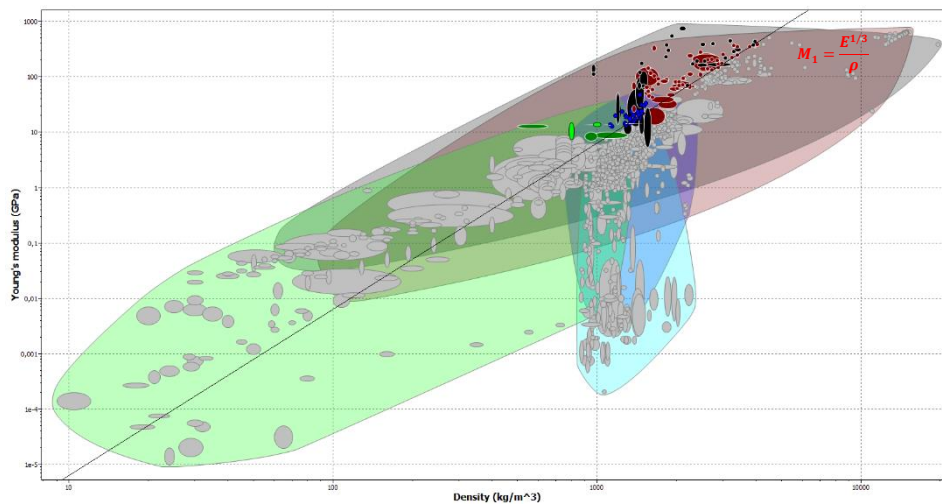


Figure 9.8 Young's Modulus Vs Density stage 2

As density is also a main constraint, which decides the mass of the product, we approximate the density of material should be maximum 1300 kg/m^3 . Also to have a good clarity of the materials selected and to further limit the materials in our case we apply limit on the price to be maximum of 75NOK/kg. The final material selection using young's modulus vs density graph is shown in below Figure 9.9.

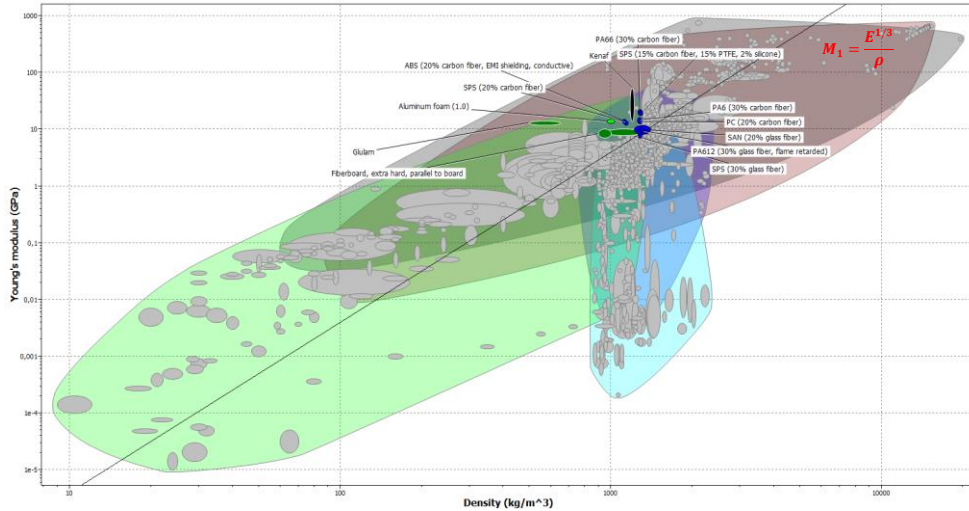


Figure 9.9 Young's Modulus Vs Density stage 3

In the next stage to make sure that the materials from the young's modulus vs density graph is correct we proceed the graph of yield strength and density and for that slope value of 2 is entered according to the calculation. limiting starts with the materials yield strength value less than 8MPas materials are eliminated, and the same procedure as above and the final materials for screening of duct is shown in Figure 9.10.

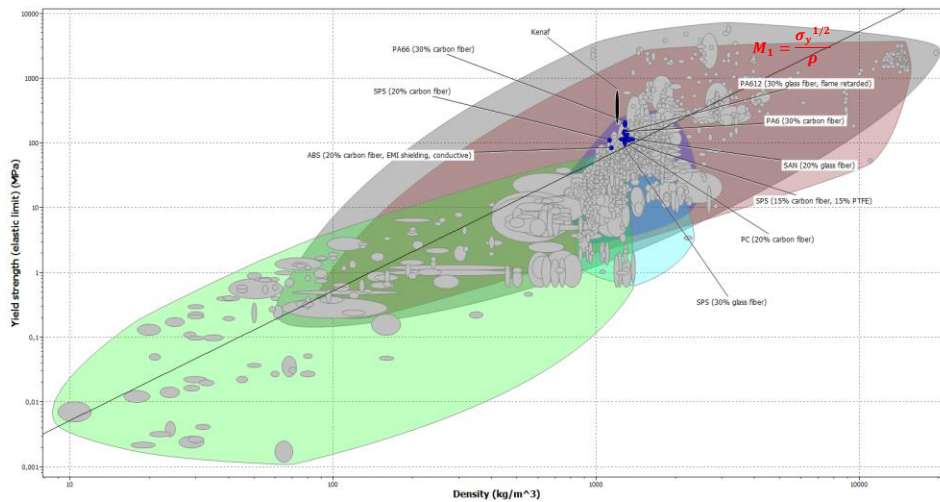


Figure 9.10 Yield strength Vs Density final stage

9.3.1.7 Ranking materials for duct

As an evident from the graph in Figure 9.7 to Figure 9.10, only small number of materials are left above the selection line and based on the different requirements in the graph's. Now we can shortlist potential material candidate, from which we can select the befitted material for the duct. Some of the potential materials, their fracture and impact properties are listed below suitable is shown in below Table 9.2.

S. No	Material	Density (kg/m ³)	Impact Strength (kJ/m ²)	Fracture toughness (M Pas)
1.	ABS (20% carbon fiber)	1.13e ³ – 1.14 e ³	5 – 5.5	3.23 – 3.98
2.	SPS (20% carbon fiber)	1.11 e ³ – 1.13 e ³	4.47 – 4.94	1.16 – 1.25
3.	P66 (30% carbon fiber)	1.27 e ³ – 1.29 e ³	12.5 – 24.2	5.6 – 6.19
4.	Kenaf	1.19 e ³ – 1.2 e ³	–	1.16 – 14.8
5.	PA612 (30% glass fiber)	1.29 e ³ – 1.31 e ³	10.2 – 19.8	4.88 – 5.39
6.	PA6 (30% carbon fiber)	1.26 e ³ – 1.28 e ³	6.77 – 13.1	5.25 – 5.81
7.	SAN (20% glass fiber)	1.22 e ³ – 1.4 e ³	5.3 - 16	4.89 – 5.87
8.	SPS (15% carbon fiber, 15% PTFE)	1.28 e ³ – 1.3 e ³	4.94 – 5.46	1.45 – 1.56
9.	PC (20% carbon fiber)	1.27 e ³ – 1.29 e ³	6.67 – 7.35	4.29 – 5.33
10.	SPS (30% glass fiber)	1.27 e ³ – 1.29 e ³	6.37 – 14.3	1.02 – 1.66

Table 9.2 Ranking materials table

In our case material selection, we have multiple number of materials which suits to duct and the choice is further narrowed by the requirement that, for impact strength must be large. From Table 9.2 the final material which is selected for further documentation process is P66 (30% carbon fiber), PA612 (30% glass fiber), PA6 (30% carbon fiber), and SPS (30% glass fiber). As we can see that the impact property eliminates the materials which are low in property, and also the materials which are selected has combination alloy of carbon fiber and glass fiber. Further documentation is carried out for their properties, uses and price.

9.3.1.8 Documentation of the selected materials

The materials selected have high values of fracture toughness and light too in terms of density. Focusing on research, and not on mass production creates a new constraint on our product which is availability and uses. Price is not a constraint in our case when compared to fracture toughness.

S. No	Material	Price (NOK/kg)	Comments	Some uses
1.	P66 (Polyamide – Nylon)	70.1 – 77.3	I. High impact property, II. Expensive.	Gears, cams, rollers, power tool housing, fuel tanks for cars, etc.,
2.	PA612 (Polyamide – Nylon)	46.8 – 51.6	I. less impact property when compared with P66, II. less expensive, III. Similar material as Frame	Mechanical parts, zips, filaments, coatings etc.,
3.	PA6 (Polyamide – Nylon)	71.1 – 78.3	I. Very less impact property, II. Expensive, III. Weight to stiffness ratio is more.	Cams, rollers, power tool housing, combs etc.,
4.	SPS (Polystyrene)	35.5 – 39.1	I. Very low fracture toughness, II. Less expensive.	Electrical and electronic components, connectors etc.,

Table 9.3 Selected materials for Duct

Polyamide plastics combined with fiber are the best choice, because of their low weight and high impact and toughness. These choices are seeming much worthy competitive to all materials and potential cost saving but according to customer's need greater the impact property best is our selection. Now using our common sense to availability of material and continuation of the process where frame manufacture procedure also uses. So, in this case even the price of the PA612 is high, we select that material to have a continuity in production and due to its better properties (42).

9.3.1.9 Final material for Duct

PA612-GF30 is in the material family of thermoplastic with base material of Polyamide/Nylon 612 and it has 30% of glass fiber. It possesses good strength & stiffness and offers increased heat deflection temperature. Exhibits fatigue endurance, dimensionally stable & provides creep and long term heat resistance. Excellent to manufacture using injection moulding of complex shapes like duct. Price is low when compared to P66 material i.e., 25NOK/kg is less. Main disadvantage of these kinds of materials are recycling and is not biodegradable (42). The various manufacturing techniques and production feasibility will be discussed in the next chapters.

9.3.2 Top cover – material selection

Top cover has a prominent work of protecting the propellers from top, this is when the quadrotor falls upside down. The property of the material that we select should absorb the impact as in duct material but yielding of the cover is not very important. It must be strong to

carry without breaking, the bending exerted by the load. Based on this functions, constraints and objectives are formulated.

9.3.2.1 Material requirements for the top cover

Our selected material should meet all the design requirements for the duct having,

- I. High material strength,
- II. Low density,
- III. Can be moulded easily as in duct.

9.3.2.2 Assumptions on design and structure

Some assumptions are made according to size and loading characteristics on cover,

- I. The cover is a circular disc made of ribs to connect together, the load is applied on the top of the cover. The load in our can be equally travelled or on one side, so the structure should be strong in all directions. In the Figure 9.11 shown below, the type of beam and forces acting on the beam,

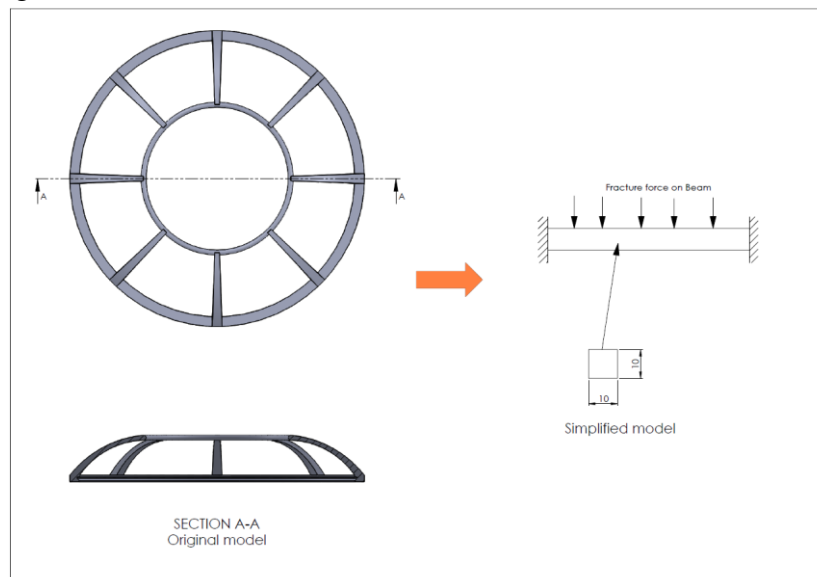


Figure 9.11 Simplified model of top cover for Material selection

- II. Stress σ_y is applied at a point y , from the neutral axis of the uniform beam loaded elastically in bending by a moment, M having section modulus Z (9.9) shown in (Appendix B.1, B.2, B.3, B.4 in (41)).

9.3.2.3 Design requirements for the top cover

Top cover should be strong, light and should not increase power usage which in turn reduces the thrust of the quad.

Function	Beam
Constraints	Strength: must not fail under design loads Length l and width b (Geometric constraints)
Objective	Minimizing mass (m)
Free variables	Plate thickness t Material of choice

Table 9.4 Translation for cover material (41)

9.3.2.4 Derivation for material indices

The objective function is same as duct to reduce mass, so we use the weight to strength as we used in the duct material selection area. Proceedings as in section 9.3.1.5.

$$M_1 = \frac{\sigma_y^{1/2}}{\rho}$$

The slope for selecting material using CES software should be 2 with σ_y (Yield strength) in the Y-axis and ρ (density) in the X-axis.

9.3.2.5 Material selection using CES Edu pack 2015

As the procedure of selecting the material in CES is same as for Duct, only the final graph is shown in below Figure 9.12.

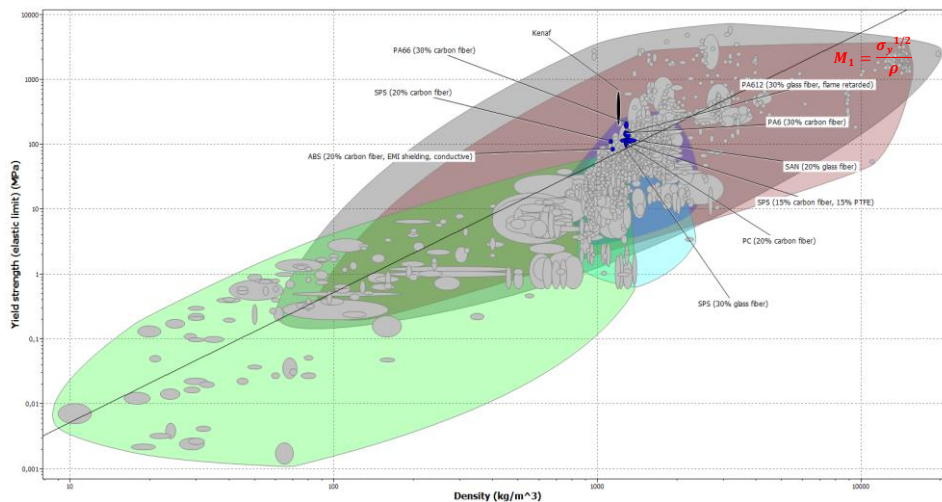


Figure 9.12 Yield strength Vs Density for top cover

9.3.2.6 Final material for top cover

As mentioned in duct screening and ranking of the top cover is done in the same way, and the best material is same as that duct. So, the production methods and price is same as that of duct Excellent to manufacture using injection moulding of complex shapes like duct and top cover. Price is low when compared to P66 material i.e., 25NOK/kg is less. The various manufacturing techniques and production feasibility will be discussed in the next chapters.

9.4 Structural analysis on the Duct and top cover

In the drop test analysis, the time varying stresses and deformations due to an initial impact of the duct with a rigid or floor surface are calculated. As the product deforms, secondary internal and external impacts are also calculated, locating critical weaknesses or failure points, as well as stresses and displacements. The test also conveys to improve the design in the critical area of the duct and the maximum ‘G-force’ experienced by the duct. ‘G-Force’ is a critical parameter for components used in selecting materials, shape and assembly characteristics, this force is fixed by the manufacturers which should be kept below specified minimum. Drop test and static fracture test is done on the duct and also on the top cover to ensure that the selected materials and design will with stand the force that applied.

9.4.1 Drop test on Duct

Initially a drop test is conducted on duct as mentioned in 9.2 from a height of 10m from ground to analyse the properties of the material chosen. The procedure of meshing and loading details are presented in Appendix C.1, here the results are displayed. Outcomes of the current analysis can be viewed and cross checked with the impact details calculation. In the Figure 9.13 shown the areas which are marked in low stress are marked in dark blue and the von Mises stress intensity is approximately $1.659 \times 10^{-7} \text{ N/m}^2$, and the regions of high stress are indicated in red and the intensity level is $1.050 \times 10^8 \text{ N/m}^2$, which occurs along the duct top end surface as shown in Figure 9.14.

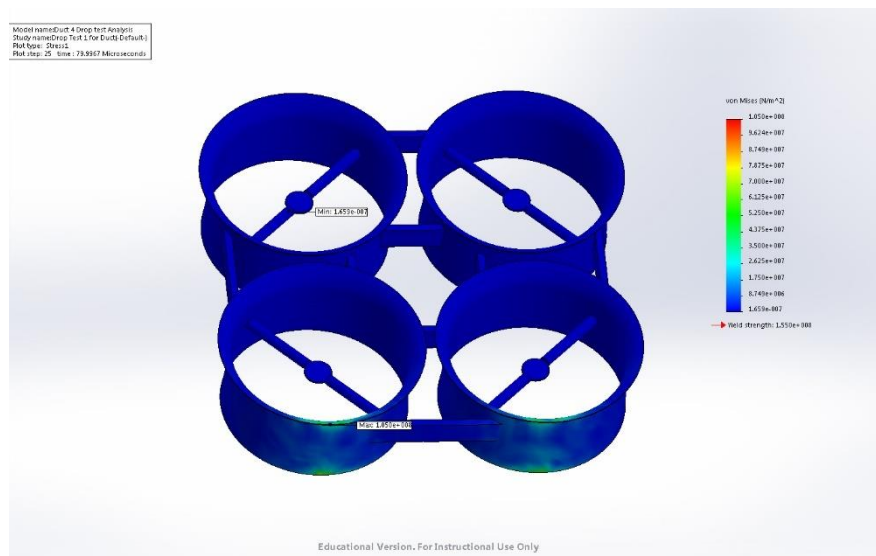


Figure 9.13 Drop test analysis on duct

Also the material yield strength is also indicated beneath the listed stress result, where it shows that the analysed stress level is lower than the designed stress that the duct can handle calculated with FOS.

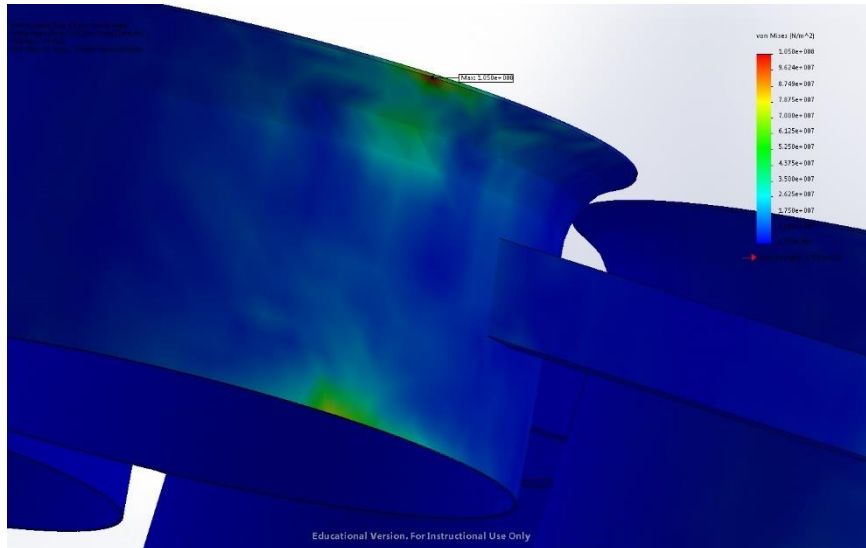


Figure 9.14 Max Von-Mises stress area on duct

When duct is dropped, the elastic modulus of the duct resists the duct to break. The minimum elasticity displacement is approximately 0.190mm which is in the bottom side of the duct and the maximum displacement occurs at the tip of the duct and the value approximately is 1.215mm and it is neglected because this maximum displacement in the tip does not affect the propeller inside the duct (Figure 9.15).

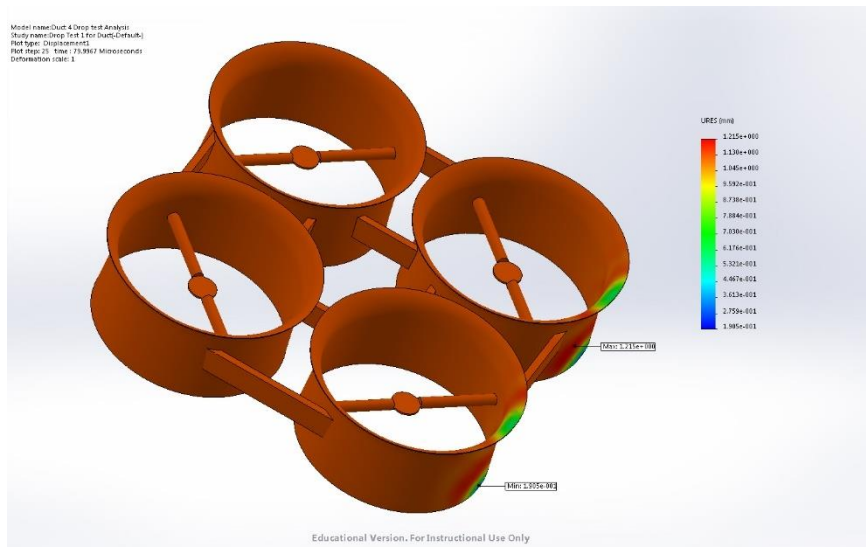


Figure 9.15 Displacement result in the duct

9.4.2 Impact test on Top cover

Impact analysis on the top cover is carried out to find the worst case areas where the component is tending to break. Factor of safety is considered and a pressure of $10 \times 10^6 \text{ N/m}^2$ is applied on the top of cover and the maximum stress developed is low in the areas where it was predicted to break (Figure 9.16).

The light green colour and the yellow colour shown in the Figure 9.16 is the maximum von – mises stress recorded, and this part is the one which has connection to duct. It has more intensity

of stress over the area, but as our material has elastic property and also the top cover has no connection with the propeller, these areas are neglected in this session. But in the future part of this thesis, the top cover area should be taken more consideration.

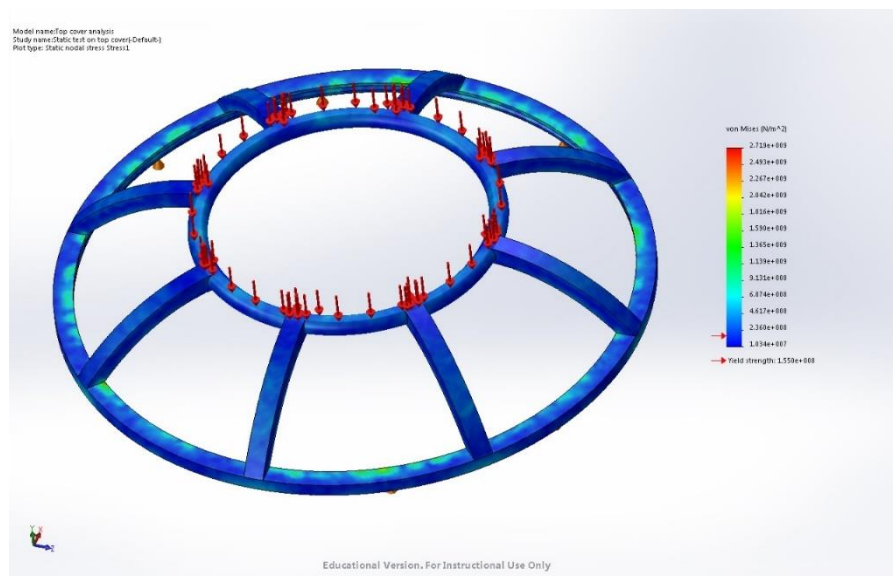


Figure 9.16 Impact analysis on Top cover

As our structural analysis on the designed parts are successful in our case, we move our product to the next stage where we develop a 3D printed prototype. All the simulation procedures and meshing tables are proceeded Appendix C.2.

Chapter 10. Duct Performance

The objective of this test is to improve the aerodynamics performance of our designed duct. To access the performance of these units, each of the rotors were tested separately which will give the approximate increment in thrust. This process starts with 3-D printing of the design model of duct.

10.1 3-D Printing of duct

3-D printing is a technology known as “additive manufacturing”, which builds objects by adding successive layers of materials. 3-D printing has its applications for niche purposes and rapid prototyping i.e., to check whether the designed product has the potential to meet the customer’s satisfaction. Duct design is incorporated with prototyping to plan and decision-making and to improve the potential sustainability of the product. MakerBot Replicator Z18 3D-printer is used for the purpose to make the prototype in our case



Figure 10.1 MakerBot Replicator Z18 (43).

Replicator Z18 uses Fused deposition modelling technology for printing with a resolution of 100microns (43). Replicator operates with a makerbot PLA filament of diameter 1.75mm which uses nozzle diameter of 0.4mm. Maximum precision achieved from this machine is 11microns in XY position and 2.5microns in Z direction. Our Duct model is converted to STL (stereo Lithography) modelling format which is supported by the printing machine and loaded into it to get our final prototyping product (Figure 10.2).



Figure 10.2 Duct 3D printed for testing

Some of the important details about 3D printed product,

S. No	Description	Product details
1.	Product material	PLA (Polylactic Acid)
2.	Colour of the product	White
3.	Weight	200grams
4.	Product thickness	3mm
5.	Precision of our product	20microns in X-Y direction, 5microns.
6.	Duct diameter printed / original diameter	243mm (3-D printed) 242.4849mm (original diameter) (7.3)

Table 10.1 3-D Printed model specification

Extra materials from the product is cleaned, because the machine built some wall around the product for reference. These reference points are removed and cleaned to fit in the thrust testing machine.

10.2 Duct thrust testing

The order of duct thrust testing is done as in open rotor thrust testing, since duct attachment is added with the rotor, supporting struts are used and a low tip clearance between the rotor tip and the wall of duct is maintained. Therefore, to maintain the original tip clearance, which is difficult to do, the ducted rotor has to be tested approximately for its improvement. Different thrust results are achieved at different levels of PWM rating (5.3) using thrust measuring device as shown in Figure 10.3. The mechanical power required to maintain the given rotor RPM remain same for both open and ducted rotors at low speeds, but at higher RPM's i.e., at higher rotor revolution speeds there appears to be a reduction in power required and improvement of thrust for the ducted rotor.

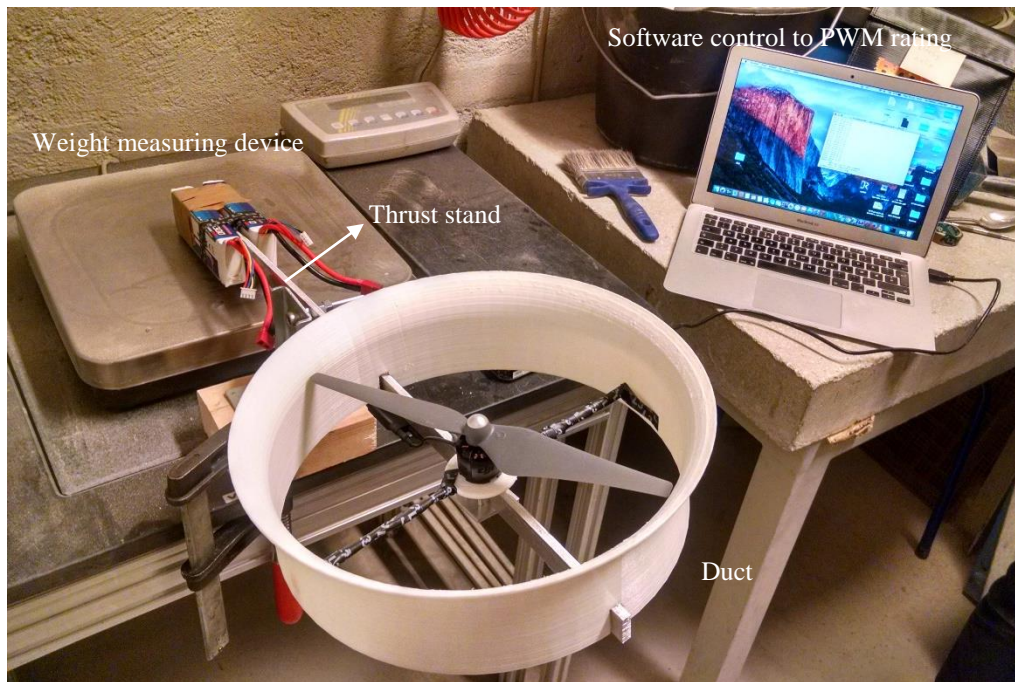


Figure 10.3 3D Printed duct on Thrust testing machine

Surprisingly at the designed ducted rotor 88gms, i.e., 35-40% improvement in thrust. Table 10.2 shows clearly the thrust measurements with ducts. Also the test results matches approximately with the Solidworks flow simulation software. Comparisons are taken with the old tests and the ducted tests to prove the difference in the thrust results.

S. No	PWM	Thrust		
		Mass (Kg)	Force (N)	Thrust (N) After model symmetricity (calculations shown below)
1	1100	0	0	0
2	1200	0.0273	0.26781	2.5991595
3	1250	0.0456	0.44733	2.808603
4	1300	0.0664	0.65138	3.046659
5	1350	0.0894	0.87701	3.309894
6	1400	0.1121	1.099701	3.5696955
7	1450	0.1417	1.39007	3.9084675
8	1500	0.177	1.73637	4.312476
9	1550	0.224	2.19744	4.850391
10	1600	0.268	2.62908	5.353971
11	1650	0.313	3.07053	5.868996
12	1700	0.363	3.56103	6.441246
13	1750	0.419	4.11039	7.082166
14	1800	0.472	4.63032	7.688751
15	1850	0.539	5.28759	8.455566
16	1900	0.600	5.886	9.153711
17	1950	0.600	5.886	9.153711
18	2000	0.600	5.886	9.153711

Table 10.2 Ducted rotor test results

Sample calculation for thrust after model symmetricity and the logic for the calculation is shown in Figure 10.4,

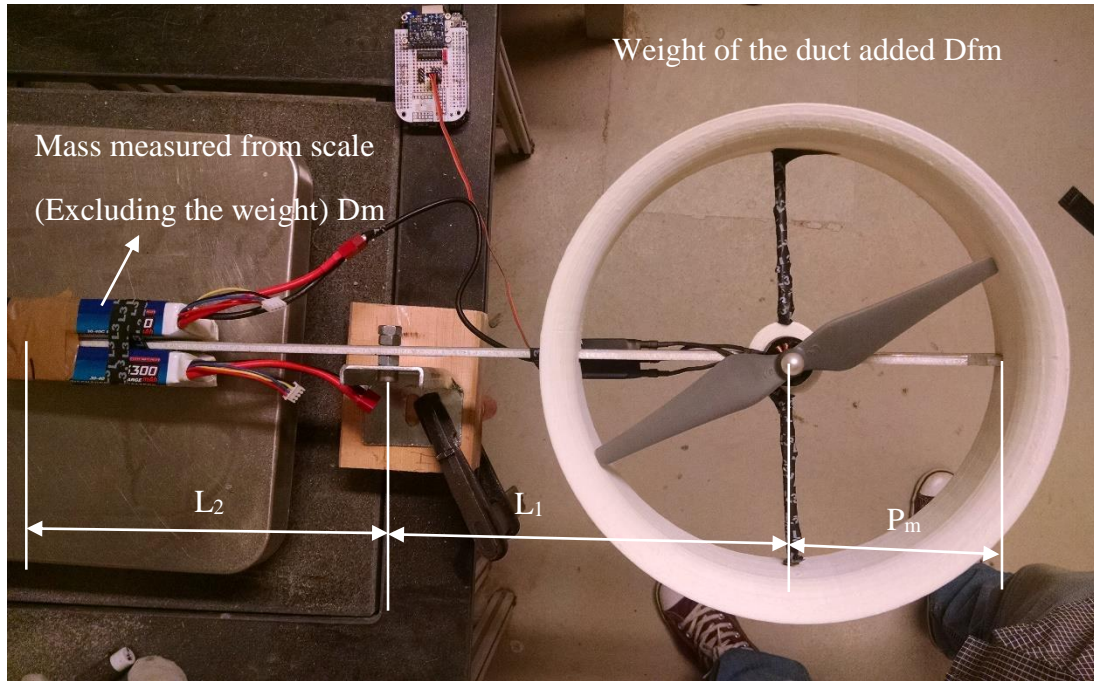


Figure 10.4 For simplified calculation of thrust

$$\text{Thrust } T = \left(\frac{l_2}{l_1} * D_m * g \right) + (D_{f_m} * g) + (P_m * g) \quad (10.1)$$

Where,

l_1 = Distance from the pivot point to the motor (0.24m),

l_2 = Distance from the pivot point to the contact point on the scale (0.28m),

g = Gravitational force constant (9.81m/s^2),

D_m = Mass measured by the scale (for example: 0.6Kg max measured),

D_{f_m} = Mass of the duct shielding (0.198Kg),

P_m = Mass of the material (aluminium) that extends past the motor (0.0351Kg).

Substituting the values in the equation (10.1) we get,

$$\text{Thrust } T = \left(\frac{0.28}{0.24} * 0.6 * 9.81 \right) + (0.198 * 9.81) + (0.0351 * 9.81)$$

$$\text{Thrust } T = 9.153711\text{N}$$

In the below Figure 10.5 PWM vs Thrust increase is shown, which clearly predicts the improvement in thrust when duct is added to the open rotor.

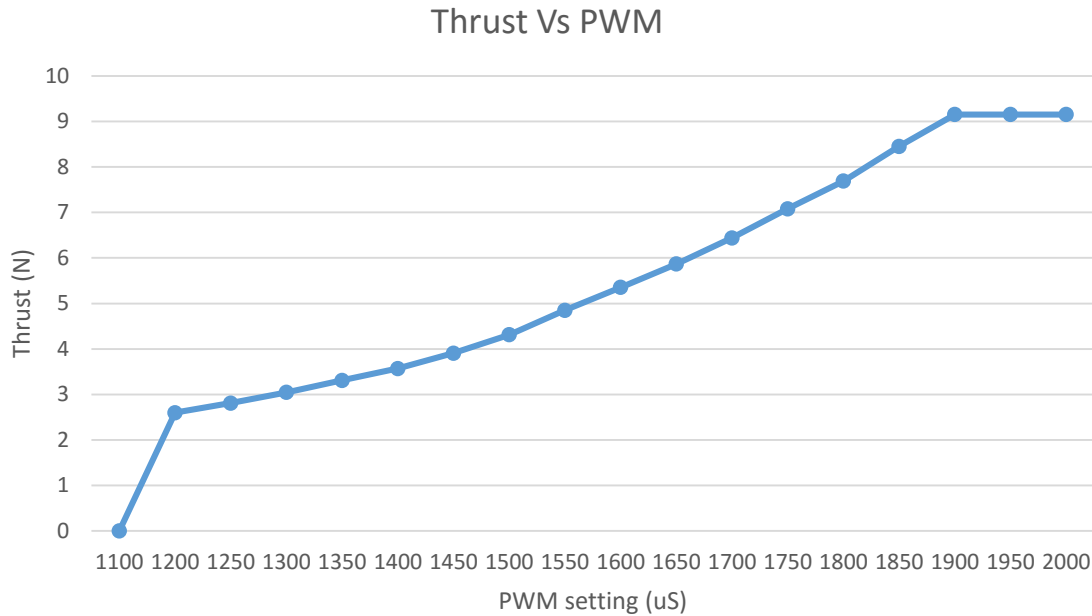


Figure 10.5 PWM vs thrust increase for Ducted quad

10.3 Observation of Quad's

A comparison of these two would then provide more reasonable estimated of Net improvement in thrust. For this to happen we chose RPM instead of PWM to compare, where the RPM is calculated approximately using the formula as below (44).

$$\left(Speed \left(\frac{rad}{s} \right) \right)^2 = T/b \tag{10.2}$$

$$b = C_t * \rho * A * r^2 \tag{10.3}$$

Where,

T = Thrust (N),

b = Constant to calculate with thrust in conversion to speed,

C_t = Thrust co-efficient (0.01025 – Non dimensional),

ρ = Density of air (1.225 Kg/m³),

r = Radius of the propeller (0.12 m),

A = Area of the propeller (0.04523 m²),

Substituting these values in equation (10.3),

$$b = 0.01025 * 1.225 * 0.04523 * 0.12^2 = 0.000008178$$

An example to find $Speed = \sqrt{\left(\frac{6.538158}{0.000008178} \right)} = 894.1372 \text{ rad/s}$

Increase in % of thrust and speeds are discussed in the Table 10.3.

S. No.	Thrust N			Speed (rad/s)	Speed (RPM)
	Open quad	Ducted quad	% Increase in Thrust		
1.	0	0	868.0657	0	0
2.	0.26849	2.5991595	489.2652	181.1926	1730
3.	0.476628	2.808603	327.9935	241.4161	2305
4.	0.711847	3.046659	252.0782	295.0324	2817
5.	0.940102	3.309894	196.8804	339.0501	3238
6.	1.202402	3.5696955	158.3813	383.4434	3662
7.	1.512674	3.9084675	122.94	430.0799	4107
8.	1.934366	4.312476	101.631	486.3465	4644
9.	2.405578	4.850391	90.77868	542.3581	5179
10.	2.806378	5.353971	75.258	585.8002	5594
11.	3.348775	5.868996	65.43622	639.9108	6111
12.	3.893492	6.441246	57.54016	689.9952	6589
13.	4.495467	7.082166	52.33853	741.4192	7080
14.	5.047148	7.688751	46.4498	785.5964	7502
15.	5.773696	8.455566	41.51165	840.2401	8024
16.	6.468521	9.153711	40.50327	889.3628	8493
17.	6.514945	9.153711	40.00443	892.5485	8523
18.	6.538158	9.153711	40.00443	894.1372	8538

Table 10.3 % Increase in thrust

A graph is constructed to show the differences on the thrust performance based on increase in speed. It can be seen from Figure 10.6 that a distinct difference between the ducted and open rotors design change the thrust according to speed change.

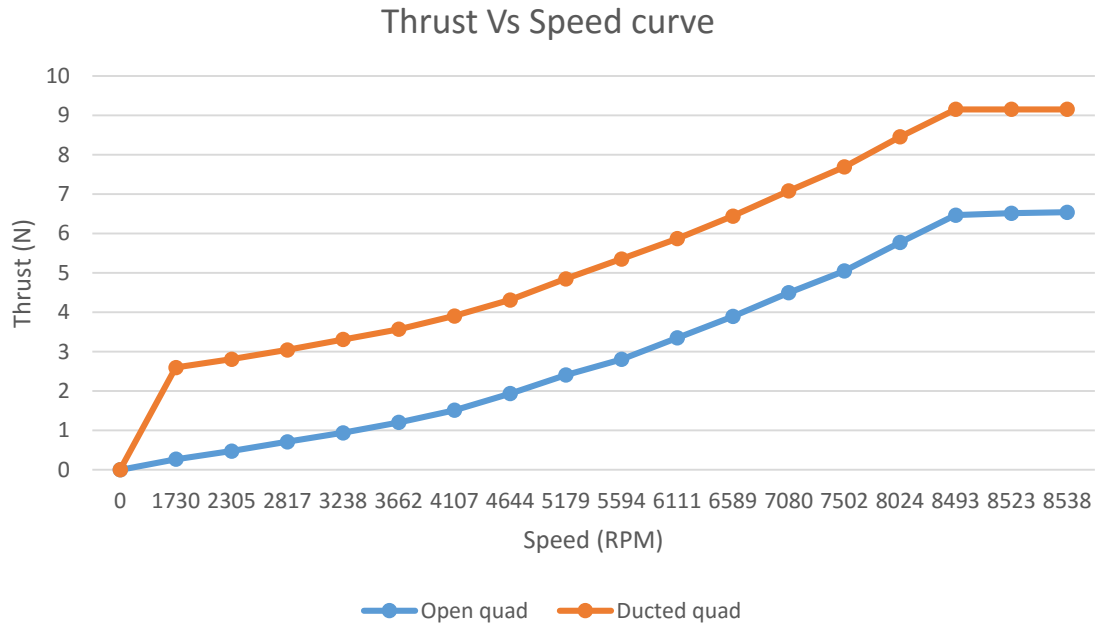


Figure 10.6 Thrust Vs speed curve

It can be clearly seen that the performance is very comparable between across both the rotors, this is an important result because it provides the rotor designer a satisfaction of increasing the performance for a given quadrotor for different duct regimes and hence aid the design process. Based on this discussion it can be generally seen that, development of duct combined with proper designing and dimensioning can substantially improve the duct performance.

Chapter 11. Manufacturing Process

11.1 Duct and Top Cover Production

This section investigates the manufacturing techniques of plastic production, final product and assembly characteristics. Final product can be achieved after following these processes with good surface finish. Manufacturing drawings are attached with the exact surface finish to be maintained and bill of materials show the components required for the assembly process.

11.1.1 Raw material Description

Thermoplastic composites that utilize a thermoplastic polymer as a matrix with a reinforcement matrix that can consist of another polymer, glass, carbon, metal, bio-based materials, etc., Processing and manufacturing of thermos-plastics is not an easy process which has some complications like High processing temperatures, high melt viscosity and fiber setting. Also after manufacturing, considerations should be made on softening temperatures, size and shape of the final product that we are manufacturing (45).

Generally, fiber treatment promotes good interfacial adhesion between the fiber and the thermoplastic resin depending on the type of fiber chosen and the nature of the thermoplastic resin. These operations often carried out during the time of fabrication, this is mainly to reduce the handling of fibers. In our case 30% of glass fiber is used as a reinforcement fiber and the length of the fiber is short which is less than 5mm, to contribute the overall property of composite (Figure 11.1).



Figure 11.1 PA612 G30 raw material (Google image search on raw material PA612)

As the property of PA612, it is used as an abrasion resistance coatings and in some mechanical parts coverings (. Usually PA612 processed in injection moulding which is a stable process and a fast process. From high precision engineering components to disposable consumer goods are manufactured in this way (46).



Figure 11.2 Parts made from PA612 (Google image search on PA612)

11.1.2 Injection moulding

Designing plastic parts is a complex task involving many factors that address a list of requirements of the application like uses, assembly areas, loading conditions etc., in addition to functional and structural issues, processing issues play a major role in the design of an injection moulded plastic part. Most thermoplastics can be processed by injection moulding, and the common materials in the manufacturing include ABS (Acrylonitrile-Butadiene-Styrene), Nylon (PA), Polycarbonate PC, and Polypropylene PP.

In injection moulding process, granular plastic is fed by gravity from a hopper into a heated barrel (Figure 11.3). As the granule particles are slowly pushed forward by a screw-type plunger, the plastic is forced into a heated chamber called barrel where it is melted. The molten plastic is forced when the plunger advances through a nozzle that seats against the mould sprue bushing, allowing it to enter the mold cavity through a gate and runner system. The mold remains at a set temperature so the plastic can solidify almost as soon as the mold is filled (47), (48), (49) & (50).

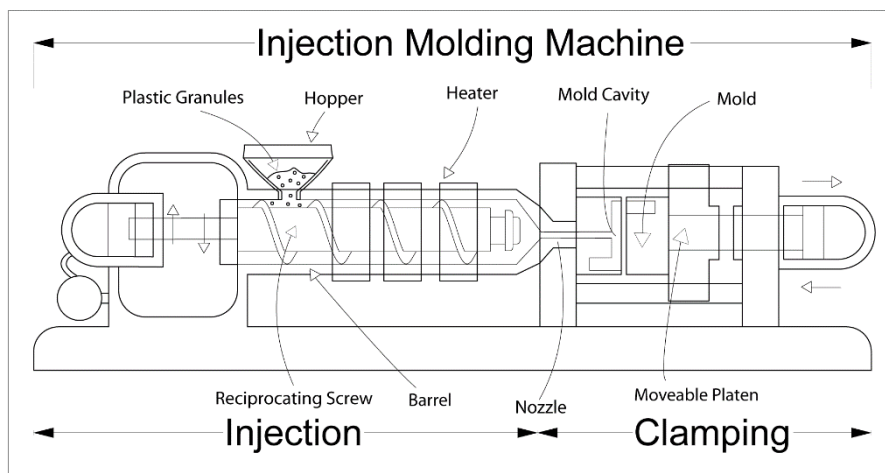


Figure 11.3 Injection molding machine and process (48).

11.1.3 Injection molding requirements

Injection molding requires the following requirements to be fulfilled to receive the final product perfect, these requirements are sequence of cycles and the operations.

11.1.3.1 Injection molding machine

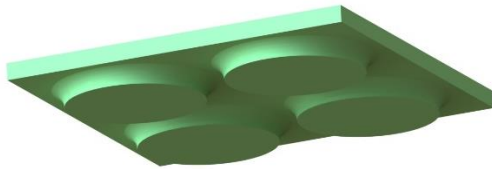
As shown in Figure 11.3 the machine for injection molding consisting of material hopper, injection ram or screw type plunger and heating unit. The mold is clamped to platen of the machine, and the plastic is injected into mold through the sprue orifice. The injected plastic is pressed by weight with the mold of about 4 or 5 tons/in. The force is determined according to the type of the material and size of the part manufactured (49).

11.1.3.2 Mold

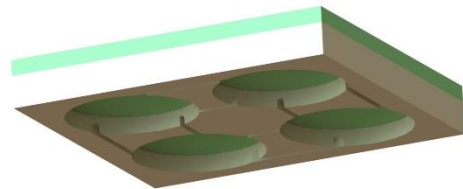
The mold or die refers to the tooling used to produce plastic parts in molding. The mold is formed in the shape of plastic part which is made of steel, aluminium, and or beryllium-copper alloy. According to the studies sharp corners should be avoided in molding to reduce stress

induced in the part which results in broken molecular bonds. For Duct the mold is designed in four parts is shown in below Figure 11.4.

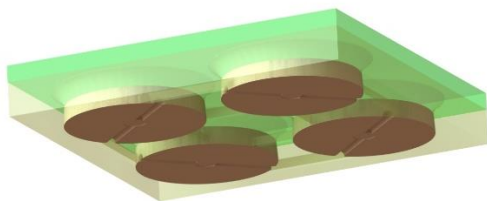
Top Mold shown in Green



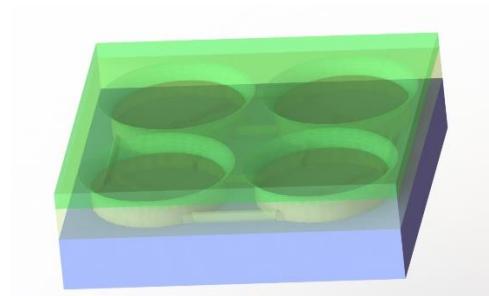
Middle mold shown in Yellow



Core part (Brown) inside the middle part



Bottom part (Blue) below the core part



Mould cavity to form the duct form

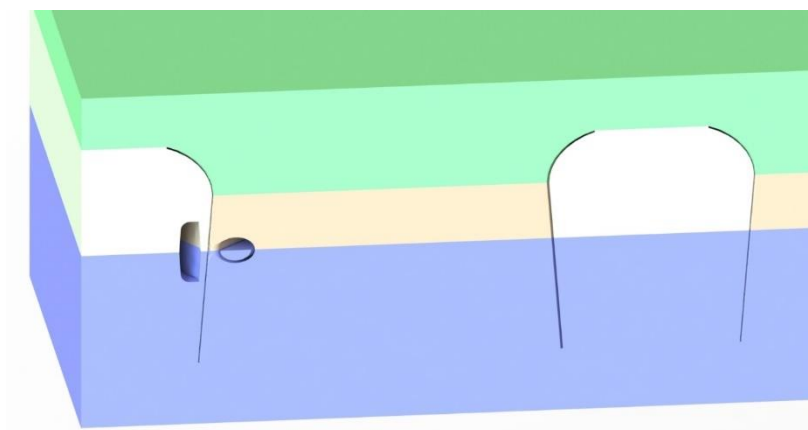


Figure 11.4 Mould forming process

Our product is made of four part mold as shown, the internal mold parts are made of precision parts to improve the air flow condition. The mold releases using ejector plates from all the sides, the four cored molds are released in four directions and the product is removed using release pins. The mold releasing principle example is shown in Figure 11.5.

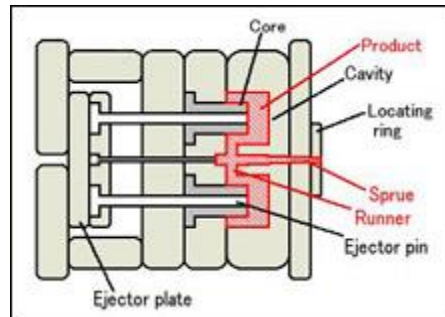


Figure 11.5 Mold releasing principle (49)

11.1.3.3 Wall thickness

Prior to the ejection from the mold, injection molded parts are cooled down from manufacturing temperatures so that they hold their shape when ejected. Choosing proper wall thickness for the product will be effective in cost and production speed of manufacturing. Thinner walls use less material which reduces cost and take less time to cool, reduce cycle time. Also for different resins the wall thickness differs and for Nylon (PA) type of resin the recommended wall thickness is 0.030 to 0.115 in, our product is maintained in this range. To avoid mold shrinkage in our product wall thickness variations are maintained less than 10%.

11.1.3.4 Draft

The injection molding plastic parts include features such as outside walls and internal ribs that are formed by opposing surfaces of tool metal inside a closed mold. To improve the part release when the mold is opened, the side walls of the mold are tapered in the direction that the mold opens. The tapering is always based on the type of surface finish, geometry and surface texture requirements of the part. In our product the draft angles are maintained about 3.5deg each side in relation with the product diffuser angle.

11.2 Duct and Top cover manufacturing drawings

Manufacturing drawings are different from engineering drawings and it explains the different surface roughness to be maintained in product. It also explains the drilling and thickness for manufacturing of product in conditions like high temperature, critical machining areas etc., In our product, manufacturing drawings for duct and top cover are drawn separately along with mold drawings in which drafts and critical features are described clearly.

It is very important to have the drawings separately since they provide different information of the product. In our duct machining is done in the bottom area where the duct is seated on the frame and drilling is done to fix the screws with motor and frame. Surface finish is maintained in those areas and it's shown clearly in the drawing for production. The duct and top cover manufacturing drawings are attached in Appendix D.

11.3 Assembly and Maintenance

Duct shielding requires proper assembly description for explaining some critical areas where the propellers are seated. To project these areas exploded views of whole quadrotor assembly is drawn and bill of materials are prepared. Bill of materials in general list the quantities and the make of different components of the product, and numbering. Exploded view is attached in Appendix D.

As there is no standard maintained in Norway for Ducted rotors and maintenance work on it, common practice of maintenance is done. In the process of designing these areas are noted to be more vulnerable and proper actions are taken in design process. If the motor bolts are removed from its position, the duct can be taken out along with the top cover, which will be easy for technicians to dismantle. The top covers are designed separately to improve the maintenance and also to help the air flow smoothly towards the propeller.

Chapter 12. Conclusion

The designing and development of a quadrotor (DJI Flame wheel F450) with ducts with an aim of increasing the thrust and improving the performance is presented. A duct prototype for one rotor was constructed to measure performance with a gross weight of 200grams and with dimensions greater than the exact model. After accounting the original duct model and the exact weight of the original duct with all the sub-attachments, the resulting weight was about 1150 grams. Our quad was successfully tested for its performance using thrust measuring device, and the results of which are promisingly satisfying for the designers. Some confirmations of early findings are drawn from this study,

- I. Solidworks flow simulation on ducted rotor with the same diameter as in original quadrotor proved a 70 – 80% improvement on thrust over an un-ducted quadrotor.
- II. Test results using thrust measuring devices over both the quad's proved that the performance is enhanced with nearly 40% improvement in thrust.
- III. Studies verified that the improvements are affected by dimensions of the duct and air inflow. Result using Flow 3D also proved that dimensions and modification made on duct can improve the thrust.
- IV. As a result, top cover as a separate part of duct will make a significant impact during maintenance and cleaning. In this way, weight of the top cover is significantly reduced to 80gms.
- V. The main challenge was the weight of the duct itself which was tried to be reduced in the design and material selection which consisted of plastic glass fiber reinforcements for all the four ducts connected using small beams in the middle to improve the structural stiffness. It helped to bring the weight of the whole duct to 1150 grams.
- VI. Although our model is successful, accurate quantitative correlation between theoretical and full scale experimental results was not yet possible due to lack of precise information on pressures, velocity and the uncertainties associated with present theories for thrust calculation.
- VII. Customer's expectations to solve this complex problem has been met.

Chapter 13. Recommendations for Future studies

The dimensions of the model used for our study is approximated, but the use of more exact values would give further insights into the behaviour of the thrust force during motion. This would allow some progress into the problem of predicting thrust loss. Furthermore, thrust testing is carried out on only one ducted systems, but if the duct is tested in full scale, losses due to weight can be predicted.

There is also an urgent need to reduce the production cost, for which effective solutions should be implemented to manufacture the duct by notifying the quadrotor manufacturers. Possibly, if the manufacturers agree in the research, there can be an opportunity to produce the product in bulk.

Appendix A

A.1 Thrust measuring test Procedure

To access the performance of these units, the rotors were first tested with the un-ducted and then in the ducted configuration (Figure A 1). Initially a long aluminium thin plate of size 665x30x3 mm is cut and the exact weight is measured (162 grams). A lever arrangement is made using L-bracket as shown is made from machining and to hold the aluminium bar, a small hole is made in the L-bracket. The hole is machined for smooth finish, so that the bar hanged over the bracket will not have any friction.

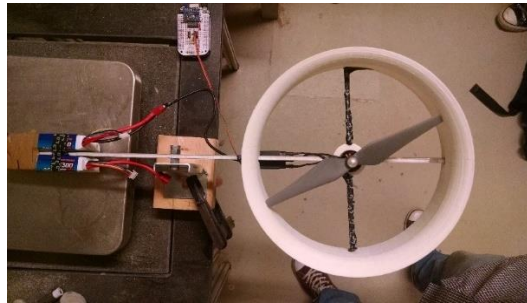


Figure A 1 Thrust measuring stand

The bar is connected with the L-bracket using bolts and nuts as shown, then the bracket is attached in a flat surface. Flatness measurement is done on the surface before fixing the bracket on the surface. A small square piece of size 35x35x2 mm is chopped for fixing the motor, the piece is then drilled with 4 holes of diameter 4 mm, the holes are drilled in the exact hole distances as in motor screw fixing holes. Using screws, the motor and square piece are fitted along with the aluminium bar, later propeller is also attached to the motor. For ducted rotor arrangement, in between the motor and aluminium bar the duct is fitted, as our duct is also designed with drilled holes it is fixed in position.

To balance the other side of the aluminium bar, a weight is added (in our case the battery used to run the motor is added to the other side), before attaching battery the exact mass is found. The extra mass is then subtracted from the thrust force. As discussed in page number 29 (section 5.3), PWM to motor speed converter is designed (Design made by industrial electronics department- Narvik University College), later this is controlled using software in the computer. Initial values of PWM settings starts from 1100 value, then the value is increased step by step until the motor reaches its maximum rpm capacity.

When the power supply is turned on, the propeller starts to rotate and lift the system, so in the other side of the bracket, the weight will push the measuring device down. In this way the mass is found by subtracting the extra weight added, this procedure is repeated for all the speed limits and also for the ducted rotor.

As we can see from the Figure A.1, attachment of duct to the stand will make the length of the aluminium bar to be non-symmetrical from the pivot point. So to make this length symmetrical a calculation is made and this is the calculation which has been explained in section 10.2 (equation (10.1)).

Appendix B

B.1 Duct initial testing setup in Flow 3D

The following (Table B 1) is the information provided by the design team on the Duct/ rotor configuration used for experimentation.

S. No	Parameters	Values
1.	Rotor Diameter D1	0.242m
2.	Duct Diameter D2	0.24240m
3.	Motor maximum velocity V (approximated)	124.384 m/s
4.	Flow rate Q	5.9392 m ³ /s

Table B 1 Parameters for loading model in Flow 3D

The Solidworks modelling for flow 3D is mentioned in Figure 7.4 and Figure 7.6. The Flow 3D simulation setup was done under the supervision of one of my supervisor (Mr. Per Arne Sundsbø). The process of setting up both the models are done in the same interface screen by duplicating the fluid meshing areas.

The domain was divided into three sections, freestream, duct area and blade area ()

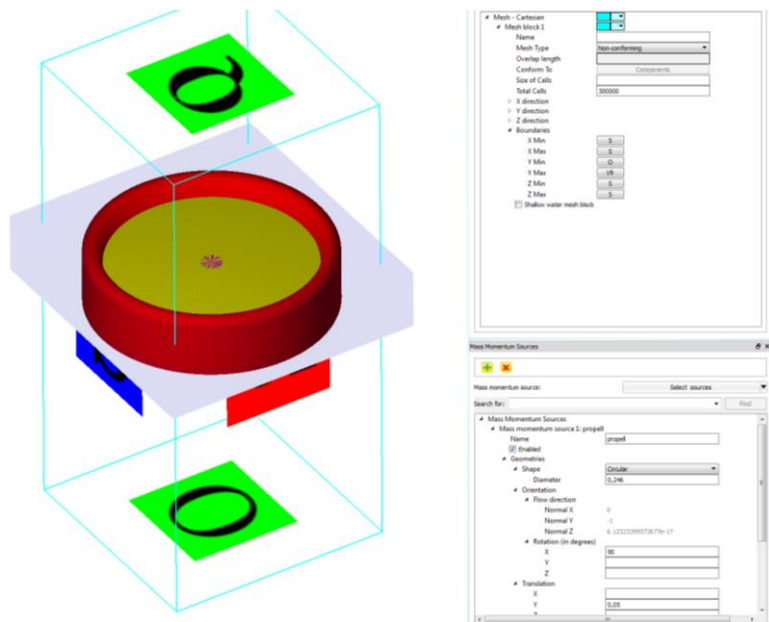


Figure B 1 Domain area in Flow 3D

The subdivision between the free stream and the duct area was for the purpose of meshing. All the relevant parameters were identical for both the ducts. The freestream is fairly coarse while the duct area is meshed slightly finer and the blade area itself is meshed very fine. This is to get the exact results of the ducting. The fluid in the freestream and the duct area is stationary while the blade area is in the rotating frame. The free stream area extends approximately 5 rotor diameters upstream and downstream.

With these setting options the model and the domain area is now ready for the meshing and the meshing parameters are given below,

x direction of real cells= 52

smallest cell= 5.3077E-03

largest cell= 5.3077E-03

maximum cell ratio = 1.0000E+00 (at cell # 52)

y direction: # of real cells= 112

smallest cell= 5.3571E-03

largest cell= 5.3571E-03

maximum cell ratio = 1.0000E+00 (at cell # 104)

z direction: # of real cells= 52

smallest cell= 5.3077E-03

largest cell= 5.3077E-03

maximum cell ratio = 1.0000E+00 (at cell # 52)

After meshing is done the parameter's described in Table B 1 is entered in the value description area, the velocity or mass flow rate is entered. Then the calculation is started and it took more than 15 hours to complete the simulation. The results for the simulation is discussed in the section 7.2.

B.2 Flow simulation setup in Solidworks for open rotor

The following (Table B.2) is the information provided by the design team on the duct/rotor configuration used for simulation,

S. No	Parameters	Values
1.	Rotor Diameter D1	0.242m
2.	Duct Diameter D2	0.24240m
3.	Rotational speed of propeller	860 rad/s, (anti-clockwise direction)
4.	Units	SI (m – kg – s)

Table B 2 Loading parameters

A Solidworks diagram of the open propeller was also provided (Figure B.2)

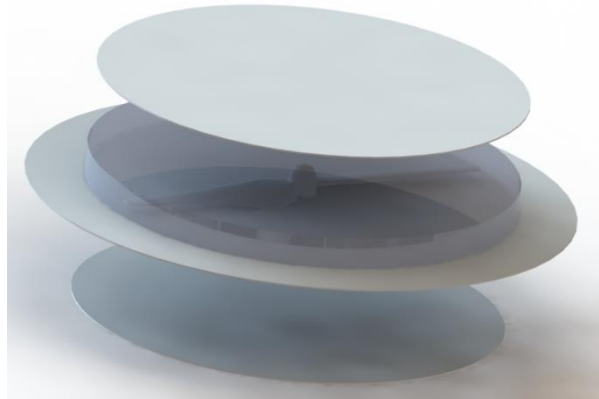


Figure B 2 Solidworks propeller for simulation

The flow simulation was followed with Solidworks flow simulation tutorial (51) & (52). The tutorial itself shows how to set up one stage of flow simulation. The domain created is a single area with finer particles in the propeller edges. The modelling is created in such a way that the air flow inside and outside is noted down by means of a flat thin surface up and down. To simplify the propeller shape and size, its created in form of a rotating disc, but the flow over the aerodynamics of the propeller is considered.

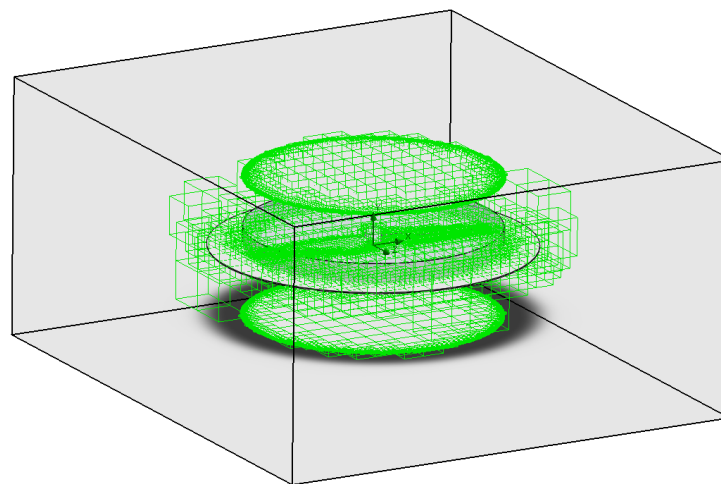


Figure B 3 Domain and meshing details

In our meshing procedure the freestream is fairly coarse but as shown in Figure B 3 the propeller area is meshed very fine. This was important for capturing the near field flow features while not consuming too much memory. Meshing details are explained in Table B 3.

S. No	Parameter	Meshing detail
1.	Basic mesh dimensions (Number of cells in X)	32
2.	Basic mesh dimensions (Number of cells in Y)	32
3.	Basic mesh dimensions (Number of cells in Z)	32
4.	Analysis mesh (Total cell count)	65066
5.	Analysis mesh (Fluid cells)	53163
6.	Analysis mesh (Solid cells)	87
7.	Analysis mesh (Partial cells)	11816
8.	Analysis mesh (Trimmed cells)	0

Table B 3 Meshing details for open rotor

After meshing the model goals for the surface of the propeller is set, in which force in Y direction is considered in our case, because this is the thrust force. Air flow condition is also specified from top to bottom and how it flows over the propeller. As mentioned earlier the air flow from top surface plate travels to middle plate more than the propeller size and travels towards the bottom plate. The simulation results are discussed in 5.5.

B.3 Flow simulation setup in Solidworks for ducted rotor

All the parameters flow velocity of the air is same as in Table B.2, but the Solidworks modelling and meshing details are quite different from the open rotor. (Figure B 4).

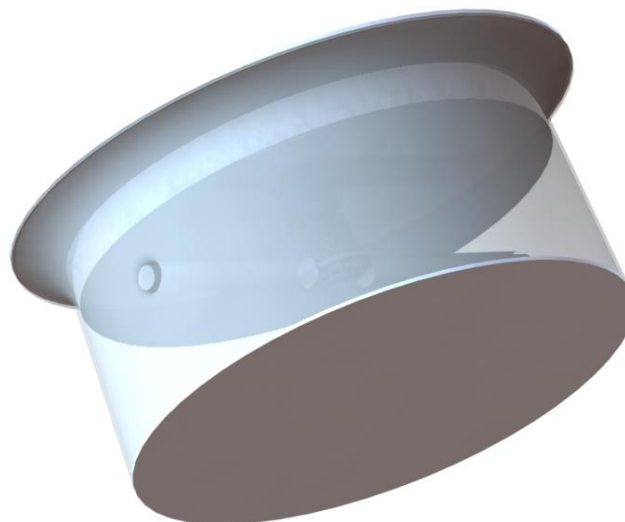


Figure B 4 Ducted rotor for Flow simulation setup

From the figure we can see that the normal duct with motor and propeller setup, but the only difference is top and bottom opening of the duct is closed and the air flow is considered from

the top lid surface to bottom lid surface. In the middle the air flows over the propeller area. As in open rotor the propeller is considered as a rotating disc structure. The meshing has three layers' outer fluid domain, inner fluid domain, duct and propeller area.

The outer fluid domain is coarsely meshed, but the inner fluid area is pressurised and medium meshed, but the fine mesh is provided to the propeller and duct areas

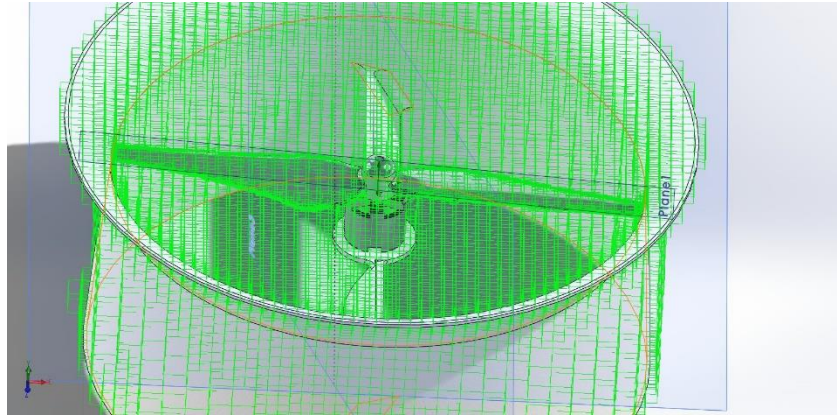


Figure B 5 Meshing details for Ducted rotors

The size of the domain, meshing details are explained in the below

S. No	Parameter	Meshing detail
1.	Computational domain (X – min)	-0.167m
2.	Computational domain (X – max)	0.163m
3.	Computational domain (Y – min)	-0.122m
4.	Computational domain (Y – max)	0.054m
5.	Computational domain (Z – min)	-0.166m
6.	Computational domain (Z – max)	0.164m
7.	Basic mesh dimensions (Number of cells in X)	32
8.	Basic mesh dimensions (Number of cells in Y)	16
9.	Basic mesh dimensions (Number of cells in Z)	32
10.	Analysis mesh (Total cell count)	65055
11.	Analysis mesh (Fluid cells)	30203
12.	Analysis mesh (Solid cells)	13563
13.	Analysis mesh (Partial cells)	21289
14.	Analysis mesh (Trimmed cells)	10

Table B 4 Meshing details for Ducted rotors

In the case of ducted rotor three boundary conditions are inserted,

- I. Inlet velocity of air that hits the propeller be at 5 – 10 m/s,
- II. Environmental pressure is normal condition after the duct area and before the air inlet,
- III. The duct is made of real walls to block the air inside it, and not allowing to pass out.

Later using these data's, the calculation for simulation is done.

Appendix C

C.1 Procedure for drop test setup

Initially in the drop test, material is chosen for the duct, as our material is PA612-GF30, we enter the details for the material, as shown in the Table C 1.

S. No	Properties	Values
1.	Model type	Linear Elastic Isotropic
2.	Yield strength	1.55e+008 N/m ²
3.	Tensile strength	1.54e+008 N/m ²
4.	Compressive strength	1.76e+008 N/m ²
5.	Elastic modulus	1.12e+010 N/m ²
6.	Poisson's ratio	0.368
7.	Mass density	1310 kg/m ³
8.	Shear modulus	3.77e+009 N/m ²

Table C 1 Properties of Material for Duct

Meshing is done on the duct and in our case we use fine mesh to all the areas of the duct, as our duct thickness is 1.5mm. Also in some areas the thickness value is less than 1.5mm, so finer mesh is provided to all the parts of the duct as shown in Figure C 1.

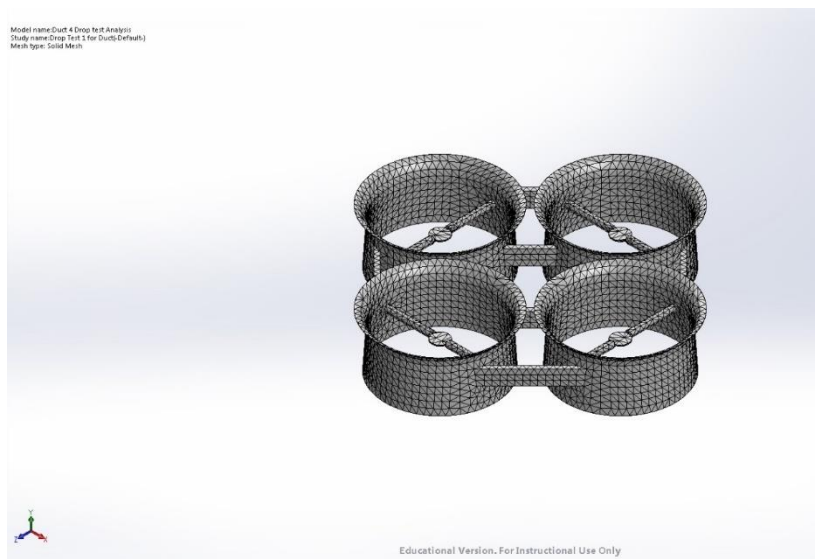


Figure C 1 Meshing in Solidworks

Meshing information and details of the mesh are shown in below Table

S. No	Mesh Information	Meshing detail
1.	Mesh type	Solid mesh
2.	Mesher used	Curvature based mesh
3.	Jacobian points	4 points
4.	Mesh Quality	High
5.	Total nodes	47939
6.	Total elements	51867
7.	Maximum aspect ratio	1221.2
8.	% of elements with Aspect ratio < 3	12.3
9.	% of elements with Aspect ratio > 10	81.2
10.	% of distorted elements (Jacobian)	0

Figure C 2 Meshing details for duct

After the meshing details are determined, in the setting up study drop height of the object is specified (that is the distance to impact) or velocity at impact is defined. In our case we develop a study based on the height which is 10m from ground. The height is always mentioned from the centre of the body and normal to the plane in which the duct falls. The duct is slightly angled to say that the duct falls in some weird position as discussed in the result section in 9.4.1. The default hitting surface to ground is considered as a rigid and the solution after the impact is taken as 80microseconds. Then the simulation is turned on.

C.2 Procedure for Impact test on Top cover

The material parameters of top cover are same as we formed for duct. But the meshing parameter vary as shown in

S. No	Mesh Information	Meshing detail
1.	Mesh Quality	High
2.	Total nodes	58444
3.	Total elements	32567
4.	Maximum aspect ratio	7.9848
5.	% of elements with Aspect ratio < 3	98.1
6.	% of elements with Aspect ratio > 10	0

Table C 2 Meshing parameter for top cover

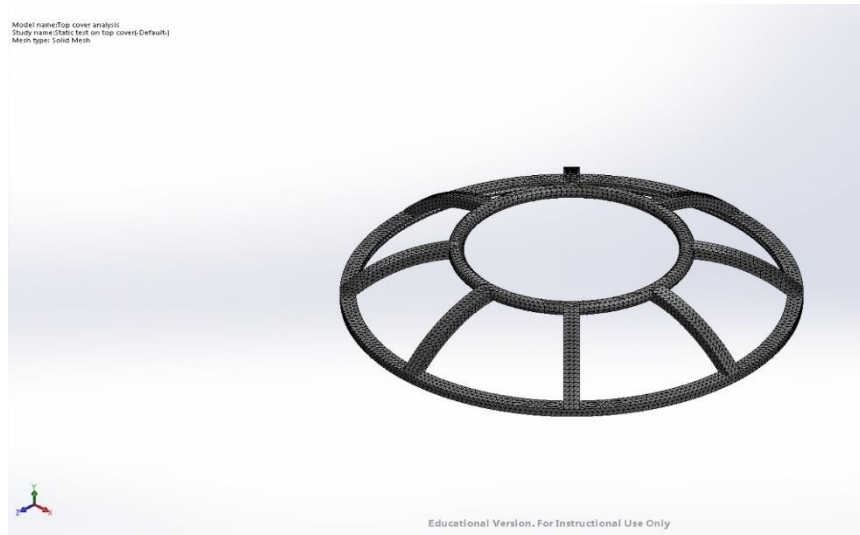


Figure C 3 Top cover Solidworks meshing

In the connector settings elastic support is given to the area where the duct is connected to the top cover. This area is considered to take the load and make the impact less worthy. The elastic support has normal stiffness value as 10 and shear stiffness value 5. Pressure is applied in the top of the cover normal to the direction of the duct, i.e., towards the gravity. After specifying the values of the impact the calculation is turned on. And as we have discussed in 9.4.2, the result values are taken to find the reaction forces and stress intensity values.

Appendix D

D.1 Bill of materials and Exploded view – Attachment 1 (Sheet: 1/3)

D.2 Duct Mechanical drawing – Attachment 2 (Sheet: 2/3)

D.3 Top cover Mechanical drawing – Attachment 3 (Sheet: 3/3)

Appendix E Task Description



Master of Science

Masterthesis by

Stud. techn. Balakrishnan, Sethuram

Duct fanned shielding design for quadrotors

Narvik University College/Høgskolen i Narvik,

Faculty of Technology

Master degree program: Engineering Design

Spring 2016

Background

Quadrotors drones are autonomous vehicles equipped with four large rotors/ propellers. The DJI FlameWheel kit does not include any type of propeller shielding for the quadrotor. Since these quadrotors are powerful, the propellers constitute a hazard risk. Therefore, the propellers need to be shielded in case of collision with an object or personnel. The propeller shielding must be mounted securely before any active flight is allowed.

Quadrotors have limited flight time and adding propeller shielding might decrease the flight time further due top added mass, increasing drag or decreasing thrust. It is therefore of interest to design the rings around the propellers in such a way that it constitutes a duct fan system. This will increase the efficiency of the propellers and balance some of the lost flight time because of the added mass. Not only is mass and aerodynamic efficiency important it is also important that the shielding exhibit high durability from extended use. Lightweight but still structurally sound. In the Figure 1 a concept art for a propeller shielding body is shown. As indicated it is also of interest to have some type of structural barrier on top of the propellers, forming a dome with its base encapsulated in the propeller shielding rings.]

The candidate for this task should thereby design a shielding system, which takes into consideration among others the following points:

1. Minimal mass
2. Improved thrust
3. Physical protection for the rotors
4. Added strength/ integrity for the rest of the design
5. Minimal vibrations
6. Usage in cold climate/ arctic regions.
7. Aesthetics
8. Easy
9. Easy service and maintenance

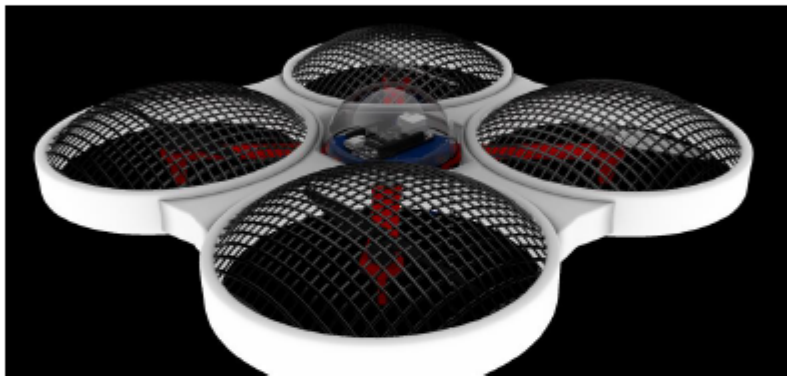


Figure 1 concept art for a propeller shielding body

The work shall include:

1. A literature study both in terms of finding state-of-the-art for these types of products, existing equipment on the market and potential competitors, as well as other literature that is necessary with a view to solving the problem (regulations, standards for materials, patents etc.). Existing equipment described with respect to behaviour, structure, performance, weight, and size.
2. Develop a specification for the product based on demands for performance under the given physical conditions, requirements for stiffness, strength, shape, weight, reliability, manufacturing, regulations and other requirements and demands of the customer.
3. Conduct a systematic design ending up with a final proposal to the technical solution for the product/system.
4. Analysis of the product/system shall be made in order to determine which aspects/ parts of the system/ product should undergo numerical and analytical calculations.
5. Modelling of the system in a 3D parametric CAD system and simulation/visualization of for instance movements. A set of 2D drawings should be generated. These drawings should include assembled drawings of the system in open and closed position and complete part production drawings with tolerances.
6. Modelling and numerical analysis of the product/ system will (also) be carried out using an appropriate numerical calculation tool (such as Ansys) and should be compared with the analytical calculations of the product / system.
7. Construction / making a (physical) prototype or a model of the product/system/structure.

8. Suggestions for future work and description of remaining work

The solution of the task should be based on typical engineering design methods and areas of study for the Master Program Engineering Design at Narvik University College.

References

1. What is a Quadcopter. *quadcopterhq.com*. [Online] 31 August 2013. quadcopterhq.com/what-is-a-quadcopter/.
2. aerospace, Krossblade. History of Quadcopters and Multirotors. [Online] Krossblade Aerospace Systems. <http://www.krossblade.com/history-of-quadcopters-and-multirotors/>.
3. "The Quadrotor's Coming of Age". Illumin. 29 December 2014, Illumin.
4. Akao. Quality Function Deployment. [Online] 1990. <http://www.becker-associates.com/thehouse.HTM> and <http://www.becker-associates.com/qfdwhatis.htm>.
5. CROW, KENNATH. npd-solutions QFD. [Online] DRM Associates, 2016. <http://www.npd-solutions.com/qfd.html>.
6. Type of drones. *Top drones for sale*. [Online] TDS, 2015. www.topdronesforsale.org/types-of-drones/.
7. Nano quadrotor. [Online] <https://www.wearechampionmag.com/best-6-smallest-nano-quadcopter-drones>.
8. Encyclopedia. AAI RQ-7 Shadow. [Online] Wikipedia, 4 February 2016. https://en.wikipedia.org/wiki/AAI_RQ-7_Shadow.
9. McDougal, Timothy. [Online] 2015. <http://www.bhphotovideo.com/explora/video/features/are-quadcopters-legal%3F>.
10. Encyclopedia. Thales Watchkeeper WK450. [Online] Wikipedia, 11 February 2016. https://en.wikipedia.org/wiki/Thales_Watchkeeper_WK450.
11. Norway, Civil Aviation Authority -. Regulation concerning aircraft without a pilot on board. *luftfartstilsynet.no*. [Online] Civil Aviation Authority - Norway, 14 Dec 2015. [Cited: 15 Feb 2016.] http://luftfartstilsynet.no/caa_no/Regulations_concerning_aircraft_without_a_pilot_on_board_etc.
12. —. Bruk av ubemannede luftfartøy i Norge. *fargisinfo*. [Online] 19 04 2013. http://www.fargisinfo.com/sensodrone/LinkedDocuments/Bruk-av-UAV_Luftfartstilsynet.pdf.
13. *DJI-F450-Flame wheel*. [Online] <http://www.buildyourowndrone.co.uk/dji-f450-flame-wheel-multi-rotor-quadcopter-artf-kit.html>.
14. Øyvind Magnussen, Kjell Eivind Skjønhaug. *Modelling, Design and Experimental study for Quadcopter system construction*. Agder : University of Agder, Department of Engineering, 2011.
15. Quadcopter parts list. [Online] Quadcopter garage. <http://quadcoptergarage.com/quadcopter-parts-list-what-you-need-to-build-a-diy-quadcopter/>.
16. Multi-rotor-quadcopter. *tomshardware*. [Online] 3 june 2014. <http://www.tomshardware.com/reviews/multi-rotor-quadcopter-fpv,3828-5.html>.
17. OscarLiang. *How to choose Motor and Propeller*. [Online] <http://blog.oscarliang.net/how-to-choose-motor-and-propeller-for-quadcopter/>.
18. Smith, Korey. Myfirstdrone. *Best-flight-controllers*. [Online] 24 July 2014. <http://myfirstdrone.com/tutorials/buying-guides/best-flight-controllers/>.
19. Gibiansky, Andrew. Quadcopter Dynamics, Simulation and Control introduction. *andre.gibiansky.com*. [Online] <http://andrew.gibiansky.com/downloads/pdf/Quadcopter%20Dynamics,%20Simulation,%20and%20Control.pdf>.
20. Allen, Clay. An Introduction to Quadcopters. [Online] 2014. http://ffden-2.phys.uaf.edu/webproj/212_spring_2014/Clay_Allen/clay_allen/works.html.

21. Mark Duptuis, Jonathan Gibbons, Maximillian Hobson-Dupont, Alex Knight, Artem Lepilov, Michael Monfreda, George Mungai. *Design Optimization of a Quad-Rotor Capable of Autonomous Flight*. Massachusetts : Worcester Polytechnic Institute, 2008.
22. *Trajectory generation and control for precise aggressive*, In *Proceedings of the International Symposium on Experimental Robotics*. D.Mellinger, N.Michael and V.Kumar. Dec 2010.
23. *Aero vinci safety on Quadrotor*. [Online] <http://www.st.ewi.tudelft.nl/~gemund/Courses/In4073/Resources/safetydoc.pdf>.
24. *Quadrotor Manufacturers*. [Online] <http://www.directindustry.com/industrial-manufacturer/quadrotor-uav-86139.html>.
25. *Quadrotor Protection covers*. [Online] <http://www.hubsan.com/product/index413.html>.
26. *Blade Protection*. [Online] <http://relaydrones.com/product/lookatool-upgrade-jjrc-h8d-4ch-5-8g-fpv-rc-quadcopter-drone-hd-camera-monitor-4-battery-free-4pcs-blades-protection-free-propeller-cover-set/>.
27. *Quadrotor Protection covers*. [Online] <http://mybestbuyever.com/en/quadcopter-accessories/28090-udi-u830-hand-sensor-rc-quadcopter-parts-protection-cover-u830-04.html>.
28. Mr.P.Cannolly. *aircraft-world*. [Online] <https://www.aircraft-world.com/Datasheet/en/hp/emeter/hp-propconstants.htm>.
29. Dickey, Jeremiah. *Static thrust calculation*. *Quadcopter project*. [Online] Airwolf II - World press . <https://quadcopterproject.wordpress.com/static-thrust-calculation/>.
30. [Online] 13 October 2015. https://en.wikipedia.org/wiki/Momentum_theory.
31. <https://www.youtube.com/watch?v=UVPITLoInOk>. NPTEL - IIT (Kanpur).
32. *Pulse-width-modulation*. [Online] https://en.wikipedia.org/wiki/Pulse-width_modulation.
33. *DIFFUSER ANGLE CONTROL TO AVOID FLOW SEPERATION*. Vinod Chandavari, Mr. Sanjeev Palekar. Issue 5, BANGALORE, INDIA : International Journal of Technical Research and Applications, Sep-Oct 2014, Vol. Volume II. ISSN: 2320-8163.
34. Oates, Gordon C. *Aircraft Propulsion Systems Technology and Design*. Washington : American Institute of Aeronautics and Astronautics, 1989. ISBN-0-930403-24-X.
35. Dr.Jason L.Pereira, Professor Inderjit Chopra. *Hover and wind-tunnel testing of shrouded rotors for improved micro air vehicle design*. University of Maryland, College Park. Aerospace Engineering : ProQuest, 2008. 0549961658, 9780549961659.
36. Leishman, J.G. *Principles of Helicopter Aerodynamics, 1st ed.,*. New york : Cambridge Aerospace series. Cambridge University Press, NY, 2000.
37. Edward.H.Smith. *Mechanical Engineers referance book 12th edition*. Lancashire : Butterworth-Heinemann Ltd, 1994. ISBN0750611952.
38. Lewis.F.Moody. *Friction factors for pipe flow*. Pg.No:671. Princeton : Transactions of ASME, Nov-1944.
39. HUDSON, GEORGE W. HOUSNER & DONALD E. *Applied Mechanics Dynamics*. United States of America : s.n., 1991.
40. O'Reilly, Oliver M. *Engineering Dynamics*. Berkley : A Primer, 2009. ISBN 978-1-4419-6360-4.
41. F.Ashby, Michael. *Materials selection Mechanical Design*. Burlington : Elsevier Ltd, 2011. ISBN 978-1-85617-663-7.
42. 2015, CES Edu pack. *Material selection software*. [Software] Cambridge, UK : Granta Design Limited, 2015.

43. Replicator Z-18 techspecs. [Online] MakerBot industries L.L.C, 2009-2016. <http://store.makerbot.com/replicator-z18#techspecs>.
44. *Multirotor Aerial vehicles*. Robert Mahony, Vijay kumar, & Peter Corke. s.l. : IEEE Robotics & Automation magazine, 27 aug 2012, Vol. 1. 1070-9932.
45. *Structural composite materials (pp. 81-90)*. F.C.Campbell. OHIO : ASM International, 2010. 978-1-61503-037-8.
46. federation, Plastic. Plastic processes. [Online] British Plastic Federation, 2016. <http://www.bpf.co.uk/plastipedia/processes/Default.aspx>.
47. V.Ryan. Injection moulding of Plastics. [Online] 2002-2009. <http://www.technologystudent.com/equip1/inject1.htm>.
48. Plastics, AV. Injection moulding. [Online] AV plastics UK. <http://www.avplastics.co.uk/what-is-injection-moulding>.
49. systems, 3D. Injection molding basics. [Online] 3Dsystems , 2015. <http://www.3dsystems.com/quickparts/learning-center/injection-molding-basics>.
50. Musa.R.Kamal. Part I: Background and overview: Injection molding; Introduction and General background PP 1, 3-70. *Injection Molding*. Munich : Carl Hanser, 2009.
51. help, Solidworks. Solidworks. [Online] Dessault systems, 2015. http://help.solidworks.com/2014/English/WhatsNew/c_Flow_Simulation.htm.
52. *Flow simulation in solidworks* (<https://www.youtube.com/watch?v=vv4gvsojKNo>). Goengineer, 2013.
53. Flamewheel 450. [Online] http://www.dji.com/showcase?from=site_brandsite_showcase.